2019

Using UV technology for microbial contamination remediation of beach water

Natasha Rahman
University of Windsor

USING UV TECHNOLOGY FOR MICROBIAL CONTAMINATION REMEDIATION OF BEACH WATER

By

Natasha Rahman

A Thesis
Submitted to the Faculty of Graduate Studies
through the Department of Civil and Environmental Engineering
in Partial Fulfillment of the Requirements for
the Degree of Master of Applied Science
at the University of Windsor

Windsor, Ontario, Canada

2019

USING UV TECHNOLOGY FOR MICROBIAL CONTAMINATION REMEDIATION OF BEACH WATER

by

Natasha Rahman

APPROVED BY:

_____

C. Weisener
Great Lakes Institute for Environmental Research

_____

N. Biswas
Department of Civil and Environmental Engineering

_____

R. Seth, Advisor
Department of Civil and Environmental Engineering

_____

D. Heath, Co-Advisor
Great Lakes Institute for Environmental Research

April 16, 2019

DECLARATION OF ORIGINALITY

I hereby certify that I am the sole author of this thesis and that no part of this thesis has been published or submitted for publication.

I certify that, to the best of my knowledge, my thesis does not infringe upon anyone's copyright nor violate any proprietary rights and that any ideas, techniques, quotations, or any other material from the work of other people included in my thesis, published or otherwise, are fully acknowledged in accordance with the standard referencing practices. Furthermore, to the extent that I have included copyrighted material that surpasses the bounds of fair dealing within the meaning of the Canada Copyright Act, I certify that I have obtained a written permission from the copyright owner(s) to include such material(s) in my thesis and have included copies of such copyright clearances to my appendix.

I declare that this is a true copy of my thesis, including any final revisions, as approved by my thesis committee and the Graduate Studies office, and that this thesis has not been submitted for a higher degree to any other University or Institution.

ABSTRACT

Microbial contamination of beach water negatively affects public health and the nation's economy. Combined sewer overflows (CSO) and sanitary sewer overflows (SSO) have repeatedly been identified as major threats to water quality. UV radiation can be used to reduce the risk of bacterial pollution. In order to quantify the efficacy of UV treatment in a timely manner, real-time quantitative polymerase chain reaction (qPCR) methods are analyzed in this thesis. First, a robust qPCR-based method was developed to quantify UV inactivation of *E. coli*. This method employed long amplicon qPCR with various gene targets in order to do a scan of DNA damage and determine suitable gene targets for reliable quantification. UV-induced DNA damage was found to be widespread through the genome of *E. coli*. Of all the gene targets, the cell division genes were found to be the most sensitive and therefore, would serve as good targets for detecting UV inactivation through qPCR. Next, the developed method was applied to simulated CSO samples. The qPCR method was found to have a linear correlation with the culture-based technique between the UV dose range of 0 – 20 mJ/cm^2. Additionally, the UV disinfection kinetics were analyzed for all the samples. It was found that a single-strain pure *E. coli* culture was more susceptible to UV damage than *E. coli* found in wastewater. Overall, UV disinfection is an effective means of reducing microbial contamination, and qPCR is a good surrogate for quantifying UV inactivation as opposed to the time-consuming culturing methods.

DEDICATION

To my mother – for everything

ACKNOWLEDGEMENTS

I would first like to express my sincere gratitude to my advisors, Dr. Rajesh Seth and Dr. Daniel Heath for their guidance, advice and encouragement throughout my work. Thank you to my committee members, Dr. Nihar Biswas, Dr. Chris Weisener, and Dr. Brian Petri for their input.

This project would not have been possible without the help of many people. I would like to express my deep gratitude towards Trojan Technologies (London, ON) for their equipment, Bill Middleton for his help and support with my experiments, Dr. Subba Rao Chaganti for training me on various molecular techniques, Dr. Po-Shun Chan for training me on UV exposure experiments, and Shelby Mackie for her help with DNA extractions and qPCR. Additionally, I would like to thanks Shannon Deehan, Fasih Rahman and the Engineering Co-op students for assisting me with my experiments. A special thank you to Razagh Shahraki and Nabeelah Lulat for sharing supplies, helping me around the lab, and for giving me tips on working in a genomics lab.

Finally, I would like to thank my family and friends for their support and encouragement over the past few years.

This work was supported by an NSERC Strategic Grant and NSERC CGS-M scholarship.

TABLE OF CONTENTS

LIST OF TABLES

LIST OF FIGURES

LIST OF ABBREVIATIONS/SYMBOLS

BLAST	Basic Local Alignment Search Tool
bp	Basepair
CSO	Combined sewer overflow
dNTPs	deoxyribonucleotide triphosphates
E. coli	*Escherichia coli*
FIB	Fecal indicator bacteria
GI illness	Gastrointestinal illness
MOECC	Ministry of Environment and Climate Change
MVT	Molecular viability testing
NCBI	National Center for Biotechnology Information
NER	Nucleotide excision repair
NTC	No template control
qPCR	Quantitative (real-time) polymerase chain reaction
RT-qPCR	Reverse transcriptase quantitative (real-time) polymerase chain reaction
sCSO	Simulated combined sewer overflow
SSO	Sanitary sewer overflow
USEPA	United States Environmental Protection Agency
UV	Ultraviolet
WHO	World Health Organization
WWTP	Wastewater treatment plant
λ	Wavelength

CHAPTER 1:

INTRODUCTION TO THE STUDY

General Introduction

Increasing populations and urbanization have compromised the world's water resources. Fresh water used for drinking and recreation is contaminated by untreated sewage, toxic chemicals, pharmaceuticals and excess nutrients. The US Environmental Protection Agency (USEPA) identifies microbial contamination as one of the major causes of water impairment, and most commonly reported cause of water pollution nationwide (USEPA, 2012; Pandey et al., 2014). Combined sewer overflows (CSO) and sanitary sewer overflows (SSO) have repeatedly been identified as major threats to water quality (WHO, 2003; McLellan et al., 2007; Templar et al., 2016). Other sources include bird droppings, animal wastes, and stormwater runoff. From all these sources, various types of pathogens are transported and discharged into receiving waters. Exposure to polluted water can lead to gastrointestinal (GI) and some upper respiratory illnesses, which are of great concern to the public (DeFlorio-Barker et al., 2018).

Need for Great Lakes Water Security

The Great Lakes contain over 20% of the world's supply of freshwater, and over 80% of North America's surface freshwater (USEPA, n.d.). Aside from hosting a diverse array of plants, animals, and ecosystems, the Great Lakes basin is Canada's densest population center and heavily contributes to the economic activity of the nation. Approximately 75% of Canada's manufacturing, 80% of Ontario's power generation, and 95% of Ontario's agriculture lands depend on the Great Lakes (Ministry of the Environment, Conservation and Parks, 2015). Due to its numerous economic advantages,

its regional economy is the fourth largest worldwide. Therefore, the strength and success of Ontario and Canada lies in the Great Lakes.

Recreational use and tourism in the Great Lakes region generated an estimated $12.3 billion in 2010 alone (Ministry of Environment, Conservation and Parks, 2016). However, the revenue from recreation and tourism is offset by the cost of water treatment, fisheries losses, health care and hospitalizations for those affected by waterborne illnesses (DeFlorio-Barker et al., 2018). With more people falling ill from poor recreational water quality, the public becomes more concerned about their quality of life and national water security. As such, there is a great need for providing proper and reliable measures to keep the Great Lakes secure and safe for everyone.

Beach Water Quality and Monitoring

The health of swimmers is of particular importance. Unlike drinking water, which undergoes a treatment process before public exposure, there is no protective engineered control separating polluted waters and swimmers. To limit the risk, regulatory agencies post advisories and close beaches when they are deemed unsafe. As sewer overflows also degrade water quality, many municipalities aim to reduce the number of overflow events by upgrading their sewer infrastructure. However, the costly price tag makes it an unappealing option. Implementing disinfection technologies, on the other hand, provide a relatively lower cost and offer a wide range of treatment options (Tondera et al., 2015; Tondera et al., 2016; Eramo et al., 2017).

The threat of fecal contamination from untreated sewage is well-established (Templar et al., 2016). Specifically, pathogens from untreated human waste pose the greatest threat to humans. Direct detection of these pathogens in water is difficult as they

are present in low numbers and yet are highly infectious. As such, bacterial water quality is assessed by quantifying fecal indicator bacteria (FIB), using total coliform, fecal coliform, *Escherichia coli*, and enterococci. These indicator organisms have been extensively used to detect the presence and assess the health risk in both fresh and marine waters. Namely, the use of *E. coli* has been recommended by the European Commission (European Union, 2006), the World Health Organization (WHO, 2003), Health Canada (Health Canada, 2012), and the USEPA (Dufour 1984; USEPA 2012). *E. coli* is found in high concentration in the intestines of humans and other warm-blooded animals, and therefore, serves as a proxy to determine the level of fecal pollution in water. It best satisfies the fecal indicator organism criteria and thus is currently regarded as the "gold standard" in assessing microbial safety of water (Bridle, 2014).

Ultraviolet Disinfection

Since the discovery of toxic by-products formed through chlorination, advanced disinfection techniques have become more popular. In particular, ultraviolet (UV) disinfection has been increasingly used in recent years, as it is a physical disinfectant that does not result in the formation of any by-products. Exposure to UV-C light (254 nm) damages DNA by causing strand breaks and/or forming pyrimidine dimers. These dimers form kinks in the helical structure of DNA that result in inhibition of transcription and DNA replication.

Methods of Quantification

The efficiency of any disinfection technique is generally monitored by measuring the concentration of indicator bacteria, such as *E. coli*, using traditional culture-based methods. There are numerous conventional methods available including, but not limited

to: multiple tube fermentation (MTF), membrane filtration technique, and IDEXX Colilert. The IDEXX Colilert technique is an approved method for culturing. Samples for Colilert, as well as other traditional methods, need to be incubated for 18 – 24 hours. Beach water quality is very weather-dependent and can often change quite significantly with time, and thus this is a significant limitation of the culture-based methods.

More recently, rapid culture-independent molecular techniques have been explored and applied for detecting waterborne microorganisms of concern. Rather than culturing the bacteria, these methods detect threats based on DNA found in the samples. The polymerase chain reaction (PCR) is a common molecular technique for DNA. In this reaction, a target DNA sequence is amplified in cycles with three steps: (1) denaturation, (2) annealing and (3) extension. The first step causes the double-stranded DNA to uncoil and become single-stranded, ready to be copied. In the second step, specific primers (forward and reverse) anneal to the DNA strands and provide a starting point for the DNA polymerase enzyme. Finally, the enzyme carries out polymerization by attaching complementary deoxyribonucleotide triphosphates (dNTP) to the growing synthesized DNA strand.

Real-time quantitative PCR (qPCR) follows the same principles as regular PCR, but measures the amplification of PCR products by using fluorescent dyes. SYBR green, TaqMan probes, and molecular beacons are commonly used fluorescent systems for qPCR. Many qPCR protocols have been developed for the detection of waterborne microorganisms of concern, including one by the USEPA (Chern, 2011; Aslan, 2015). However, the majority of these protocols have not been developed with quantification of disinfection efficiency in mind. Whether chemical or physical disinfectants are used, they

alter the cell in different ways and the molecular detection methods developed thus far do not account for the discrepancies. Researchers have developed modified protocols, using additional steps, chemical reagents and dyes to minimize false-positive and false-negative qPCR results. Though qPCR-based techniques are much faster than conventional culturing methods, they still require some developments, especially for UV radiation. There is currently no consensus on a qPCR-based technique for quantifying UV disinfection efficiencies.

Thesis Objectives

The main objective of this thesis was to address the issue of microbial contamination of recreational water using UV light as a disinfectant. In order to determine the efficacy of UV as a treatment option, both culture-based and qPCR-based methods will be used. The aim was to determine a correlation between the two techniques and determine if the rapid nucleic acid technique can be used as a surrogate for the more time-consuming traditional method.

The objective of Chapter 2 was to develop a reliable qPCR-based method that can quantify UV inactivation of *E. coli*. A review of relevant literature was conducted to determine the deficiencies in applying qPCR to UV-exposed samples. In order to quantify disinfection efficiency, the first objective was to identify the criteria for suitable gene targets and then use the *E. coli* genome to determine targets for qPCR. Primers were designed and tested for the selected targets, and standard curves were developed and evaluated. The next objective was to determine the effect of UV light on *E. coli*. This

study compared the culture-based and qPCR-based methods, short-amplicon (SA) and long-amplicon (LA) qPCR, and LA-qPCR of seventeen selected gene targets. Then correlations were tested for LA-qPCR versus IDEXX Colilert. The final aim was to suggest suitable target(s) that can be applied for quantifying UV disinfection with qPCR.

In Chapter 3, the primary aim was to evaluate the efficacy of UV treatment for managing microbial beach contamination using qPCR. The focus was specifically on fecal contamination of recreational waters caused primarily by CSO and SSO. For this study, simulated CSO (sCSO) samples were generated using wastewater. Since Ontario requires primary level treatment on CSO, primary-treated sCSO were also generated. The UV disinfection kinetics of the samples was first examined. Comparisons were made between inactivation rates of pure *E. coli*, untreated and primary-treated sCSO. Then, the disinfection efficiency was quantified using culture-based and qPCR methods. Correlations were developed between the two methods, and the applicability of the developed qPCR was discussed.

Finally, Chapter 4 summarizes the main conclusions from this investigation and provides future research recommendations based on the findings of this thesis.

References

Aslan, A., Kinzelman, J., Dreelin, E., Anan'eva, T., & Lavendar, J. (2015). A guidance document for testing recreational waters using USEPA qPCR method C.

Bridle, H. (2014). Waterborne Pathogens: Detection Methods and Applications, first ed. Amsterdam: Academic Press.

Chern, E., Siefring, S., Paar, J., Doolittle, M., & Haugland, R. (2011). Comparison of quantitative PCR assays for Escherichia coli targeting ribosomal RNA and single copy genes. Letters in Applied Microbiology, 52, 298-306. doi:10.1111/j.1472-765X.2010.03001.x

DeFlorio-Barker, S., Wing, C., Jones, R., & Dorevitch, S. (2018). Estimate of incidence and cost of recreational waterborne illness on United States surface waters. Environmental Health, 17(3). doi:10.1186/s12940-017-0347-9

Dufour A. (1984) Health Effects Criteria for Fresh Recreational Waters. Toxicology and Microbiology Division, U.S. Environmental Protection Agency Report EPA- 600-1-84-2004. , Cincinnati, OH

Eramo, A., Morales Medina, W., & Fahrenfeld, N. (2017). Peracetic acid disinfection kinetics for combined sewer overflows: indicator organisms, antibiotic resistance genes, and microbial community. Environmental Science Water Research & Technology. doi:10.1039/c7ew00184c

European Union. (2006). Bathing water quality directive. Official Journal of the European Union.

Health Canada. (2012). Guidelines for Canadian Recreational Water Quality. Ottawa.

McLellan, S., Hollis, E., Depas, M., Van Dyke, M., Harris, J., & Scopel, C. (2007). Distribution and fate of Escherichia coli in Lake Michigan following contamination with urban stormwater and combined sewer overflows. Journal of Great Lakes Research, 33, 566-580.

Ministry of Environment, Conservation and Parks. (2016, October 11). Ontario's Great Lakes strategy. Retrieved from https://www.ontario.ca/page/ontarios-great-lakes-strategy

Ministry of the Environment, Conservation and Parks. (2015, February 18). Protecting the Great Lakes. Retrieved from https://www.ontario.ca/page/protecting-great-lakes

Pandey, P., Kass, P., Soupir, M., Biswas, S., & Singh, V. (2014). Contamination of water resources by pathogenic bacteria. AMB Express, 4(51). Retrieved from http://www.amb-express.com/content/4/1/51

Templar, H., Dila, D., Bootsma, M., Corsi, S., & McLellan, S. (2016). Quantification of human-associated fecal indicators reveal sewage from urban watersheds as a source of pollution to Lake Michigan. Water Research, 100, 556-567. doi:10.1016/j.watres.2016.05.056

Tondera, K., Klaer, K., Gebhardt, J., Wingender, J., Koch, C., Horstkott, M., . . . Pinnekamp, J. (2015). Reducing pathogens in combined sewer overflows using ozonation or UV irradiation. International Journal of Hygiene and Environmental Health, 218, 731-741. doi:10.1016/j.ijheh.2015.09.002

Tondera, K., Klaer, K., Koch, C., Hamza, I. A., & Pinnekamp, J. (2016). Reducing pathogens in combined sewer overflows using performic acid. International Journal of Hygiene and Environmental Health, 219, 700-708. doi:10.1016/j.ijheh.2016.04.009

USEPA. (2012). Summaries of water pollution reporting categories. Retrieved from https://watersgeo.epa.gov/ATTAINS/34PARENTATTAINSDESCRIPTIONS.pdf

USEPA. (n.d.). Facts and figures about the Great Lakes. Retrieved from https://www.epa.gov/greatlakes/facts-and-figures-about-great-lakes

WHO. (2003). Guidelines for safe recreational water environments. Volume 1, Coastal and fresh waters. Geneva.

CHAPTER 2:

DEVELOPMENT OF ROBUST QPCR METHOD FOR QUANTIFYING UV INACTIVATION OF *E. COLI*

Introduction

In recent years, more attention has been given to ultraviolet (UV) disinfection for water treatment. Compared to chemical disinfectants such as chlorine and ozone, it has a greater germicidal efficiency and does not produce any disinfection by-products. UV light is a physical disinfectant and its mechanism differs from that of chemical disinfectants. Specifically, UV-C ($200\ nm < \lambda < 280\ nm$) is a well-known mutagen at a molecular genetic level. Where chlorine and ozone oxidize the bacterial cell membrane causing it to rupture, UV disinfection generally maintains cellular integrity. UV-C light targets DNA, forming pyrimidine dimers in the helical structure that cause DNA to lose its functionality.

The evaluation of disinfection efficiency is commonly performed by applying standard microbiological methods which rely on culturing of *E. coli*. The culture-based methods for enumeration of *E. coli* have several limitations including the long incubation period required. For this reason, rapid molecular techniques have been proposed as alternatives to the traditional methods. One such technique is real-time quantitative polymerase chain reaction (qPCR) which amplifies and quantifies a specific region of the genome of a target organism. qPCR offers several advantages over the culture-based methods. It is able to provide quantitative results within a few hours and has a greater quantification range. Additionally, it is able to examined any microbe of interest. The

technique is promising enough for the USEPA to issue a draft method which uses qPCR for *E. coli* detection in recreational waters (Aslan et al., 2015).

To evaluate the performance of disinfection technologies, it is crucial to select an appropriate and reliable method. Currently, there are deficiencies that need to be filled before qPCR can be applied for quantifying UV disinfection efficiency. Firstly, UV light causes DNA damage at random points across the genome. When a small region of a gene is targeted in qPCR, it is not a good representation of the damage occurring over the entire genome and it may seem as though there is no damage. Whether quantifying bacteria, viruses or other organisms, amplification of short DNA fragments (less than 200-bp) is easier, efficient, and is currently commonly used for such applications (Nocker et al., 2007; Süß et al., 2009; Banihashemi et al., 2012; Zhang et al., 2015; Ho et al., 2016; Leifels et al., 2016; Kibbee & Ormeci, 2017; Xu et al., 2017). Banihashemi et al. (2012) used one short- and one long-amplicon for detecting DNA damage after a single UV dose to pure bacterial cultures, and found the long-amplicon was able to detect more damage. Their limited study has shown the potential for long amplicon qPCR (LA-qPCR), but the 1000-bp amplicons used in their work may not be ideal. Ho et al. (2016) have argued that increasing amplicon length beyond 500-bp was not suitable. As amplicon length increases beyond this size, longer elongation times are required during qPCR amplification, which result in the formation of unspecific products. Furthermore, LA-qPCR tends to have a lower amplification efficiency which is a sign of a poor qPCR method. Ho et al. (2016) have suggested 500-bp to be a good compromise between the limited information gained from short amplicons and the issues that arise from very long amplicons. However, to date, there has been no work done using the suggested 500-bp

amplicon length for UV disinfection, nor have any correlations been made between 500-bp qPCR and conventional culturing techniques.

The structure of DNA allows it to persist in the environment even after cell death. DNA-based qPCR methods quantify all DNA present in a sample, and cannot distinguish between live or dead cells. For enumeration, majority of cells are assumed to be living so this does not pose a concern. Thus, emphasis is put on selecting qPCR gene targets that are present in high concentration and specific to the bacteria of interest (i.e., *E. coli*). For quantifying disinfection, it is important to determine cell viability. Propidium monoazide (PMA), a photo-activated DNA intercalating dye, can be used to correct for false signal from membrane-compromised cells; thus, leaving only the signal from living cells. However, UV radiation does not damage the membrane, so contribution from dead cells cannot be eliminated by PMA. UV light damages DNA directly, preventing DNA replication. However, if the gene target chosen is not essential for cell functioning, damage to that gene may not be reflective of the efficacy of disinfection. Currently, gene targets are not chosen based on importance to cell functioning. For example, rRNA genes are common PCR targets due to their high copy numbers and specificity to bacteria. Yet for determining disinfection efficiency, rRNA genes do not provide insight on essential functioning of the cell. For UV treatment, three gene target categories that better indicate cell viability were chosen in this study: UV repair, cell division, and metabolism. UV repair genes were chosen because damage to them would prevent the cell from repairing itself. Bacterial UV repair pathways were examined for determining target UV repair genes (Reuven et al., 1999; Goosen & Moolenaar, 2008; Janion, 2008). Next, cell division genes were chosen because damage to them would prevent the cell from

multiplying and increasing in number. The bacterial cell division pathway outlined in Ouellette et al. (2015) was used to identify key cell division genes. Lastly, metabolic genes were chosen to give insight on the cell's overall health and its ability to maintain itself. The *E. coli* core metabolism map from the BiGG Model was used to identify important intersections that, if damaged, would reduce the production of essential metabolic precursors (Noor et al., 2010). To provide a comparison, rRNA genes which are commonly used were chosen as well.

Based on review of relevant literature, there is limited information available and no consensus on a reliable qPCR method for quantifying the efficacy of UV disinfection. The first objective of this study was to identify suitable gene targets that serve important functions. The second objective was to design and test primers, aiming for a 500-bp amplicon length. Consequently, standard curves for each primer set were evaluated for acceptable amplification efficiency and goodness of fit. The next objective was to determine the effect of UV on a pure *E. coli* culture by exposing it to UV in collimated beam experiments and calculating the efficiency of treatment through both a culturing technique and qPCR. This work also compared short and long amplicon qPCR results, and compared the newly selected target to the commonly used rRNA and *uidA*. Subsequently, correlations were developed for the LA-qPCR and culturing methods. The final goal was to suggest one or multiple gene target(s) that can be applied for quantifying UV disinfection with qPCR.

Materials and Methods

Gene Target Selection Process

Gene targets were selected from three categories that would give insight on cell viability post-UV exposure. First, UV repair genes were chosen because damage to them would prevent the cell from repairing itself. Bacterial UV repair pathways were examined for determining target UV repair genes (Reuven et al., 1999; Goosen & Moolenaar, 2008; Janion, 2008). Next, cell division genes were chosen because damage to them would prevent the cell from multiplying and increasing in number. The bacterial cell division pathway outlined in Ouellette et al. (2015) was used to identify key cell division genes. Lastly, metabolic genes were chosen to give insight on the cell's overall health and its ability to maintain itself. The *E. coli* core metabolism map from the BiGG Model was used to identify important intersections that, if damaged, would reduce the production of essential metabolic precursors (Noor et al., 2010).

To provide a comparison, rRNA genes which are commonly used were chosen as well. These genes not only help identify a bacterial species, but their products are essential for translation of RNA and the production of various proteins.

Primer Design

Primers were designed using Geneious 10.1 software. The sequences for target genes found in various *E. coli* strains were downloaded from the NCBI database. *E. coli* sequences were aligned with those of other common bacteria of concern and bacteria closely related to *E. coli* (i.e., Salmonella, Shigella, Citrobacter, Klebsiella, Enterobacter,

etc.). Primers were designed for regions specific to *E. coli*. Forward and reverse primer pairs met the following requirements:

- 20 bp in length
- 40 – 60% GC content
- Primer pair ΔT_m less than 2°C
- Avoid dinucleotide repeats
- Avoid regions of secondary structures (i.e., hairpins, self-dimers, primer-dimers)
- 3' should end with C/G, or at least 2C/G in the last 5 bp
- $T_m \approx 60°C$
- 410 – 530 bp amplicon length

For comparison, two short amplicon primer pairs were chosen: 23S (EC23S857 F- and R-primers from Chern et al., 2011) and *uidAS* (Shahraki, unpub. data).

Testing Primers

Chosen primers (Table 1) were first tested on the NCBI BLAST database to determine overlaps with other microorganisms. Subsequently, all primers were tested using PCR and gel electrophoresis. PCR was conducted with a 25-µL reaction volume, containing: 16.4 µL nuclease-free water, 2.5 µL 10x Taq buffer, 3.5 µL 20-mM $MgSO_4$, 0.5 µL of each 10-mM F- and R-primer, 0.1 µL Taq polymerase, and 1 µL *E. coli* genomic DNA template. A negative control (nuclease-free water) was included. All reactions were conducted in duplicates. The program started with an initial incubation at 95°C for 1 minute, followed by thirty-five cycles of 95°C for 15s, 60°C for 15s, and 72°C for 40s. The last step included one cycle of 72°C for 7 min to complete elongation.

PCR products were then run on a 2% agarose gel. The product size was measured against the DNA ladder to confirm that the designed primers only produced a single product and all products were the expected length.

E. coli Culture

E. coli ATCC® 8739™ cells were obtained in six 300-µL glycerol stock vials. A single vial was added to 20 mL sterile nutrient broth (Becton Dickinson) and incubated at 37°C for 20 hours. Sterile nutrient broth agar plates were prepared with 1.5% agar. Cultured cells were streaked on the plates to separate colonies. A single isolated colony from the agar plates was inoculated in 40 mL sterile nutrient broth and incubated for 16 – 24 hours at 37°C. The culture was then centrifuged for 20 min at 4,000 rpm. The nutrient broth supernatant was disposed and the settled cells were re-suspended in 20 mL sterile phosphate-buffered saline (PBS). Cell concentration was estimated using UV-vis spectrophotometry according to section 4.3.2. of the USEPA Draft Method C (Aslan et al., 2015). For developing standard curves, *E. coli* cells were serially diluted and aliquots in triplicate were frozen at -20°C until extraction. For UV exposure experiments, *E. coli* cells were diluted in 1 L sterile PBS to approximately 7-log cells per mL.

UV Exposure Experiments

UV exposure experiments were conducted with a low-pressure collimated beam apparatus (Trojan Technologies, Canada) according to manufacturer's standardized protocols. Intensity measured at the sample surface with the IL1700 radiometer (Trojan Technologies, Canada). For each sample, 53-mL *E. coli* suspension was filled in clear glass petri dish with a stir bar. 3 mL was taken out for UVT readings using Real Tech Water's UV254 portable meter with split sense technology. Based on the UVT readings,

an excel sheet was used to calculate the time required for the desired dose. Each dose was done in triplicate. Calculations for the dose accounted for the petri, divergence, and reflection factors as per Bolton & Linden (2003).

After exposure, each sample was split into aliquots for DNA extraction and for culturing. Six 1.75-mL aliquots were frozen at -20°C for extraction, and the remaining sample was used for culturing.

Culture-dependent Method

IDEXX Colilert Quanti-Tray®/2000 was used as the culture-based method in this study. It is able to detect both total coliform and *E. coli* up to 2,419 MPN/100mL. Each sample, UV-exposed and non-exposed, was serially diluted with sterile PBS to a concentration that would be within the range of this method.

DNA Extraction

Frozen 1.75-mL samples were thawed at room temperature and centrifuged at 10,000 rpm for 15 min. The supernatant was taken out and 400 µL sterile PBS was added. For each sample, 500 µL 1-mm sterile glass beads and 400 µL sucrose lysis buffer were added. Sucrose lysis buffer was made according to Shahraki et al. (2018). After adding lysis buffer, samples were subjected to bead-beating using the Mini-beadbeater-16 (Lab Services BV, Nederland) for 40s three times at an intensity of 3,450 oscillations/min. 100 µL 1% SDS and 50 µL 20 mg/mL lysozyme (Sigma-Aldrich, USA) were added to each tube. Samples were then incubated at 37°C on a shaker overnight. The next day, 2 µL of 20 mg/mL proteinase K (Thermo Scientific, USA) was added, and samples were again kept in the incubator at 37°C on a shaker overnight. Finally, the next morning, proteinase K was deactivated in a 95°C water bath for 10 min. The digest from

Table 1: *E. coli* primers chosen for qPCR

Category	Gene	Forward (5' -> 3' on + strand)	Reverse (5' -> 3' on - strand)	Product (bp)	T_m
rRNA	*rrsA*	CGGGGAGGAAGGGAGTAAAG	CGGTCGACTTAACGCGTTAG	440	60
	rrlA	GTGAGCTCGATGAGTAGGGC	CCTTGCCGAAACAGTGCTCT	519	60
UV repair	*uvrB*	TATGGTCTGGGCGATCCTGA	AACAGTAGCCCAGCTCGTTC	475	60
	umuC	TAAGCTTGCCAATCATGCGG	ATTGAGCGCAAATGGTGACG	460	60
Cell division	*ftsZ*	TTGGGTATCCTGACCGTTGC	TTGTCGGAAGCAAATGCACG	500	60
	ftsQ	CTCTGAACACGCGAAACAGC	CCCTGCAACACTTCATTGGC	505	60
Metabolic	*gltA*	TACGGTCCATAGCACGTTCC	CAGCTGGCGACCGATTCTAA	440	60
	ptsG	TGCGGGTAAACTGTCTGGTG	CCAAATGCAGCAACCAGAGC	492	60
	pgl	GACACAGGTTGTCGATGTGC	CCCAGACATCCACTGAGCTG	527	60
	tktA	GATGTCGCGAATAACGTGCC	GGTTACGATCTGCCGATGGA	410	60
	fbaA	CCGATTTTGGACATGCGCTC	AAACAACTTCGCACTGCCAG	426	60
	tpiA	GTTTACAGAGCCGCCGTACT	GCAAAACGTGGACCTGAACC	454	60
	ppsA	GTAACCCTGGTGCACACGAT	TTCCGGAATGGGTGTTTCCG	430	60
	pck	GTGGGCAGACAAAGGCAAAG	CCGAAGAACACCGCAACATC	495	60
	dfp	TGAGCTGGGTAAATGGGCTG	TGATACCAGCGTGACGTTCG	478	60
	*uidAL**	ATAACGGTTCAGGCACAGCA	TAATGGACTGGATTGGGGCC	455	60
	gadA	CAATCATGCGTTTCGGGTCC	CACGAAATGCGCGATGATGT	484	60
Short amplicon	*23S*	GGTAGAGCACTGTTTtGGCA**	TGTCTCCCGTGATAACtTTCTC**	88	60
	*uidAS**	GTAATGTTCTGCGACGCTCA	AATAACGGTTCAGGCACAGC	70	60

*L is used to denote the long amplicon primers of the *uidA* gene, and S for short amplicon

**Lower case nucleotide denotes deliberate mismatch basepair

each tube was plated in a 96-well extraction plate, and DNA was extracted by magnetic bead robotic extraction according to Shahraki et al. (2018). Extracts were kept in the freezer at -20°C until qPCR analysis.

qPCR

First, qPCR was used to create standard curves for each primer, developing a relationship between C_T and the log cell numbers. Afterwards, DNA extracts from the UV exposure experiments were used with each primer set. Due to the large number of samples and primer pairs, 384-well qPCR plates were utilized with a 9-µL reaction volume. To prepare the 384-well plate, four 96-well plates were prepared with 12-µL reactions containing: 4.4 µL nuclease-free water, 6 µL 2x PowerUp™ SYBR® Green Master Mix (Applied Biosystems), 0.3 µL of each 10-mM F- and R-primers, and 1 µL DNA template. Then 9 µL was transferred from the four 96-well plates into a single 384-well plate. The QuantStudio™ 12K Flex System (ThermoFisher Scientific) ran the following program: initial step at 95°C for 20s, followed by forty cycles of 95°C for 10s and 60°C for 20s. All results were exported into Microsoft Excel files for analysis.

Results and Discussion

Selected Gene Targets

The first objective of this study was to identify appropriate gene targets for quantifying UV damage to *E. coli* cells. Three major gene function categories were chosen, representative of the cell function and viability: UV repair, cell division, and metabolism. Within each category, the goal was to choose a gene target that, if damaged,

would disrupt cellular function. For comparison, commonly used rRNA genes were also included.

UV repair genes were selected because repair of UV damage would defeat the purpose of disinfection. Goosen & Moolenaar (2008) present an overview of different UV damage repair enzymes found in bacterial cells. Exposure to UV light induces an SOS-response in *E. coli*, and nucleotide excision repair (NER) is an important mechanism to remove DNA damage caused by UV light, environmental carcinogens, or other compounds that cause DNA structure damage. The *uvrA*, *uvrB*, and *uvrC* proteins play an important role in NER and any mutations in these proteins have resulted in UV sensitivity in *E. coli* (Goosen & Moolenaar, 2008). Of the three, *uvrB* plays an essential role, as it is needed to interact with both *uvrA* and *uvrC* in the NER reactions. Therefore, the *uvrB* gene was selected as one of the UV repair genes of interest, as damage to it would disrupt the cell's ability to repair through NER.

The SOS-response to UV light can also lead to SOS mutagenesis, creating a DNA polymerase that is capable of translesion replication (Reuven et al., 1999). The mutagenic gene *umuC* is activated by several other genes and is an important active agent for replicating across DNA lesions (Woodgate et al., 1989; Janion, 2008). Thus, *umuC* was chosen as the second UV repair gene of interest. It is representative of the cell's last resort for error-prone repair.

Cell division was chosen as the second category because damage would prevent an increase in bacterial concentration. Ouellette et al. (2015) present the cell division pathway for bacterial cells based on an *E. coli* model. The process of cell division begins

with the recruitment of the *ftsZ* protein to the division site. The *ftsZ* gene encodes for an "early" division protein; therefore, it was selected as it can prevent initiation of cell division. Buddelmeijer & Beckwith (2004) mention three membrane proteins required for cell division of *E. coli*, and the most crucial of the three is *ftsQ* as the other two are dependent on it. For this reason, *ftsQ* was chosen as the second cell division target, and also represents a "late" cell division protein.

Lastly, the health and viability of a cell is reflected by its cellular metabolism. Certain metabolites serve as precursors for downstream building blocks for the cell. Noor et al. (2010) list twelve precursor metabolites needed for biomass gain in *E. coli*. These precursors eventually produce amino acids, glycogen, nucleotides, etc. When choosing gene targets for metabolic pathways, the goal was to select those which would reduce the production of these precursor metabolites. Selected metabolic targets and the reasoning behind their selection is presented in Table 2. A map of the targets, including the precursor metabolites is presented in Figure 1. Collectively, the selected genes prevent the production of nine precursor metabolites. Certain genes that were chosen are not related to precursor metabolites; however, they serve another metabolic function. For example, presence of *gadA* helps *E. coli* survive extreme acidic conditions such as the low pH of a host's stomach.

16S and 23S were chosen as the rRNA gene targets. Both targets are commonly used for other molecular techniques such as next-generation sequencing (NGS) and provide a comparison for the other genes. *rrsA* is one of seven 16S rRNA genes and a component of the 30S small subunit ribosome. *rrlA* is one of seven 23S rRNA genes and

Table 2: Selected metabolic genes and their reasoning

Gene	Reasoning
gltA	Encodes for citrate synthase Catalyzes the first reaction of the tricarboxylic acid (TCA) cycle TCA cycle is responsible for majority of the electron transfer which create energy (ATP) for a cell
ptsG	Encodes for component of glucose-specific phosphotransferase system (PTS) Transports glucose into the cell, which is later phosphorylated into glucose 6-phosphate (G6P) G6P is an essential precursor metabolite
pgl	Encodes for 6-phosphogluconolactonase, an intermediate enzyme in the conversion of glucose into ribose 5-phosphate
tktA	Encodes for transketolase I (responsible for majority of transketolase activity compared to transketolase II) Catalyzes the reversible reaction between two precursor metabolites: glyceraldehyde 3-phosphate (G3P), ribose 5-phosphate
fbaA	Encodes for fructose-bisphosphate aldolase class II Catalyzes the reversible reaction during glycolysis and gluconeogenesis, forming or breaking down glyceraldehyde 3-phosphate (G3P)
tpiA	Encodes for triose-phosphate isomerase Catalyzes the isomerization between glyceraldehyde 3-phosphate (G3P) and dihydroxyacetone phosphate (DHAP) G3P is an essential precursor metabolite
ppsA	Encodes for phosphoenolpyruvate (PEP) synthase Synthesizes PEP from pyruvate and water PEP is an essential precursor metabolite
pck	Encodes for phosphoenolpyruvate (PEP) carboxykinase Synthesizes PEP from oxaloacetate PEP is an essential precursor metabolites
dfp	Encodes for a bi-functional protein that catalyzes two sequential reaction to synthesize coenzyme A Coenzyme A is needed to form acetyl-coA and succinyl-coA, two of the twelve essential precursor metabolites
uidA	Encodes for β-glucuronidase Used commonly as a qPCR target for *E. coli* Used in this study as a reference to current practice
gadA	Encodes for glutamate decarboxylase α Helps to maintain pH when exposed to extreme acidic conditions (i.e., human stomach)

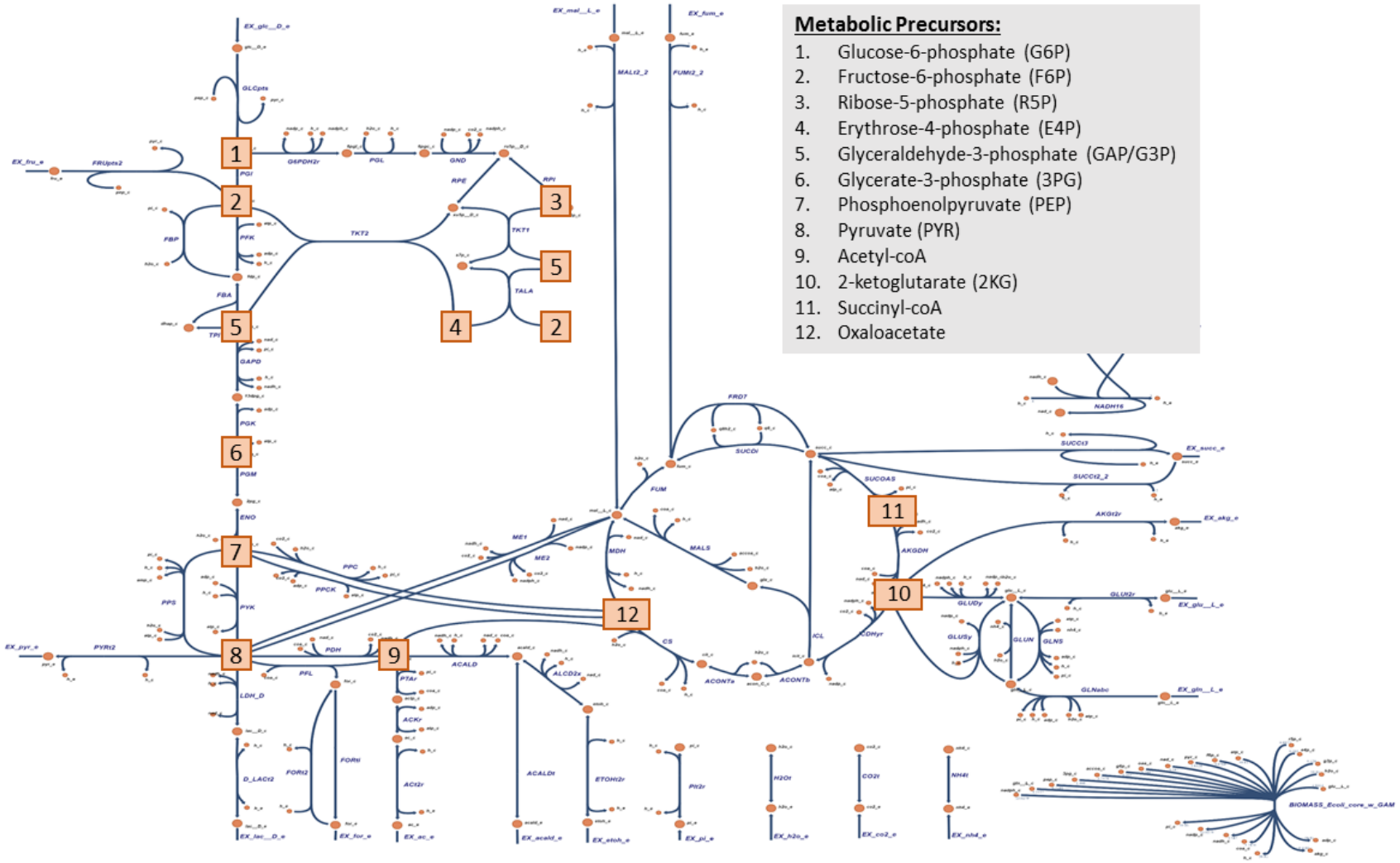

Figure 1: Map of Core Metabolism of *E. coli*. Original map obtained from the BiGG Model, http://bigg.ucsd.edu/models/e_coli_core

a component of the 50S large subunit ribosome. Problems with the ribosomal structure would eventually lead to arrested translation, as ribosomes are basically protein-synthesizing machines.

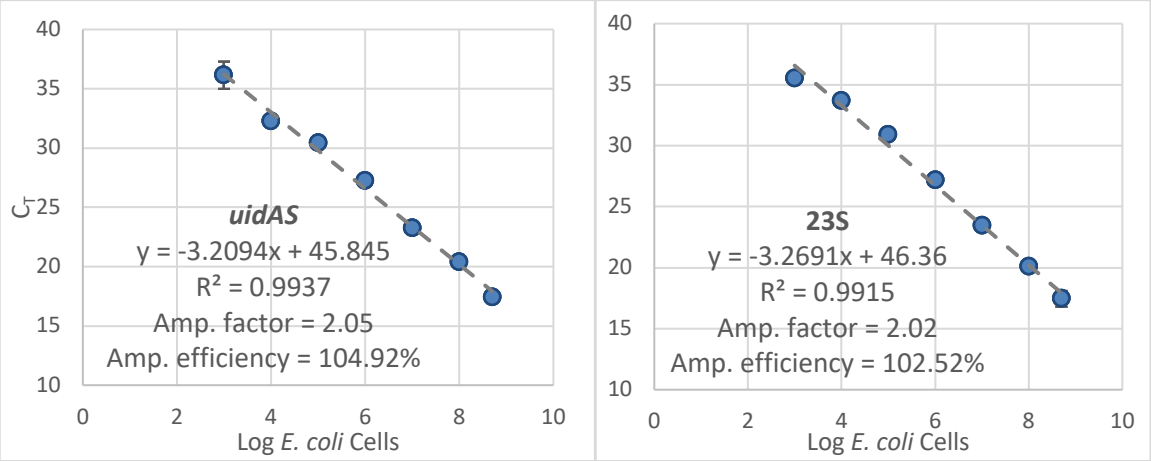

Figure 2: Standard curves for qPCR for two short amplicon gene targets. The no template control (NTC) had an undetermined C_T. Cell counts less than 1,000 also had an undetermined C_T value, and are not plotted. Error bars represent standard deviation between replicates. Some error bars are smaller than the markers.

Standard Curves

Standard curves were developed for each primer set. Determining qPCR efficiency based on the standard curves is very important for determining the performance of qPCR, as poorly optimized assays will have poor sensitivity and specificity. An optimized qPCR assay is described as one that is linear ($R^2 > 0.98$), efficient (amplification efficiency 90 – 105%), and consistent across replicates. All of these factors were checked in this study before the primers were applied for UV exposure experiments.

As the amplicon length increases, the efficiency of qPCR will decrease. Ho et al. (2016) reported amplification efficiencies dropped 20% when amplicon size was increased from 250-bp to 456-bp. In this study, the amplification efficiencies of the two

short-amplicon targets, *uidAS* and 23S, were 104.92% and 102.52%, respectively (Figure 2). These targets both fall within the acceptable range of 90 – 105%. Efficiencies greater than 100% are a result of polymerase inhibition caused by excessive amounts of DNA or carry-over contamination (i.e., proteinase K, ethanol, SDS). Presence of inhibitors

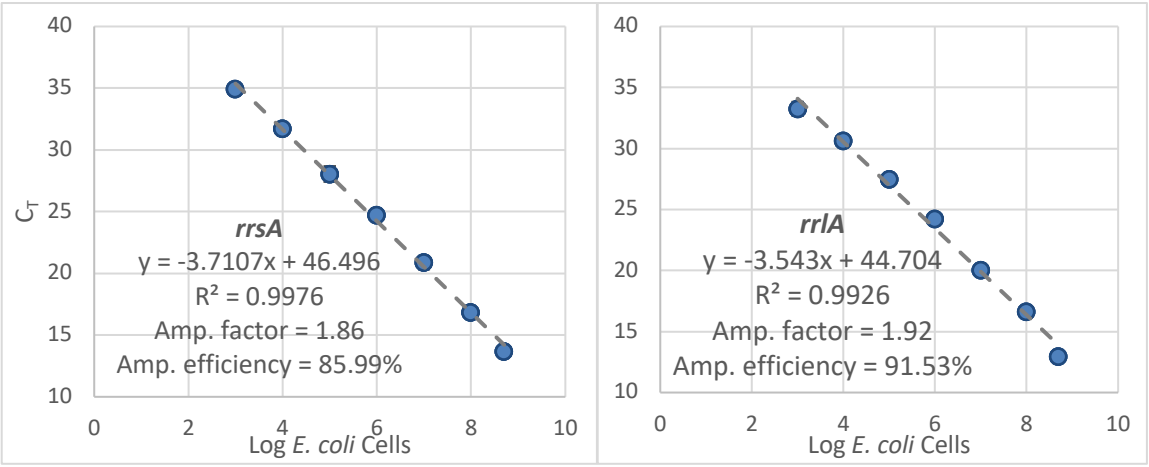

Figure 3: Standard curves for qPCR for two rRNA gene targets. The NTC had an undetermined C_T. Error bars represent standard deviation between replicates. Some error bars are smaller than the markers.

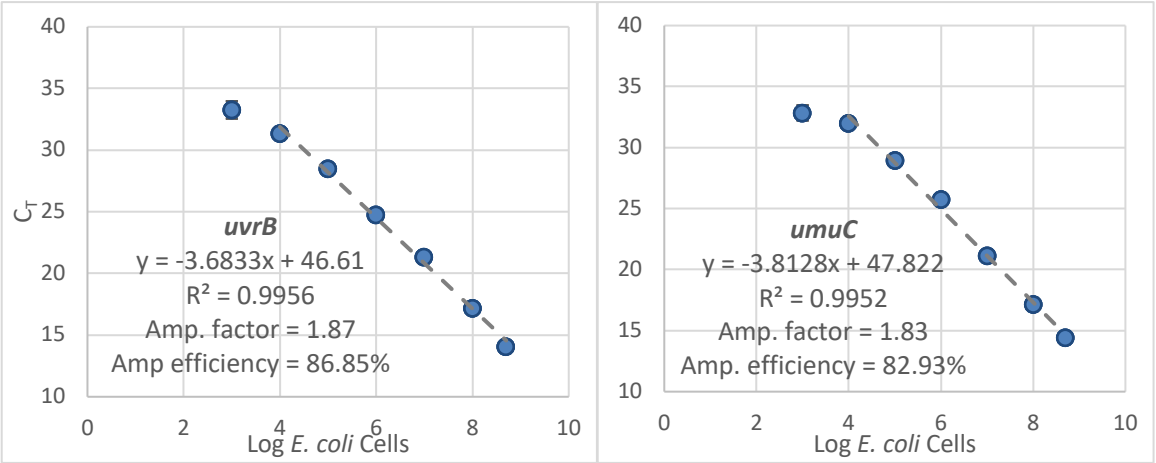

Figure 4: Standard curves for qPCR for two UV repair gene targets. The NTC had an undetermined C_T. The highest point is neglected from the linear regression. Error bars represent standard deviation between replicates. Some error bars are smaller than the markers.

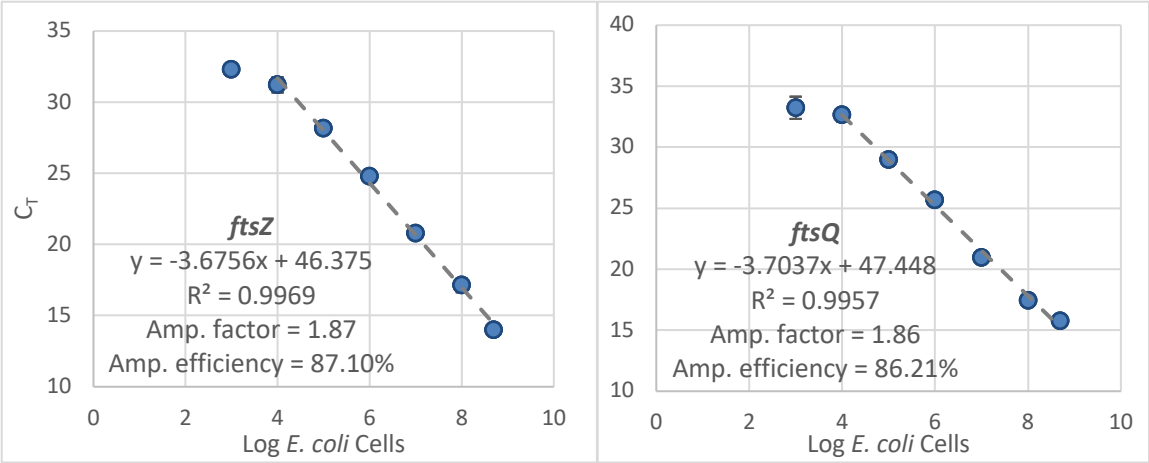

Figure 5: Standard curves for qPCR for two cell division gene targets. The NTC had an undetermined C_T. The highest point is neglected from the linear regression. Error bars represent standard deviation between replicates. Some error bars are smaller than the markers.

increases the C_T value, causing a shallower slope which in turn results in an amplification efficiency greater than 100%.

Figures 3 – 6 show the standard curves for all the targets selected. The first criteria for an optimized qPCR assay was met by all targets, with each target having an r-squared value greater than 0.99. Most targets had a linear relationship down to 4-log cells; however, some targets were more sensitive and continued to be linear until 3-log cells. Anything less than 1,000 cells had an undetermined C_T value and was not plotted.

The second condition for the qPCR assays was to have an amplification efficiency between 90 – 105%. This criterion is primarily set for short amplicons. Work done with longer amplicons is expected to have lower efficiencies and therefore the range can be expanded. For long amplicons, if the amplification efficiency is found to be greater than 80%, the primers may be used considering the remaining criteria for an optimized assay are met (Ho et al., 2016). The long-amplicon primer sets designed in this study all had

amplification efficiencies greater than 80%. Targets with the greatest efficiencies were the metabolic genes *uidAL*, *gadA*, and *ppsA* with 100.89%, 97.64% and 97.44%, respectively.

While checking the amplification factors and efficiencies, the melt curves should also be taken into account. In this qPCR assay, SYBR Green was used as the fluorescent reporter. SYBR Green is a DNA-intercalating dye that binds to double-stranded DNA during the PCR process and emits a fluorescent signal that is quantified by the instrument. This dye is unspecific to the product, as it binds to any double stranded DNA product. Therefore, the melt curves should be assessed to ensure that a single product was formed and that the C_T values are not skewed by additional PCR products. The melt curves for each primer set designed in this study was examined to ensure that there was only a single melting temperature (Appendix A).

The last measure of a good qPCR assay was consistency between replicates. As shown by the standard deviation error bars in the graphs, the replicates produced similar results.

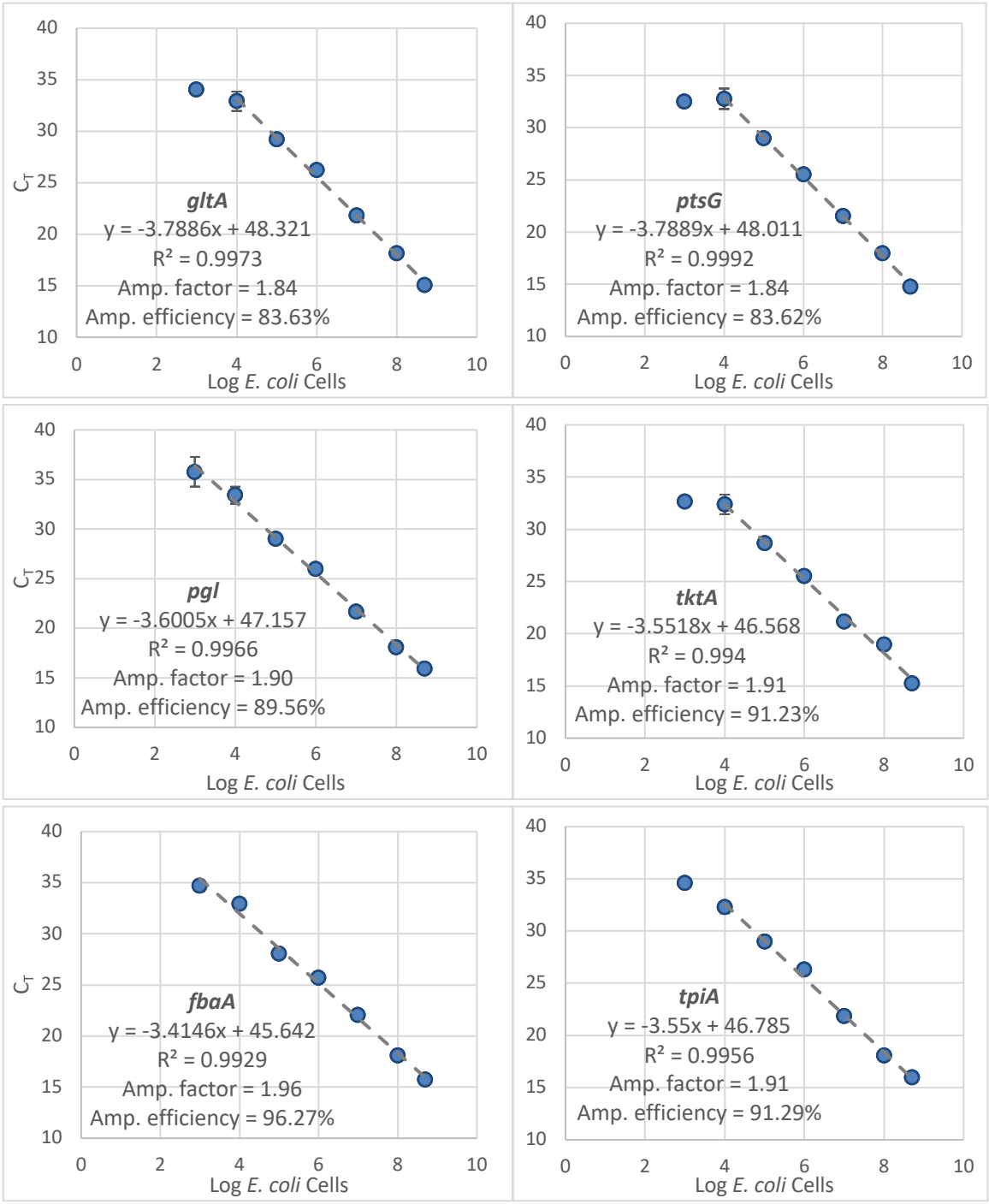
gltA
y = -3.7886x + 48.321
R² = 0.9973
Amp. factor = 1.84
Amp. efficiency = 83.63%
ptsG
y = -3.7889x + 48.011
R² = 0.9992
Amp. factor = 1.84
Amp. efficiency = 83.62%
pgl
y = -3.6005x + 47.157
R² = 0.9966
Amp. factor = 1.90
Amp. efficiency = 89.56%
tktA
y = -3.5518x + 46.568
R² = 0.994
Amp. factor = 1.91
Amp. efficiency = 91.23%
fbaA
y = -3.4146x + 45.642
R² = 0.9929
Amp. factor = 1.96
Amp. efficiency = 96.27%
tpiA
y = -3.55x + 46.785
R² = 0.9956
Amp. factor = 1.91
Amp. efficiency = 91.29%
C_T
Log E. coli Cells

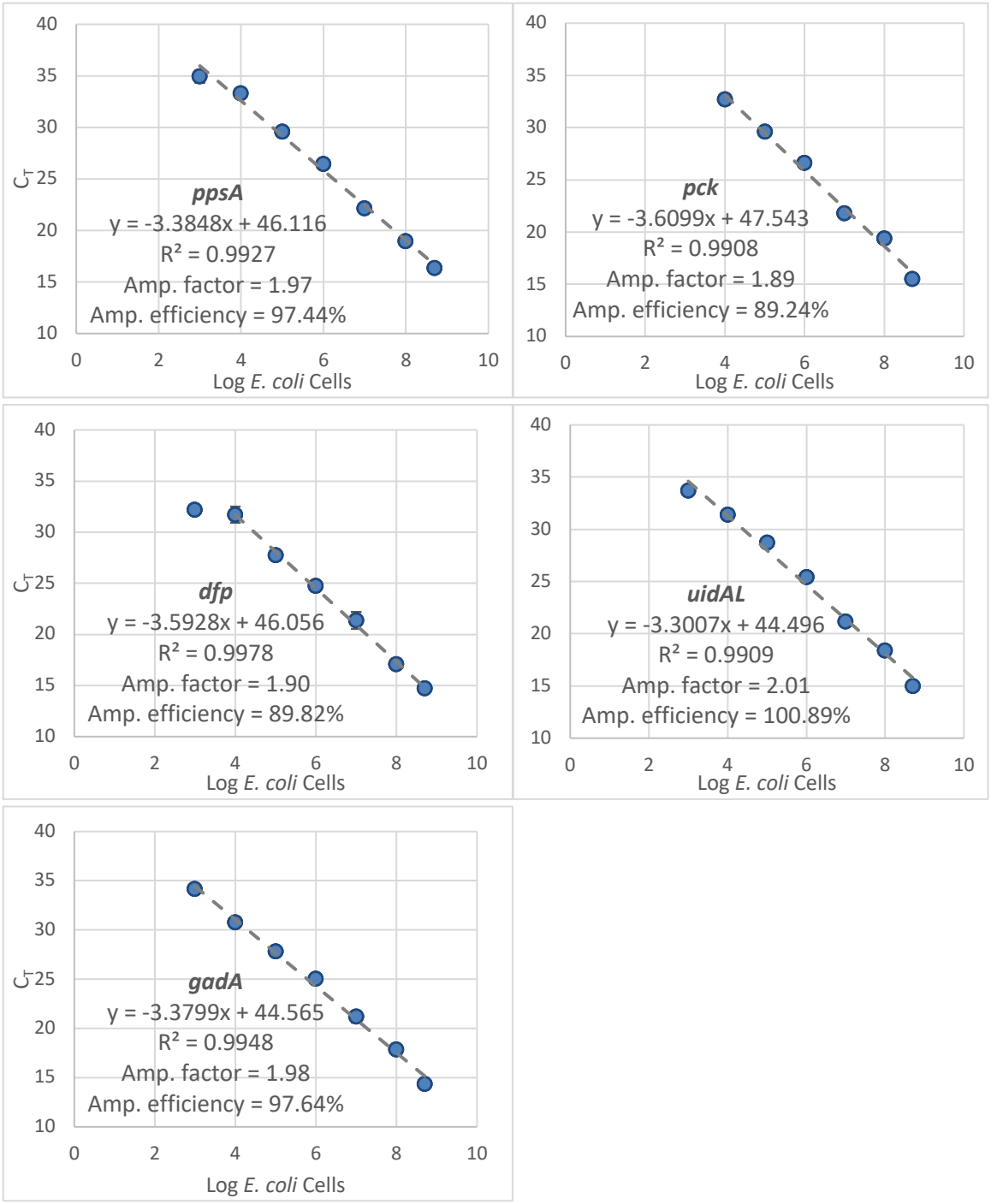

Figure 6: Standard curves for qPCR for metabolic gene targets. The NTC had an undetermined C_T. The highest point is neglected from some of the linear regressions. Error bars represent standard deviation between replicates. Some error bars are smaller than the markers.

Note: The C_T value for 1,000 cells (3-log cells) with the pck primer set was undetermined, and therefore, not plotted.

Dose-Response of E. coli

The dose-response curves for *E. coli* under UV light are presented in Figure 7. UV dose up to 20 mJ/cm^2 are commonly applied for pure *E. coli* cultures (Hijnen et al., 2006). Within this range, the culture based method shows approximately a 5.5-log reduction in culturable cells. After a dose of 20 mJ/cm^2, the curve plateaus. On the other hand, the dose-response curve from LA-qPCR shows the damage continues to occur even after 20 mJ/cm^2. It is assumed that damage continues to occur as long as there is DNA present, independent of whether the cell has lost culturability. It is important to note that traditional methods measure the ability of cells to culture and propagate on a specific media, whereas qPCR measures damage done to a specific region of the genome.

Short amplicon qPCR was less sensitive at detecting damage compared to the long amplicon alternative (Figure 7(b) & (c)). Over the 100 mJ/cm^2 range, short amplicon *uidA* was only able to detect two cycle changes, whereas the long amplicon was able to detect approximately a five cycle difference. Also, the short amplicon is less sensitive after 20 mJ/cm^2, as damage continues to occur in other regions of the genome. This agrees with the work of other researchers that larger amplicons should be used as opposed to short amplicon when quantifying UV damage.

The use of various gene targets allowed for a genomic scan of *E. coli*, and provided insight on the damage caused by UV light. This study found that UV causes widespread damage to the genome, as shown by the increase in C_T of every selected gene target (Appendix A).

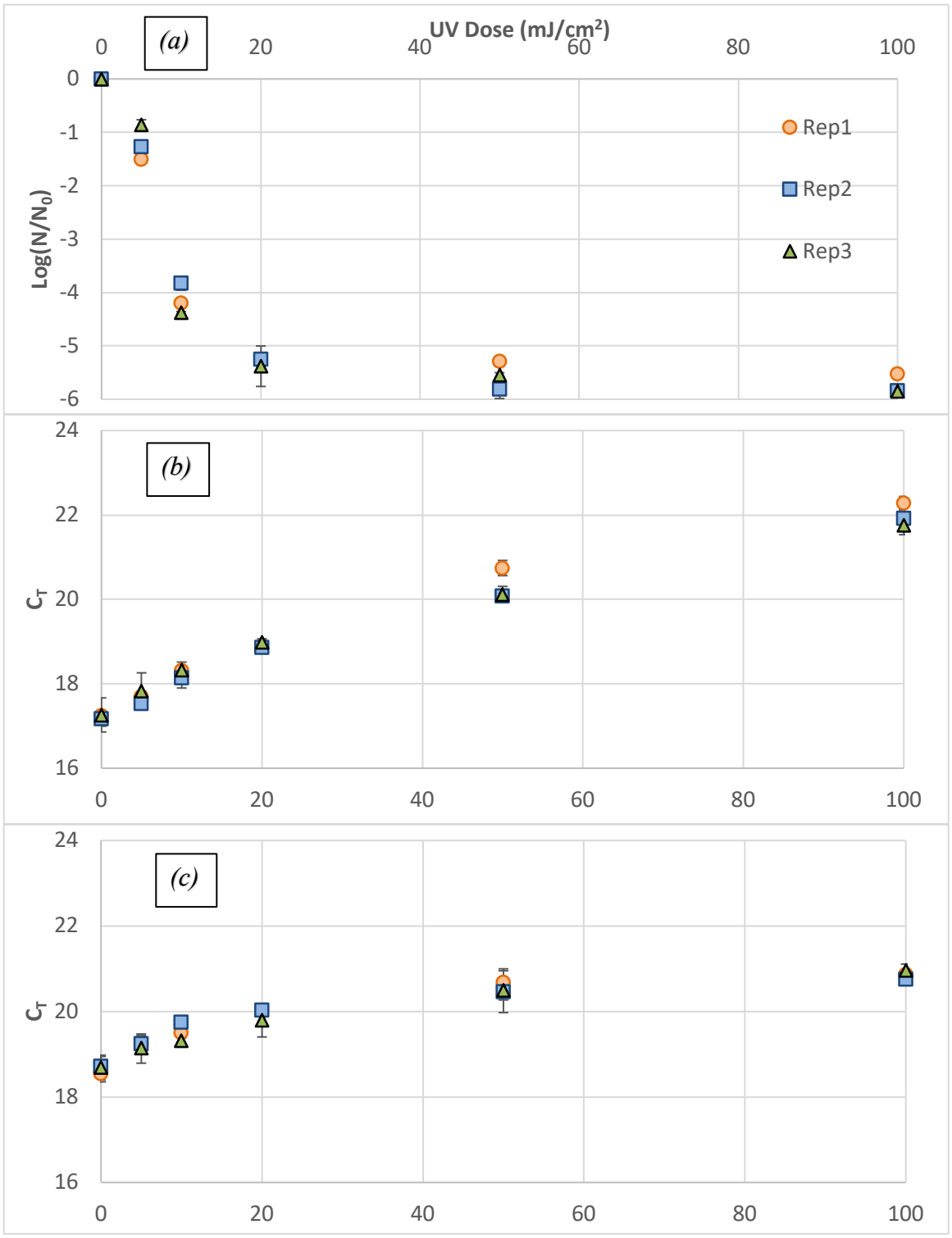

Figure 7: Inactivation curve of *E. coli* ATCC 8739 disinfected by UV-C as measured by **(a)** IDEXX Colilert Quanti-Tray®/2000, **(b)** long amplicon and **(c)** short amplicon qPCR of the same gene target, *uidA*. Error bars represent the standard deviation between triplicates. Some error bars are smaller than the size of the marker.

Analysis of rRNA Genes

The two rRNA genes that were selected were both found in *E. coli* in high concentrations. The average C_T values of *rrsA* and *rrlA* before UV exposure was 15.8 for both for 10^7 cells/mL. Of all the targets, they had the highest concentration and thus, met the first criterion of being a 'good target' for qPCR. These targets also met the second criterion, as they were both sensitive to UV damage and saw a 5-cycle change throughout the 0 – 100 mJ/cm^2 dose range. Additionally, both targets are important for ribosomal activity and therefore, serve an important function in the cell. Thus, the selected rRNA targets are well-suited for quantifying disinfection using qPCR.

The log reduction from IDEXX Colilert and the change in C_T from qPCR using these targets were plotted, shown in Figure 8. Between the range of 0 – 20 mJ/cm^2, the log reduction and change in C_T were found to be directly proportional. Past this range, the log reductions did not increase further; however, the C_T values continued to increase due

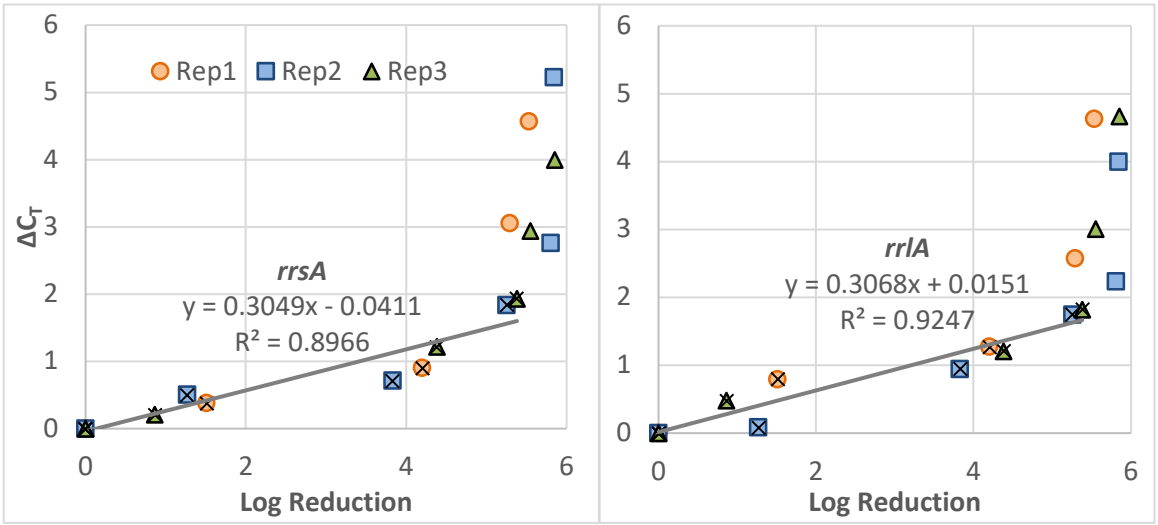

Figure 8: Correlation between log reduction and change in C_T for rRNA gene targets. Points marked with an X were used for the linear regression.

to ongoing DNA damage. A linear relationship was developed between log reduction and ΔC_T between 0 – 20 mJ/cm^2 (up to 5-log reduction). To date, correlations such as these have not been developed for the rRNA targets, or any other gene target. A higher slope for this correlation implies that the target is more sensitive to UV damage. In the case of the rRNA targets, both genes had similar correlations and therefore, they are both equally sensitive to UV damage. However, if looking for a suitable rRNA target, *rrlA* is recommended as the R-squared value for this target was found to be better than *rrsA*. It can then be assumed that the damage done to *rrsA* is similar due to their similar inactivation rates.

Analysis of UV Repair Genes

The target concentration of the two selected UV repair genes was found to be high. The average C_T values of *uvrB* and *umuC* before UV exposure was 17.5 and 16.6, respectively for 10^7 cells/mL. Each of them met the first criterion of being a 'good target' for qPCR. Additionally, both genes saw a 5-cycle change throughout the 0 – 100 mJ/cm^2 dose range. They were both sensitive enough to detect UV damage, and therefore, each met the second criterion mentioned earlier. Lastly, both gene targets serve important functions (NER and SOS mutagenesis), and damage done to these targets implies that the cells will not be able to undergo UV repair. Thus, both targets serve as good gene targets for quantification of UV disinfection through qPCR.

Correlations were developed for the *uvrB*- and *umuC*-based qPCR results (Figure 9). Again, there was a linear relationship between the UV dose range of 0 – 20 mJ/cm^2. The slopes for both UV repair targets were not different, implying that the similar damage was done to both genes. However, the R-squared value for the *umuC* gene target

was poor compared to *uvrB*. Hence, if looking for a UV repair gene target, *uvrB* was found to be more suitable. It can be assumed that the damage done to the *uvrB* target is similar to the damage done to *umuC*.

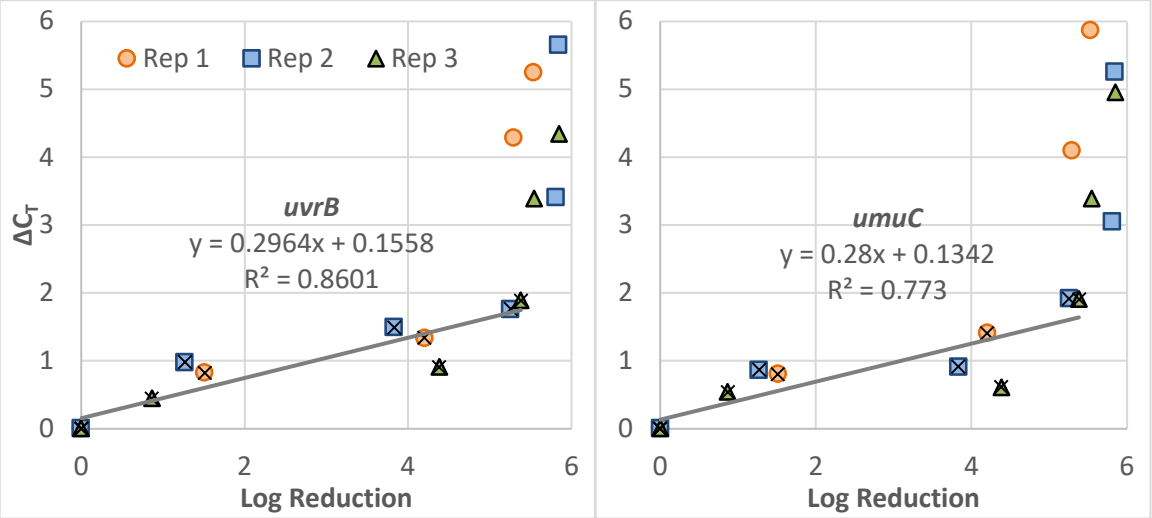

Figure 9: Correlation between log reduction and change in C_T for UV repair gene targets. Points marked with an X were used for the linear regression.

Analysis of Cell Division Genes

The selected cell division genes both met the first criterion of a 'good target' as they were found in high concentration in *E. coli*. The average C_T values of *ftsZ* and *ftsQ* were 16.8 and 17.0, respectively for 10^7 cells/mL. Furthermore, both targets saw a 6-cycle change throughout the 0 – 100 mJ/cm^2 dose range; hence, meeting the second condition. *ftsZ* and *ftsQ* play important roles in "early" and "late" cell division processes, respectively. UV-induced damage to either target impairs the cell and prevents an increase in cell count. Thus, the chosen genes serve as good targets for qPCR when quantifying UV disinfection.

For these targets, correlations between culture-based and qPCR methods were developed, again showing a linear relationship between 0 – 20 mJ/cm^2 (Figure 10). The inactivation of both gene targets was found to be similar, with the *ftsQ* gene having a better correlation. Thus, if looking for a cell division gene target that is suitable for quantifying UV disinfection, *ftsQ* is recommended. The damage done to *ftsZ* can be assumed to be similar.

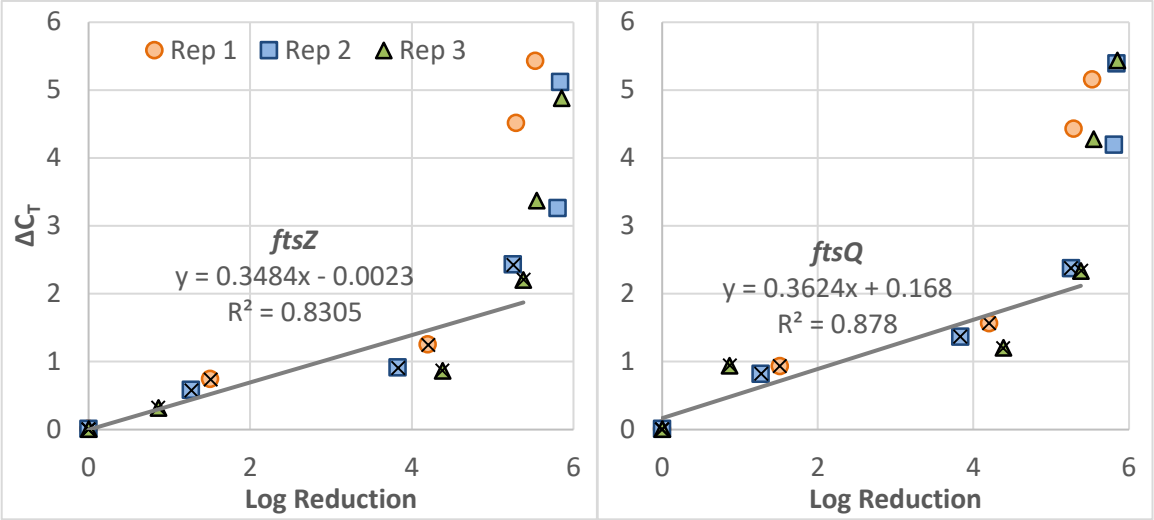

Figure 10: Correlation between log reduction and change in C_T for cell division gene targets. Points marked with an X were used for the linear regression.

Analysis of Metabolic Genes

A total of eleven metabolic gene targets were selected. All metabolic targets were found in high concentrations in *E. coli*, with C_T values ranging from 17.0 to 18.5 for 10^7 cells/mL. Thus, each of the eleven targets met the first condition of being a 'good target'. Each target was sensitive enough to UV light, thereby meeting the second condition. On average, a 5-cycle change was seen throughout the 0 – 100 mJ/cm^2 range. The function of each of the targets was mentioned in Table 1. With the exception of *gadA* and *uidA*, the

remaining nine targets serve an important role in the core metabolism of *E. coli*. Therefore, those nine meet the third measure of a 'good target'. *gadA* and *uidA*, though present in high concentrations and sensitive, are only important in certain conditions, (i.e., acidic environments, catalysis of complex carbohydrates).

Again, correlations were developed for all eleven gene targets (Figure 11). Most metabolic targets were similar to one another. The most sensitive of all the targets was found to be *tpiA*, and the least sensitive was *gltA*. The *uidA* target had the best R-squared value of 0.9422. However, use of the *uidA* should be avoided as mentioned earlier, it does not serve an important function. Any of the nine gene targets mentioned earlier can be used as suitable targets for qPCR, as they all have similar slopes and good R-squared values.

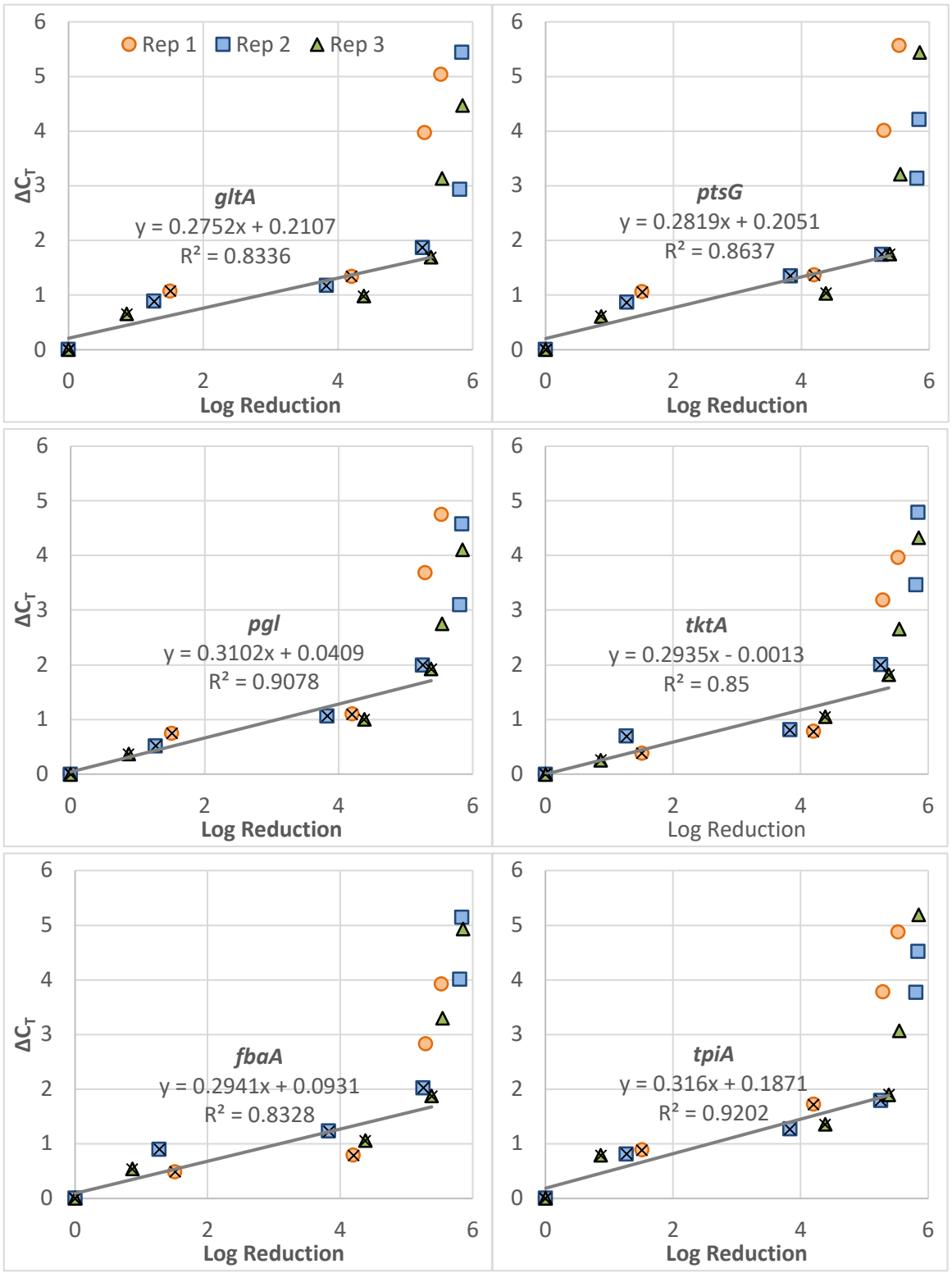
Rep 1
Rep 2
Rep 3
gltA
y = 0.2752x + 0.2107
R² = 0.8336
ptsG
y = 0.2819x + 0.2051
R² = 0.8637
pgl
y = 0.3102x + 0.0409
R² = 0.9078
tktA
y = 0.2935x - 0.0013
R² = 0.85
fbaA
y = 0.2941x + 0.0931
R² = 0.8328
tpiA
y = 0.316x + 0.1871
R² = 0.9202
ΔCT
Log Reduction

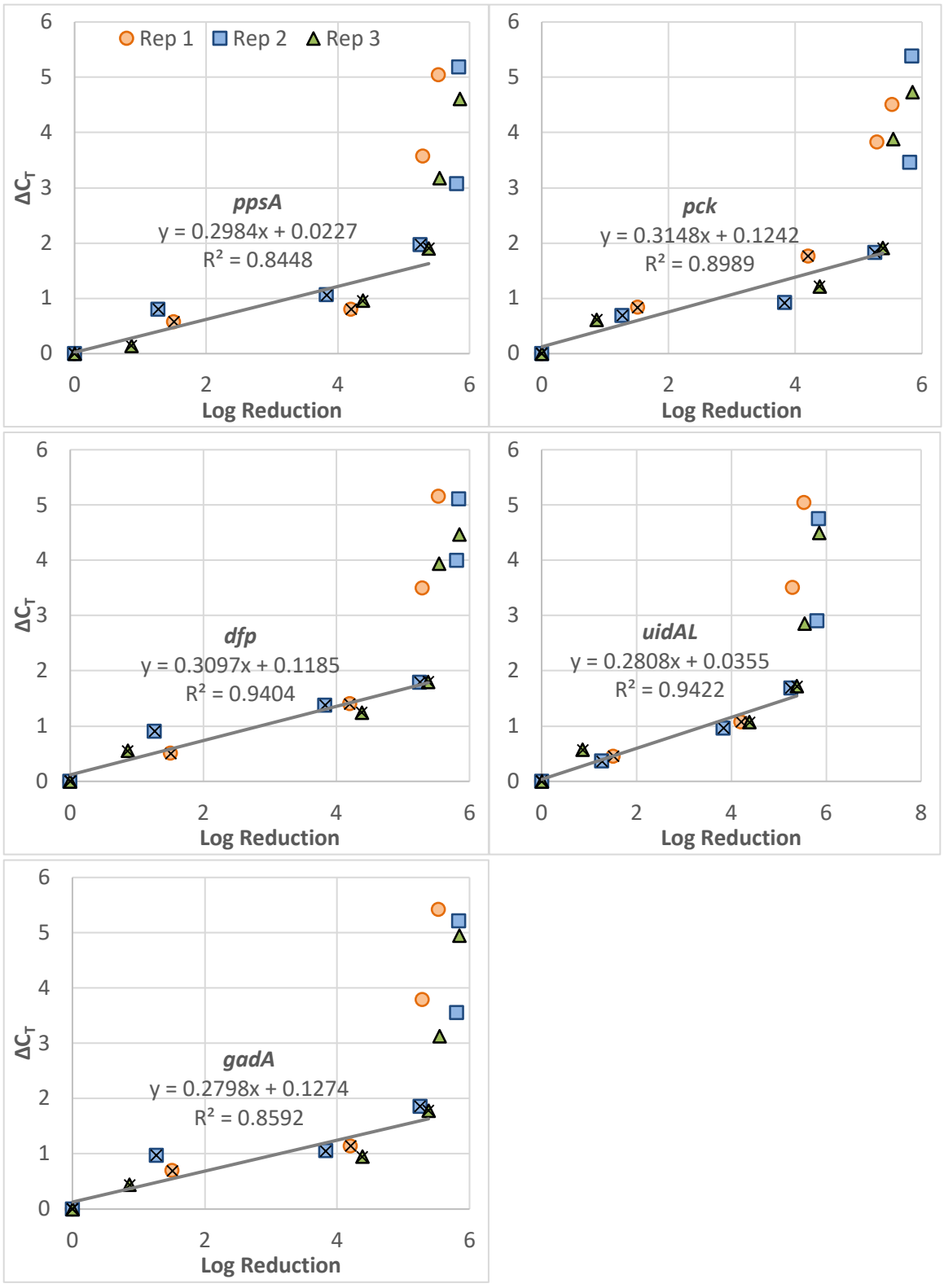

Figure 11: Correlation between log reduction and change in C_T all metabolic gene targets. Points marked with an X were used for the linear regression.

Comparison of All Targets

Most of the selected gene targets in this study served as good options for quantifying UV disinfection through qPCR. The target concentration for all the selected genes was similar for 10^6 cells, as shown in Table 3. rRNA gene targets are used for enumeration because they are easily detected. This study shows that the other targets can also be easily detected, yet provide more information on cell functioning post-disinfection than the rRNA genes. In order to compare the seventeen targets against one another, the total change in C_T over the linear range of 0 – 20 mJ/cm^2 was compared. Figure 12 shows this comparison for each gene target within each category. In term of sensitivity, the cell division targets were found to be the most sensitive to UV light (Table 3, Figure 12).

Table 3: Summary table of all gene targets

Gene	C_T for 10^6 cells	ΔC_T from 0 – 20 mJ/cm^2	Amp. efficiency	Correlation R^2	Important for cell function	Good marker?
rrsA	24.2	1.89	86%	0.897	No	Good
rrlA	23.4	1.79	92%	0.925	No	Good
uvrB	24.5	1.82	87%	0.860	Yes	Very good
umuC	24.9	1.91	83%	0.773	Yes	Very good
ftsZ	24.3	2.31	87%	0.831	Yes	Excellent
ftsQ	25.2	2.35	86%	0.878	Yes	Excellent
gltA	25.6	1.78	84%	0.834	Yes	Very good
ptsG	25.3	1.75	84%	0.864	Yes	Very good
pgl	25.6	1.96	90%	0.908	Yes	Very good
tktA	25.3	1.91	91%	0.850	Yes	Very good
fbaA	25.2	1.95	96%	0.833	Yes	Very good
tpiA	25.5	1.84	91%	0.920	Yes	Very good
ppsA	25.8	1.94	97%	0.845	Yes	Very good
pck	25.9	1.87	89%	0.899	Yes	Very good
dfp	24.5	1.79	90%	0.940	Yes	Very good
uidA	24.7	1.70	101%	0.942	No	Good
gadA	24.3	1.82	98%	0.859	No	Good

For quantifying UV disinfection with qPCR, it is not necessary to use all seventeen selected gene targets. It is preferred that a single reliable target be used. From the results of this study, it is recommended that *ftsQ* be used for measuring UV disinfection efficiency. This target was found in high concentration in *E. coli*, most sensitive for quantifying UV-induced DNA damage, served an important cellular function, and had a good correlation with culture based methods. On the other hand, if other genes are of interest for some work, a ratio of the change in C_T between the gene and *ftsQ* may be used to determine the damage. However, it should be kept in mind that the ratios from this study should only be used with a pure *E. coli* 8739 culture, or should be recreated with the different sample in order to be applied.

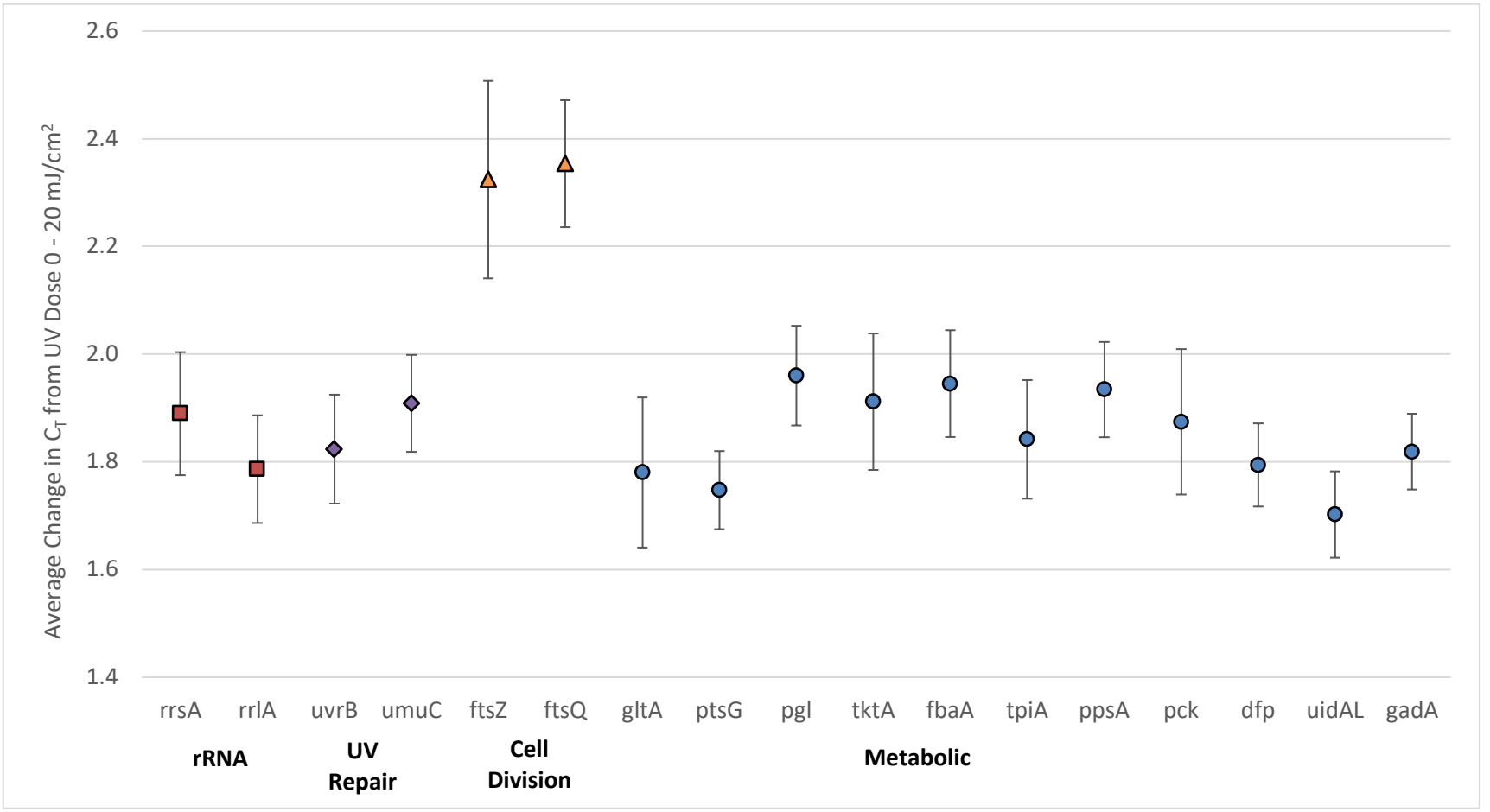

Figure 12: Average change in C_T from UV Dose 0 – 20 mJ/cm^2. Error bars represent standard deviation of replicates.

Conclusion

In order to develop a robust qPCR method for quantifying UV inactivation of *E. coli*, long amplicon qPCR was applied with various gene targets, as short amplicons were not sensitive. The results of this study show that UV causes widespread damage across the genome. There was a correlation between the qPCR method and conventional culture-based methods, within the commonly used UV dose range. This correlation allows the qPCR method to serve as a faster alternative to the conventional culture-based methods, and the log reduction can be estimated from the curve. It is recommended that for application the *ftsQ* gene be used as the target for qPCR. However, if for some reason, another gene target is of interest, a ratio can be made between the response of the two genes. Thus, multiple primers do not need to be used. The method developed in this study worked well for a pure *E. coli* culture. Real-world samples, such as wastewater, may pose challenges due to the presence of suspended particles, different *E. coli* strains, and interference from other bacteria. Application of the method developed in this study needs to be tested with real-world samples.

References

Aslan, A., Kinzelman, J., Dreelin, E., Anan'eva, T., & Lavendar, J. (2015). A guidance document for testing recreational waters using USEPA qPCR method C.

Banihashemi, A., Van Dyke, M., & Huck, P. (2012). Long-amplicon propidium monoazide-PCR enumeration assay to detect viabl Campylobacter and Salmonella. Journal of Applied Microbiology, 113, 863-873. doi:10.1111/j.1365-2672.2012.05382.x

Bolton, J. R., & Linden, K. G. (2003). Standardization of methods for fluence (UV dose) determination in bench-scale UV experiments. Journal of Environmental Engineering, 129(3), 209-215.

Buddelmeijer, N., & Beckwith, J. (2004). A complex of the Escherichia coli cell division proteins ftsL, ftsB and ftsQ forms independently of its localization to the septal region. Molecular Microbiology, 52(5), 1315-1327. doi:10.1111/j.1365-2958.2004.04044.x

Chern, E., Siefring, S., Paar, J., Doolittle, M., & Haugland, R. (2011). Comparison of quantitative PCR assays for Escherichia coli targeting ribosomal RNA and single copy genes. Letters in Applied Microbiology, 52, 298-306. doi:10.1111/j.1472-765X.2010.03001.x

Goosen, N., & Moolenaar, G. (2008). Repair of UV damage in bacteria. DNA Repair, 7, 353-379. doi:10.1016/j.dnarep.2007.09.002

Hijnen, W., Beerendonk, E., & Medema, G. (2006). Inactivation credit of UV radiation for viruses, bacteria and protozoan (oo)cysts in water: a review. Water Research, 40, 3-22. doi:10.1016/j.watres.2005.10.030

Ho, J., Seidel, M., Niessner, R., Eggers, J., & Tiehm, A. (2016). Long amplicon (LA)-qPCR for the discrimination of infectious and noninfectious phix174 bacteriophage after UV inactivation. Water Research, 103, 141-148. doi:10.1016/j.watres.2016.07.032

Janion, C. (2008). Inducible SOS response system of DNA repair and mutagenesis in Escherichia coli. International Journal of Biological Sciences, 4(6), 338-344.

Kibbee, R., & Ormeci, B. (2017). Development of a sensitive and false-positive free PMA-qPCR viability assay to quantify VBNC Escherichia coli and evaluate disinfection performance in wastewater effluent. Journal of Microbiological Methods, 132, 139-147. doi:10.1016/j.mimet.2016.12.004

Leifels, M., Hamza, I. A., Krieger, M., Wilhelm, M., Mackowiak, M., & Jurzik, L. (2016). From lab to lake - evaluation of current molecular methods for the detection of infectious enteric viruses in complex water matrices in an urban area. PLOS One. doi:10.1371/journal.pone.0167105

Li, D., Tong, T., Zeng, S., Lin, Y., Wu, S., & He, M. (2014). Quantification of viable bacteria in wastewater treatment plants by using propidium monoazide combined with quantitative PCR (PMA-qPCR). Journal of Environmental Sciences, 26, 299-306. doi:10.1016/S1001-0742(13)60425-8

Nocker, A., Sossa, K., & Camper, A. (2007). Molecular monitoring of disinfection efficacy using propidium monoazide in combination with quantitative PCR. Journal of Microbiological Methods, 70, 252-260. doi:10.1016/j.mimet.2007.04.014

Noor, E., Eden, E., Milo, R., & Alon, U. (2010). Central carbon metabolism as a minimal biochemical walk between precursor for biomass and energy. Molecular Cell, 39, 809-820. doi:10.1016/j.molcel.2010.08.031

Nucleotide excision repair. (n.d.). Retrieved from KEGG: https://www.genome.jp/kegg-bin/show_pathway?map=ko03420&show_description=show

Ouellette, S. P., Rueden, K. J., AbdelRahman, Y. M., Cox, J. V., & Belland, R. J. (2015). Identification and partial characterization of potential ftsL and ftsQ homologs of Chlamydia. Frontiers in Microbiology, 6. doi:10.3389/fmicb.2015.01264

Reuven, N. B., Arad, G., Maor-Shoshani, A., & Livneh, Z. (1999). The mutagenesis protein umuC is a DNA polymerase activated by umuD', recA, and ssb and is specialized for translesion replication. Journal of Biological Chemistry, 274(45), 31763-31766.

Shahraki, A., Chaganti, S., & Heath, D. (2018). Assessing high-throughput environmental DNA extraction methods for meta-barcode characterization of aquatic microbial communities. Journal of Water and Health, 17(1), 37-49. doi:10.2166/wh.2018.108

Süß, J., Volz, S., Obst, U., & Schwartz, T. (2009). Application of a molecular biology concept for the detection of DNA damage and repair during UV disinfection. Water Research, 43, 3705-3716. doi:10.1016.watres.2009.05.048

Varma, M., Field, R., Stinson, M., Rukovets, B., Wymer, L., & Haugland, R. (2009). Quantitative real-time PCR analysis of total and propidium monoazide-resistant fecal indicator bacteria in wastewater. Water Research, 43, 4790-4801. doi:10.1016/j.watres.2009.05.031

Woodgate, R., Rajagopalan, M., Lu, C., & Echols, H. (1989, October). UmuC mutagenesis protein of Escherichia coli: purification and interaction with umuC and umuD'. Proceedings of the National Academy of Sciences USA, 86, 7301-7305.

Xu, L., Zhang, C., Xu, P., & Wang, X. (2018). Mechanism of ultraviolet disinfection and chlorination of Escherichia coli: culturability, membrane permeability, metabolism, and genetic damage. Journal of Environmental Sciences, 65, 356-366. doi:10.1016/j.jes.2017.07.006

Zhang, S., Ye, C., Lin, H., Lv, L., & Yu, X. (2015). UV disinfection induces a VBNC state in Escherichia coli and Pseudomonas aeruginosa. Environmental Science & Technology, 49, 1721-1728. doi:10.1021/es505211e

CHAPTER 3:

APPLICATION OF QPCR METHOD FOR EVALUATING UV TREATMENT OPTIONS TO MANAGE MICROBIAL BEACH CONTAMINATION

Introduction

Pollution of recreational waters has been of public concern for decades, especially microbial pollution from fecal sources. In most municipalities, urban stormwater and sanitary sewage are conveyed in separate sewers. However, older sections of many cities are still serviced by combined sewer systems, which transport both stormwater and sanitary sewage to the wastewater treatment plant (WWTP). At times of heavy precipitation, the large volume can exceed the capacity of the plant, resulting in both stormwater and sanitary sewage being released as part of combined sewer overflow (CSO). Separated sanitary sewers may also be overwhelmed during wet weather conditions, resulting in sanitary sewer overflows (SSO). Urban wet weather pollution is recognized as a major source of water quality impairment, including in the Great Lakes region (Weatherbe & Sherbin, 1994; Marsalek & Rochfort, 2004; McLellan et al., 2007; Templar et al., 2016). Recreational waters contaminated by fecal pollution pose a serious threat to human health.

Disinfection of CSO is required in Ontario in areas upstream of recreational waters, under Procedure F-5-5 (MOECC, 2016). During wet weather conditions, the minimum level of treatment required is primary treatment or equivalent. To meet this requirement, some cities (such as Windsor, ON) employ a retention treatment basin (RTB) which collects CSO and offers a primary level of treatment by settling solids

through polymer coagulation. The effluent should be disinfected to less than 1,000 *E. coli* per 100 mL (monthly geometric mean). The most common processes for disinfection include chlorination, ozonation, and ultraviolet (UV) radiation. Compared to the chemical disinfectants, UV light does not produce hazardous by-products and therefore, would be the preferred option. Furthermore, as a result of primary treatment, the reduced suspended solids concentration allows UV light to be more effective. Additionally, having an RTB may reduce the cost of infrastructure required for implementing UV disinfection. Since the main concern of sewer overflows is the fecal contamination component, disinfection of CSO or SSO can be considered to be similar to disinfection of wastewater. Disinfection of wastewater has been widely studied. The use of UV radiation for disinfection of wastewater was first introduced in the 1970s and has since become highly developed and implemented in treatment plants around the world (Whitby & Scheible, 2004). Although many studies on wastewater disinfection have been done, few studies have been conducted to explore the effectiveness of different disinfectants on CSO or SSO (Tondera et al., 2015; Tondera et al., 2016; Eramo et al., 2017). Of these studies, the focus has been on chemical disinfectants and less on UV light.

The effectiveness of UV and the sensitivity of a selected microorganism for UV can be described by the inactivation kinetics (Lazarova et al., 1999; Gehr et al., 2003; Hijnen et al., 2006). Inactivation is defined as the reduction of the concentration of culturable microorganisms (N) due to the exposure to a disinfectant of a certain concentration (C) during a specific contact time (t). UV inactivation kinetics can be described similar to chemical disinfectants, with the first-order disinfection model of

Chick (1908) and Watson (1908). There is a linear relationship between log inactivation and the UV dose as described by the following equation:

$$\log_{10}\left(\frac{N_t}{N_0}\right) = -kD$$

where N_t is the microbial concentration after contact time t, N_0 is the initial microbial concentration, k is the inactivation rate constant (cm^2/mJ), and D is the UV dose (mJ/cm^2). Microorganisms that are more sensitive to UV have a high k-value and require a lower UV dose for inactivation. Previous work has been done on the UV disinfection kinetics of bacterial cultures, drinking water and wastewater, but there is lack of information on the kinetics of UV disinfection of CSO.

Evaluating the performance of disinfection technologies has been primarily done with standard microbiological methods that rely of culturing. Due to the long incubation times required by these methods, rapid molecular techniques such as real-time quantitative polymerase chain reaction (qPCR) methods have been investigated. A limited number of studies have been done on the applicability of qPCR for quantifying disinfection of wastewater (Chatzisymeon et al., 2011; Li et al., 2014; Kibbee & Ormeci, 2017). Again, the focus of these studies has been on chemical disinfectants such as ozone. The reason for this is because chemical disinfectants directly damage the cell membrane, and qPCR-based techniques have been proposed to take into account the membrane damage (i.e., PMA-qPCR). Due to the different disinfection mechanism of UV light, there is no consensus on a qPCR method that would be able to reliably quantify UV disinfection. The previous chapter developed a qPCR-based method and demonstrated its applicability for a pure *E. coli* culture exposed to various UV doses.

However, the applicability of the method for quantifying UV disinfection efficiency of CSO was not tested. Due to the various bacterial strains and populations present in CSO, the UV inactivation may be significantly different than that of a single-strain *E. coli* culture.

This study explored the effectiveness of UV disinfection on CSO. Due to lack of information on inactivation kinetics for CSO, the first objective was to determine the inactivation rates for treated and untreated CSO and also compare with the kinetics of a pure *E. coli* culture. After conducting UV exposure experiments, disinfection performance was quantified through culture-based and qPCR-based methods. Correlations were developed between the log reduction and DNA damage of UV-exposed samples. The final objective of this work was to check the applicability of the developed qPCR method from Chapter 2 to quantify UV inactivation of CSO samples, and to compare the results of the CSO samples with those of a pure *E. coli* culture.

Materials and Methods

Sample preparation

As the main concern of CSO/SSO is the untreated wastewater component, artificially generated CSO/SSO samples were used for this study. Approximately 1-L of each raw wastewater (WW) and primary treatment effluent was collected from the Little River Wastewater Treatment Plant (Windsor, ON, Canada). To simulate CSO/SSO, raw WW and primary effluent were each diluted 50:50 with sterile tap water. Each sample was stirred in a flask for 10 – 15 minutes before UV exposure experiments to ensure

proper mixing and prevent settling of particles. Two replicates were conducted from January 2019 – February 2019.

E. coli ATCC® 8739™ cells were obtained in six 300-µL glycerol stock vials. A single vial was added to 20 mL sterile nutrient broth (Becton Dickinson) and incubated at 37°C for 20 hours. Sterile nutrient broth agar plates were prepared with 1.5% agar. Cultured cells were streaked on the plates to separate colonies. A single isolated colony from the agar plates was inoculated in 40 mL sterile nutrient broth and incubated for 16 – 24 hours at 37°C. The culture was then centrifuged for 20 min at 4,000 rpm. The nutrient broth supernatant was disposed and the settled cells were re-suspended in 20 mL sterile phosphate-buffered saline (PBS). Cell concentration was estimated using UV-vis spectrophotometry according to section 4.3.2. of the USEPA Draft Method C (Aslan et al., 2015). For developing standard curves, *E. coli* cells were serially diluted and aliquots in triplicates were frozen at -20°C until extraction. For UV exposure experiments, *E. coli* cells were diluted in 1 L sterile PBS to approximately 7-log cells per mL.

UV Exposure Experiments

UV exposure experiments were conducted with a low-pressure collimated beam apparatus (Trojan Technologies, Canada) according to manufacturer's standardized protocols. Intensity measured at the sample surface with the IL1700 radiometer (Trojan Technologies, Canada). For each sample, 53-mL *E. coli* suspension was filled in clear glass petri dish with a stir bar. 3 mL was taken out for UVT readings using Real Tech Water's UV254 portable meter with split sense technology. Based on the UVT readings, an excel sheet was used to calculate the time required for the desired dose. Each dose was done in triplicate. Calculations for the dose accounted for the petri, divergence, and

reflection factors as per Bolton & Linden (2003). After UV exposure, each sample was split into aliquots for DNA extraction and for culturing.

Culture-based Method

IDEXX Colilert Quanti-Tray®/2000 was used as the culture-based method in this study. It is able to detect both total coliform and *E. coli* up to 2,419 MPN/100mL. Each sample was diluted with sterile PBS to a concentration that would be within the range of this method.

DNA Extraction

Frozen samples were thawed at room temperature and centrifuged at 10,000 rpm for 15 minutes. The supernatant was taken out and 400 µL of sterile PBS was added. For each sample, 500 µL of 1-mm sterile glass beads and 400 µL of sucrose lysis buffer was added. Sucrose lysis buffer was made according to Shahraki et al. (2018). After adding lysis buffer, samples were subjected to bead-beating using the Mini-beadbeater-16 (Lab Services BV, Nederland) for 40 seconds (three times) at an intensity of 3,450 oscillations/min. 100 µL of 1% SDS and 50 µL of 20 mg/mL lysozyme (Sigma-Aldrich, USA) were added to each tube. Samples were then incubated at 37°C on a shaker overnight. The next day 2 µL of 20 mg/mL proteinase K (Thermo Scientific, USA) was added, and the samples were again kept in the incubator at 37°C on a shaker overnight. Finally, the next morning, proteinase K was deactivated in at 95°C water bath for 10 minutes.

The digest from each tube was plated in a 96-well extraction plate, and DNA was extracted by magnetic bead robotic extraction according to Shahraki et al. (2018). Extracts were kept in the freezer at -20°C until qPCR analysis.

qPCR

DNA extracts from UV exposure experiments were used with various primer sets. Due to the large number of samples and primer sets, 384-well qPCR plates were utilized with a 9-µL reaction volume. To prepare the 384-well plate, four 96-well plates were prepared with 12-µL reactions containing: 4.4 µL nuclease-free water, 6 µL 2x PowerUp™ SYBR® Green Master Mix (Applied Biosystems), 0.3 µL each of 10-mM F- and R-primers, and 1 µL DNA template. Then 9 µL was transferred from the fourt 96-well plates into a single 384-well plate. The QuantStudio™ 12K Flex System (ThermoFisher Scientific) ran the following program: initial step at 95°C for 20s, followed by forty cycles of 95°C for 10s and 60°C for 20s. All results were exported into Microsoft Excel files for analysis.

Results and Discussion

Dose-Response of E. coli

A typical dose-response curve of *E. coli* shows two stages: an initial steep decline attributed to the suspended free-swimming bacteria which are easily exposed to UV light, followed by a second step with a much shallower slope, referred to as tailing. Figure 13 shows the dose-response curve of the three sample types in this study: (a) pure *E. coli* ATCC® 8739™ culture, (b) sCSO (50% raw WW, 50% tap water), and (c) primary-treated sCSO (50% primary effluent, 50% tap water).

From Figure 13, it can be noted that the inactivation rate of pure *E. coli* is higher than that of *E. coli* derived from wastewater, whether untreated or primary-treated. This difference in inactivation rate may be due to several factors. Firstly, the cultured *E. coli* is

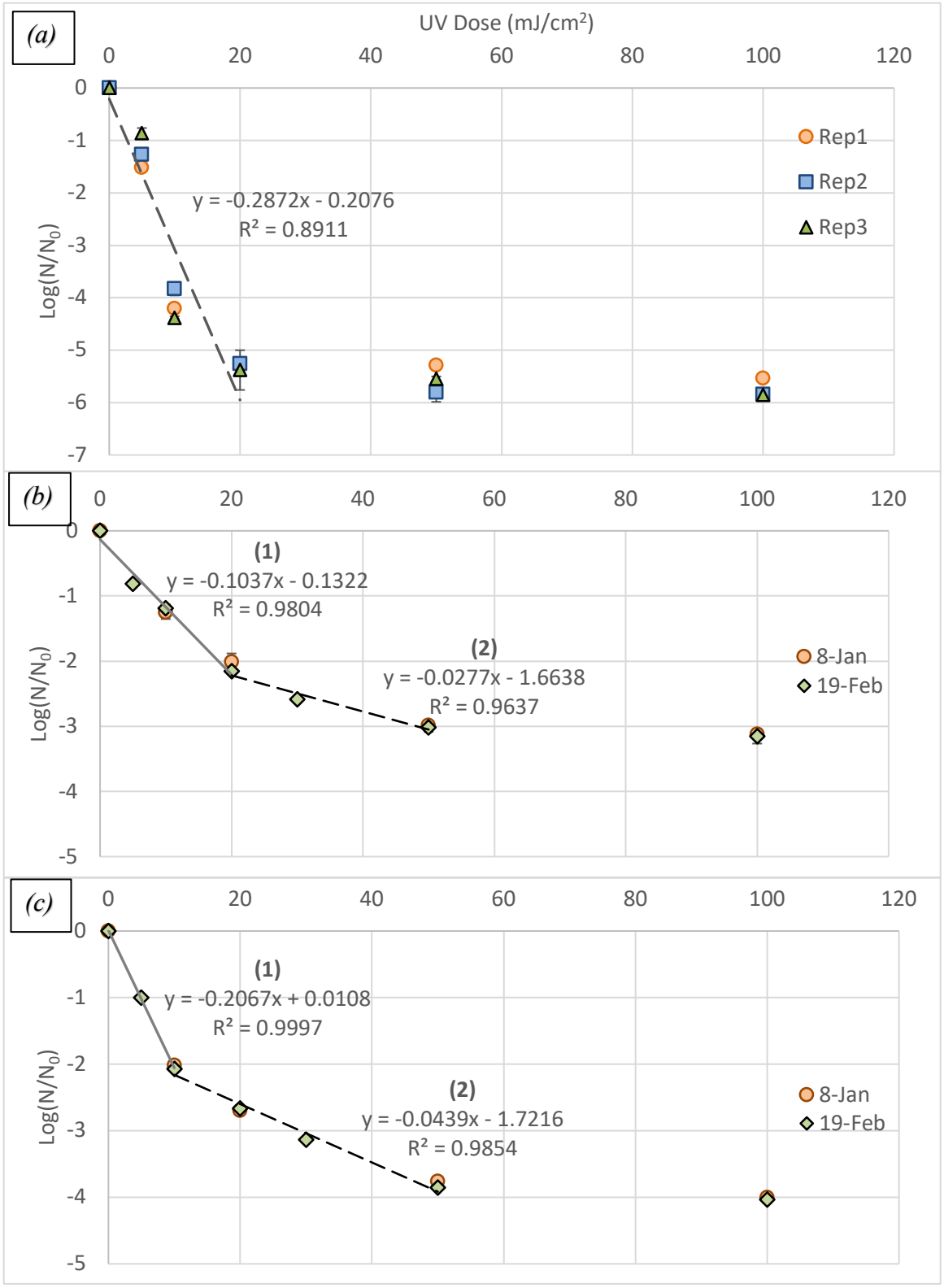

Figure 13: Dose-response curves for (a) pure *E. coli* ATCC® 8739™, (b) sCSO, and (c) primary-treated sCSO. Error bars represent standard deviation. Some error bars are smaller than the size of the marker.

a single strain, whereas multiple strains of *E. coli* are present in wastewater. Strain diversity has been established as a reason for observed differences in UV sensitivity (Sommer et al., 2000; Malley et al., 2004; Hijnen et al., 2006). Secondly, the metabolic state of *E. coli* can be another reason for the difference in inactivation rates. For pure culture experiments, the *E. coli* cells were harvested when in a growth phase. On the other hand, bacteria in wastewater can be present in a stationary phase due to unfavourable environmental conditions and stress. Bacteria exposed to UV light while in the growth phase are easily inactivated compared to cells in a stationary phase (Malley et al., 2004; Hijnen et al., 2006). Additionally, the turbidity of wastewater has an influence on the effectiveness of UV disinfection. Low inactivation rates are observed in wastewater due to suspended solids which either absorb or scatter UV light, shade microorganisms, or shield embedded microorganisms (Madge & Jensen, 2006; Azimi et al., 2012). Lastly, the level of particle association also affects a cell's susceptibility to UV light. If microorganisms are present on the 'loose shell' (i.e., the outer layer of a particle), they are easier to damage than those compacted in the core of a wastewater biofloc (Ormeci & Linden, 2002; Azimi et al., 2012).

The concept of tailing of the dose-response curve is well-known; however, the cause is still under debate. Several reasons have been hypothesized to date, including but not limited to: experimental bias, highly resistant subpopulations, aggregation of microorganisms, and particle association. In general, Hijnen et al. (2006) found tailing occurs when at least 99% of the initial microorganisms have been inactivated. Microorganisms more susceptible to UV light see greater than 99% damage before tailing starts to occur. From Figure 13 (a), it is noted that tailing occurs after 5-log reduction for

E. coli 8739. On the other hand, the dose response curves of untreated sCSO and primary-treated sCSO begin to tail after approximately 2.5- and 3.5-log reduction, respectively. This further enforces the conclusion that environmental bacteria, such as the *E. coli* strains found in wastewater, are more resistant to UV light than a single-strain *E. coli* exposed to near-ideal laboratory conditions.

UV disinfection kinetics also vary for untreated and treated wastewater. At the primary level of wastewater treatment, coagulation polymers are added to aid in the settling of suspended particles. Based on the logic presented by Madge & Jenson (2006) and Azimi et al., (2012), the reduction in suspended solids should increase the UV inactivation rate. This is illustrated in Figure 13 (b) and (c), as the slope of the primary-treated sCSO was shown to be approximately twice the slope of untreated sCSO. To achieve a 2-log reduction, or 99% removal, a UV dose of 20 mJ/cm^2 is required for untreated sCSO, whereas half the dose is needed for primary-treated sCSO. The presence of particles in wastewater hinder UV disinfection. As noted from the dose-response curves, the *E. coli* culture sees a single log-linear relationship between dose 0 – 20 mJ/cm^2. However, treated and untreated sCSO samples see (1) an initial steep decline, followed by (2) a slightly shallowed slope, and eventually (3) a plateau. Based on the literature, the first rate represents the inactivation of free-swimming cells and the second may be due to the shade or shielding of particles on microorganisms. Since the primary-treated sCSO had fewer suspended solids, the second rate is two times higher than that of untreated sCSO and inactivation continues to occur past 3-log reduction.

Using the qPCR method, a greater reduction was observed in the primary treated samples, showing the reduction in suspended solids increased the amount of DNA lesions. DNA damage was observed in all the selected targets in this study, to a greater degree in primary-treated sCSO and to a lesser degree in untreated sCSO. Nonetheless, UV light caused widespread damage to the genome of wastewater *E. coli* (Appendix B). Widespread damage was also observed in pure *E. coli*; however, the extent of damage was to a greater degree in the culture (Figure 14). It can be noted that although the culture-based dose-response curves show tailing, damage continued to occur to the DNA of the cells. It is hypothesized that DNA damage would continue to occur, regardless of cell viability, as long as DNA is present. Thus, it is important to note that the two methods measure two different parameters: conventional culturing techniques measure the ability of cells to propagate on a specific media, whereas molecular techniques such as qPCR measure the amount of damage done to a specific region of DNA.

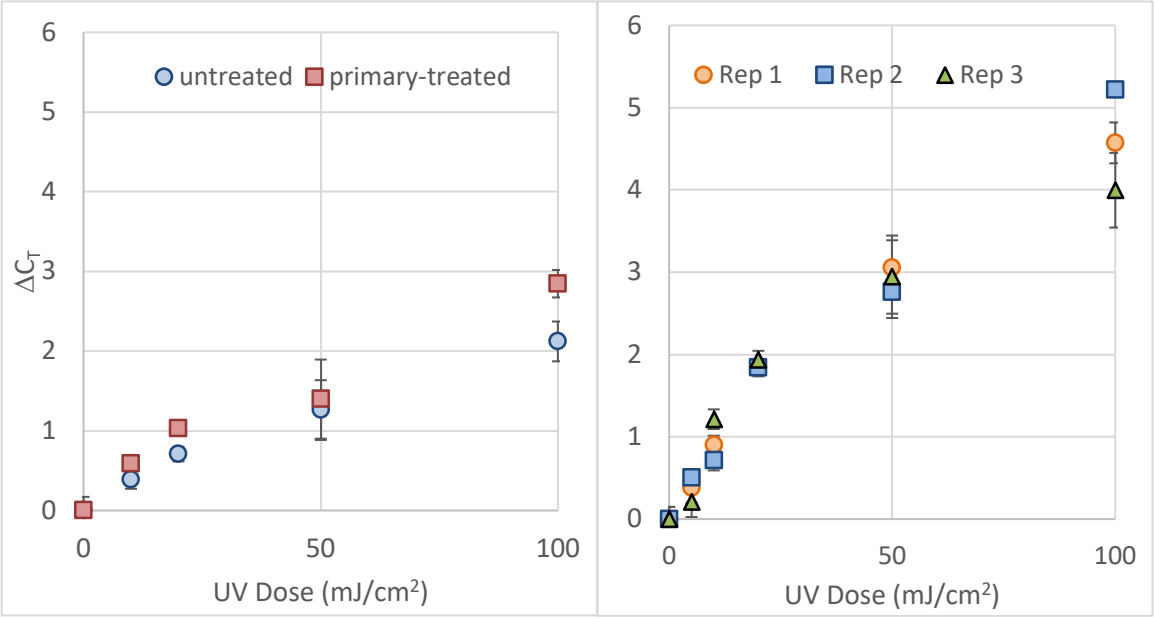

Figure 14: DNA damage to *rrsA* gene in sCSO (left) and *E. coli* (right) samples. Error bars represent standard deviation in replicates. Some error bars are smaller than the markers.

Table 4: Initial cell count per 100 mL from Colilert and estimated from qPCR standard curves

	Untreated sCSO	**Primary-treated sCSO**
IDEXX Colilert	1.30×10^6	7.28×10^5
rrsA	2.73×10^7	1.68×10^7
rrlA	1.59×10^7	1.33×10^7
uvrB	2.68×10^7	7.77×10^6
umuC	2.04×10^7	1.45×10^7
ftsZ	1.17×10^7	6.24×10^6
ftsQ	1.54×10^7	9.82×10^6
ptsG	1.65×10^7	9.24×10^6
pgl	2.13×10^7	1.66×10^7
pck	3.22×10^7	1.89×10^7
uidA	9.90×10^6	7.83×10^6

Analysis of rRNA Genes

Two rRNA genes, *rrsA* and *rrlA*, were selected for quantifying *E. coli*. They were both found in high concentration in the pure culture. Since the concentration of *E. coli* was lower in the sCSO samples as compared to the pure culture, it was expected that the C_T value would be higher. Both targets were still quantifiable in untreated and primary-treated sCSO. For *rrsA*, the average initial C_T values were 25.5 and 26.2 for untreated and primary-treated sCSO, respectively. The *rrlA* gene had similar concentration, with average C_T values of 25.4 and 25.7 for untreated and primary-treated sCSO. The cell concentration of the untreated and primary-treated sCSO samples as determined by IDEXX Colilert is shown in Table 4. Using the qPCR results and the standard curves developed in the previous chapter, the estimated initial cell counts were determined, as shown in Table 4. For comparison, the cell count numbers as determined by IDEXX Colilert for each sample were also tabulated. The estimated cell counts using the two rRNA genes were 1.1 – 1.4 log greater than the most probable number (MPN) determined by IDEXX Colilert. It was assumed that the difference in numbers was due to the

designed primers not being specific enough to *E. coli*. The lack of specificity resulted in the quantification of other bacteria with similar gene sequences as *E. coli*. Nonetheless, the results from qPCR still quantified DNA damage, whether the damage was done to *E. coli* or to another bacterial cell closely related to *E. coli*.

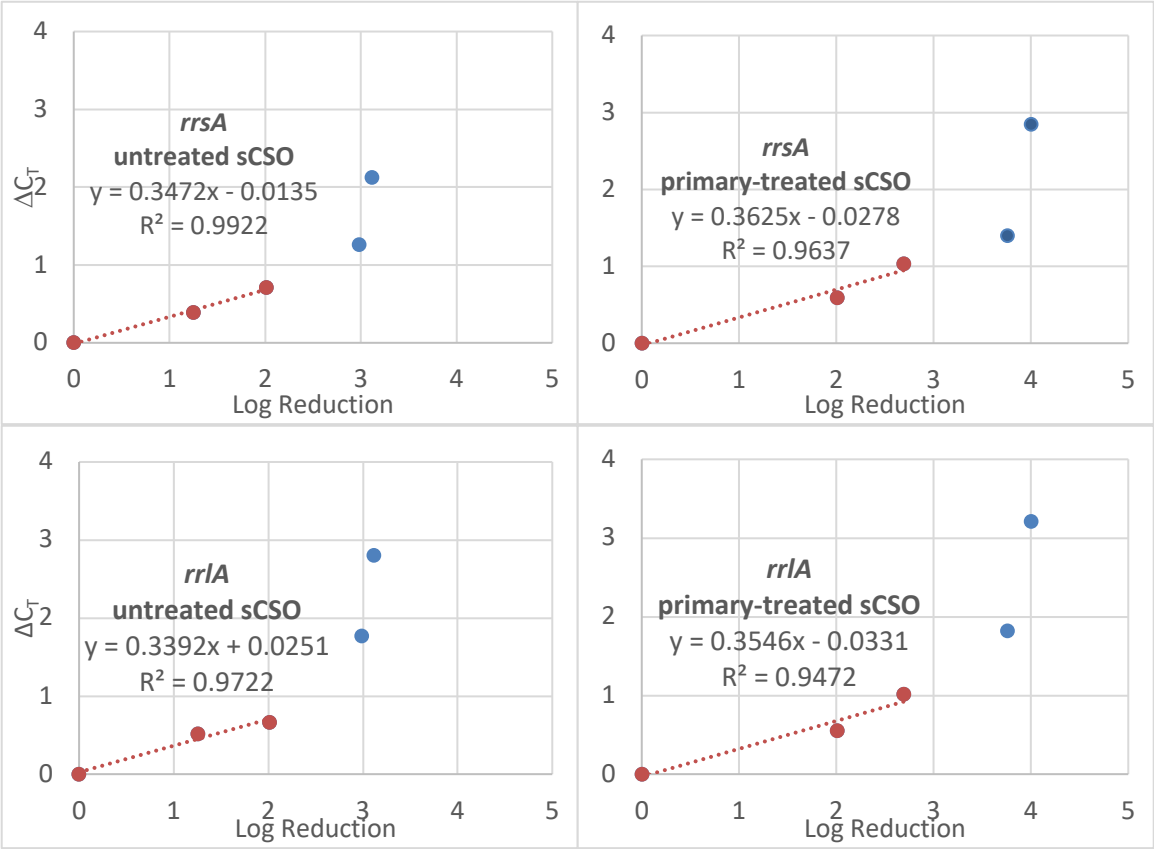

Figure 15: Correlation of culture-based and qPCR-based methods for rRNA genes with untreated and primary-treated sCSO samples.

Correlations between the log reduction from IDEXX Colilert and the change in C_T from qPCR were developed for the two rRNA targets (Figure 15). Between the UV dose range of 0 – 20 mJ/cm^2, there was a linear relationship. Past this range, the log reduction plateaued, while the C_T values continued to increase due to continuous DNA damage. To date, these type of correlations have not been developed for CSO samples

using any kind of gene target. Both targets have similar slopes within the linear range, which implies that damage occurs to both genes at a similar rate. The *rrsA* targets had a better r-squared value than the *rrlA* gene.

The results vary between the pure *E. coli* 8739 culture and the sCSO samples. The slopes observed with sCSO samples were slightly greater than those of pure *E. coli*. Again, it was hypothesized that this increase was due to the lack of specificity of the primers, detecting DNA damage of *E. coli* and other bacteria whereas the Colilert method quantified only *E. coli* reduction. One commonality was that the slopes of *rrsA* and *rrlA* were not different from each other within a particular sample. Damage occurs to both genes at the same rate, therefore, either target may be used for qPCR and its results would be indicative of the damage done to the other gene.

Analysis of UV repair genes

The two UV repair genes for quantifying *E. coli* were *uvrB* and *umuC*. Both were found in high concentration in the pure culture, and were still quantifiable in the sCSO samples. For the *uvrB* gene, the average initial C_T values were 25.7 and 27.7 for raw and primary-treated sCSO, respectively. The average initial C_T values for *umuC* were 27.0 and 27.6 for raw and primary-treated sCSO, respectively. Based in these results and the standard curves developed in Chapter 2, the estimated initial cell counts were determined and tabulated in Table 4. The estimated cell counts for the two UV repair genes were 1.2 – 1.3 log higher than the MPN from IDEXX Colilert. It was hypothesized that the difference in numbers was due to the lack of specificity of the primers designed. This may have caused the detection of bacterial cells with similar gene sequences as *E. coli*. qPCR still measured DNA damage done, whether it was to *E. coli* or other bacteria.

The log reduction from the culture-based method and the DNA damage quantified from the qPCR method were plotted (Figure 16). A linear relationship was observed between the range of 0 – 20 mJ/cm^2. Out of this range, continued DNA damage was observed, however, there was no further reduction in the number of cultured cells. The two targets have similar slopes within the linear range but the r-squared value for *umuC* was better than that of *uvrB*.

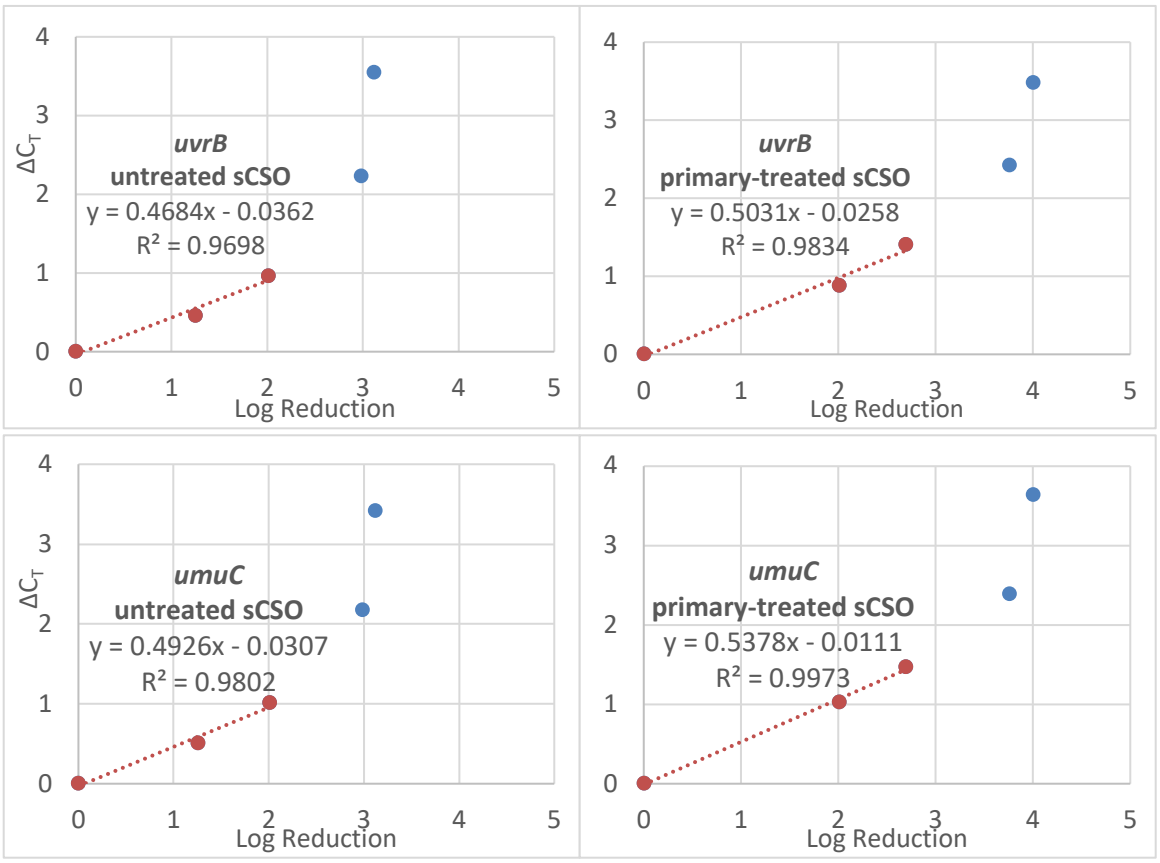

Figure 16: Correlation of culture-based and qPCR-based methods for UV repair genes with untreated and primary-treated sCSO samples.

Some variation between the pure *E. coli* 8739 culture and the sCSO samples was observed. The slopes for the raw and treated sCSO samples were slightly greater than those of the single-strain *E. coli* culture, most likely due to the lack of specificity of the primers. The qPCR method quantified more damage, most likely damage done to *E. coli*

and other bacteria, whereas the plotted log reduction from Colilert was of solely *E. coli*. It should be noted that for a particular type of sample, the damage done to both UV repair genes occurred at similar rates and the slopes were within 10% error. Therefore, either UV repair target may be used for qPCR and its results would be representative of the UV-induced damage to the other gene.

Analysis of Cell Division Genes

The *ftsZ* and *ftsQ* genes were selected as the cell division targets, and both had similar target concentrations. The average initial C_T values for *ftsZ* were 26.8 and 27.9 for untreated and primary-treated sCSO, respectively. For *ftsQ*, the average initial C_T values were 27.3 and 28.1 for untreated and primary-treated sCSO, respectively. From the results, the estimated cell counts based on the two cell division genes were 0.9 – 1.1 log higher than the MPN from IDEXX Colilert. The difference in the counts may be due to the primers used, which may not be specific to *E. coli*. However, the qPCR method still quantified the damage done to DNA by UV light, whether it was *E. coli* DNA or DNA of a similar bacteria.

Correlations were developed for the two different methods using the cell division genes (Figure 17). There was again a linear relationship between the UV dose range of 0 – 20 mJ/cm^2. The two targets similar slopes within the linear range for each sample type.

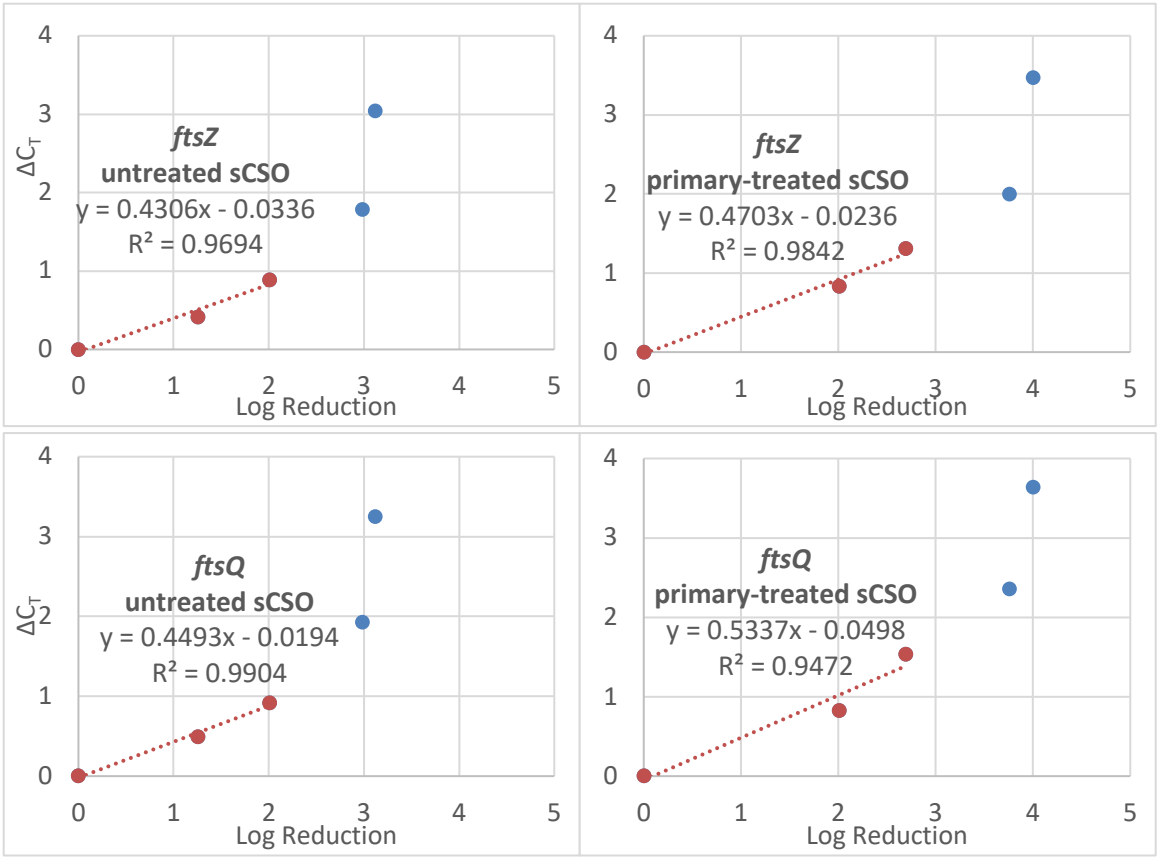

Figure 17: Correlation of culture-based and qPCR-based methods for cell division genes with untreated and primary-treated sCSO samples.

The correlation graphs developed for sCSO were different than those of the *E. coli* culture. The former had a higher slope, most likely due to the lack of specificity of the primers for these gene targets. For a particular sample, the damage done to the two cell division genes occurred at a similar rate. Thus, either target may be used for qPCR.

Analysis of Metabolic Genes

For this study, only four metabolic targets were selected for analysis. As shown in the previous chapter, metabolic targets showed similar DNA damage after UV exposure, and thus, there was no need to use all eleven targets. The four selected were: *ptsG*, *pgl*, *pck*, and *uidA*. The first three were chosen based on the amount of damage seen within

the linear range (Chapter 2, Figure 12). *ptsG* was the least damaged, *pgl* was the most damaged, *pck* was representative of the average damage to all metabolic targets. *uidA* was selected because it is commonly used as a qPCR target for *E. coli* and served as a comparator. The four targets were found to have similar target concentrations, with average C_T values ranging from 26.8 – 27.3 for untreated sCSO, and 27.5 – 28.0 for primary-treated sCSO. The estimated cell counts based on these four targets was 0.9 – 1.4 log greater than the MPN determined through IDEXX Colilert, most likely due to the lack of specificity of the primers. Nonetheless, the qPCR method quantified DNA damage caused by UV, whether *E. coli* or other bacteria were damaged.

Graphs correlating the log reduction and change in C_T were made for the four metabolic targets (Figure 18). Between the UV range of 0 – 20 mJ/cm^2, there was a linear relationship. Within this range, the *ptsG* gene was still the least damaged and the *pgl* was the most, with approximately 20% difference between the two.

In comparison with the correlations developed from the pure culture, the sCSO samples had greater slopes. It is assumed that the higher slope is due to the qPCR method detecting more damage (i.e., from *E. coli* and other bacteria), whereas the culture method is quantifying only *E. coli*. For pure culture, treated and untreated sCSO, the *pgl* gene continued to show the most damage, and the *ptsG* continued to show the least damage.

Comparison of All Targets

All targets had similar target concentrations and could be easily detected using qPCR, with the rRNA genes having the highest target concentration and the *ftsQ* gene having the least. Each target estimated a higher cell count that the IDEXX Colilert

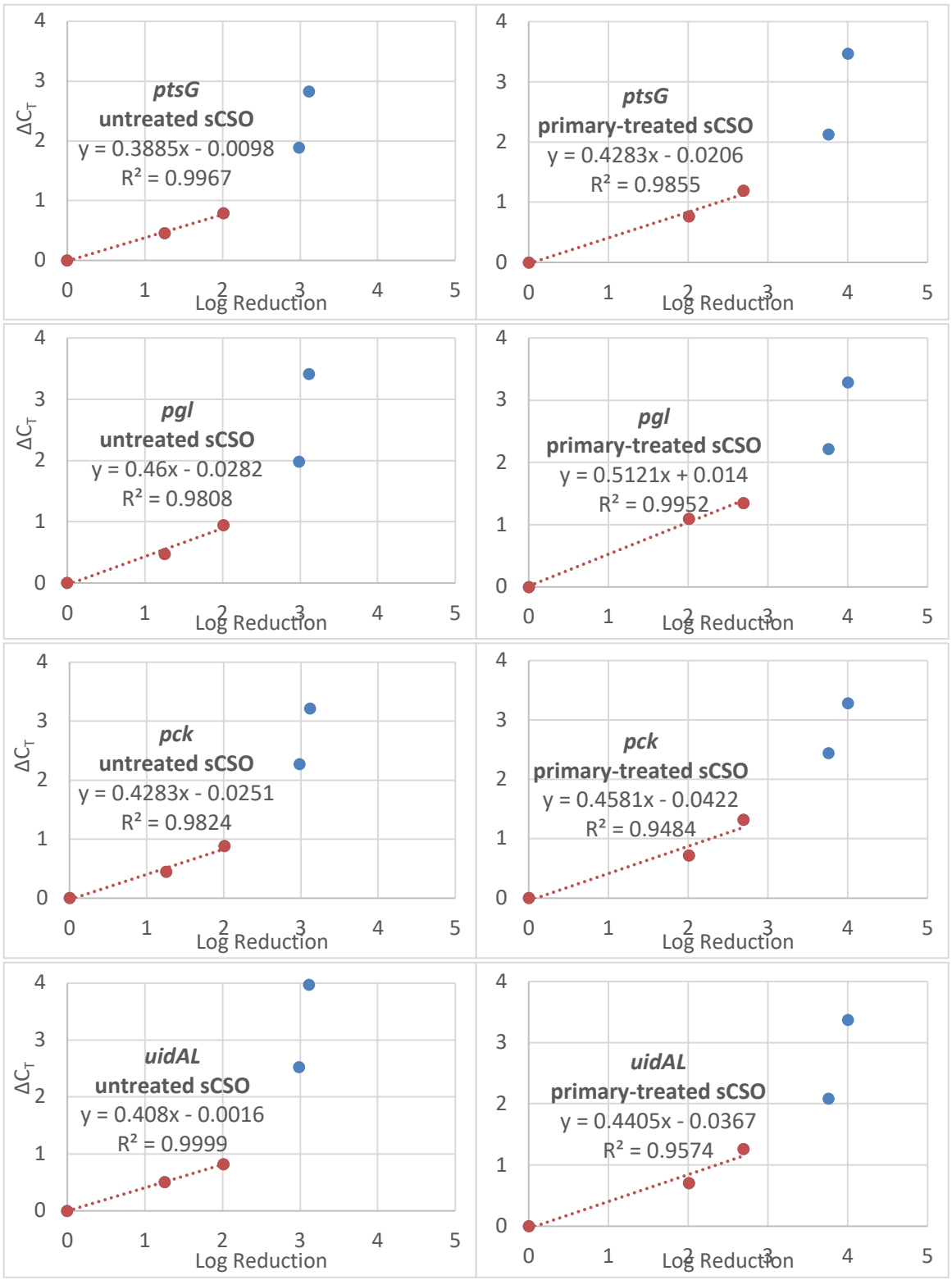

Figure 18: Correlation of culture-based and qPCR-based methods for selected metabolic genes with untreated and primary-treated sCSO samples.

method, which suggests that none of the targets were specific to *E. coli* and require improved primer design. The *uidA* target was the closest in estimating the *E. coli* count, but still on average 1-log higher. Nonetheless, the amount of UV damage that occurs is the difference between the C_T value at a specific dose and the initial C_T value. Even if the damage being detected is from other non-*E. coli* cells, UV is still fulfilling its role as a disinfectant. Furthermore, it induces damage to all the targets and therefore, causes widespread damage. As damage is done to gene targets that serve important functions, the cell will not be able to survive.

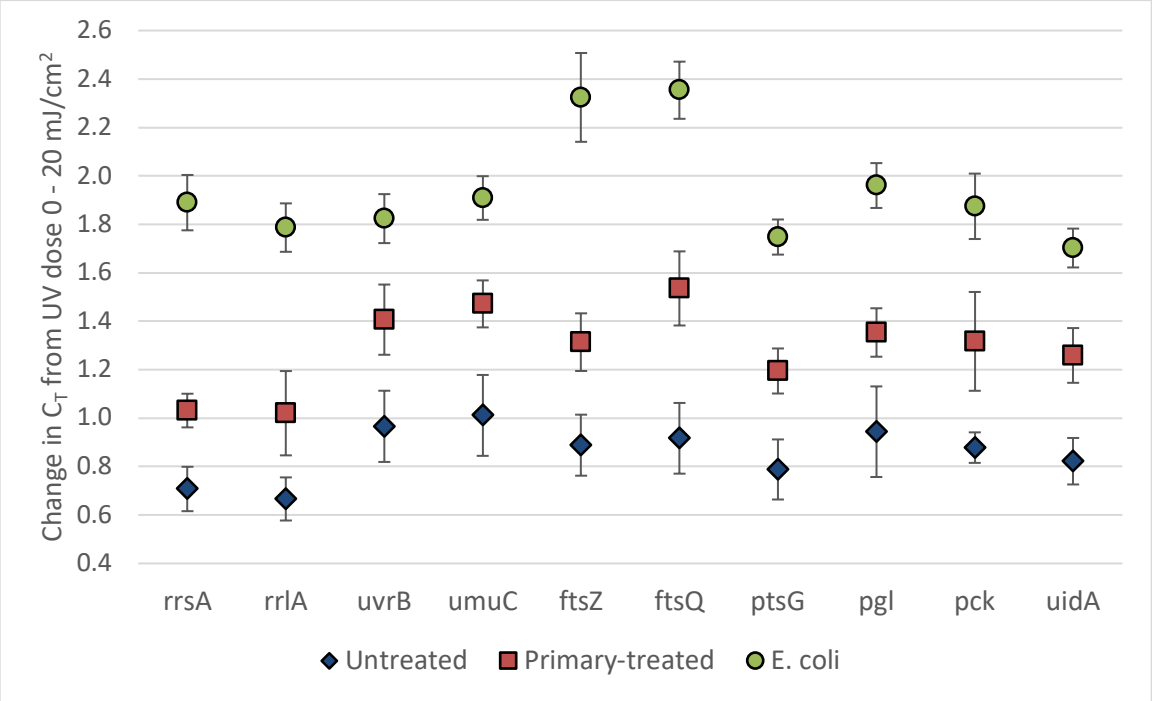

Figure 19: Change in C_T for each target from UV dose 0 – 20 mJ/cm^2 for all samples

Correlations were developed for targets within each category, and all showed a linear relationship between the range of 0 – 20 mJ/cm^2. Figure 19 compared the change in C_T for each target within the linear dose range of 0 – 20 mJ/cm^2 for all three sample

types: pure *E. coli* 8739, untreated sCSO, and primary-treated sCSO. With the pure *E. coli* culture, all gene targets had greater damage than with the CSO samples. This shows that the pure *E. coli* was more sensitive to UV than the *E. coli* obtained from wastewater. The particles in wastewater provided shielding to some *E. coli* from the UV light. With the pure *E. coli*, the cell division genes were found to be more sensitive. However, with the CSO samples, UV repair genes, cell division genes and metabolic genes are all equally sensitive. Between the CSO samples, the primary treatment aided in the effectiveness of UV to damage DNA. Overall, the results show that there is variation between the pure culture and sCSO samples. Therefore, if applying qPCR as a surrogate method for quantifying UV disinfection of CSO, CSO samples should be used for developing the correlations.

Conclusion

In order to target a major source of recreational water contamination, the effectiveness of UV radiation on CSO treatment was evaluated. UV kinetics showed that *E. coli* from wastewater was more resistant than *E. coli* grown in an ideal laboratory setting. The observed differences were assumed to be due to several factors: strain diversity, metabolic state, particle association and low water quality. UV disinfection efficiencies were quantified using IDEXX Colilert, a culturing technique, and qPCR. Based on the results of this study, the developed qPCR method can be applied for real-world application, such as quantifying UV disinfection of CSO. Evaluation of DNA damage to various gene targets demonstrated that UV light caused widespread genomic damage. The reduction from both culture-based and qPCR-based method were correlated

for each gene target and were linear within a certain range. Using the correlations, the qPCR method can serve as a rapid surrogate for traditional culture-based techniques. It is recommended that correlations be made with real CSO samples rather than simulated CSO or pure bacterial cultures.

References

Aslan, A., Kinzelman, J., Dreelin, E., Anan'eva, T., & Lavendar, J. (2015). A guidance document for testing recreational waters using USEPA qPCR method C.

Azimi, Y., Allen, D., & Farnood, R. (2012). Kinetics of UV inactivation of wastewater bioflocs. *Water Research, 46*, 3827-3836. doi:10.1016/j.watres.2012.04.019

Banihashemi, A., Van Dyke, M., & Huck, P. (2012). Long-amplicon propidium monoazide-PCR enumeration assay to detect viabl Campylobacter and Salmonella. Journal of Applied Microbiology, 113, 863-873. doi:10.1111/j.1365-2672.2012.05382.x

Bolton, J. R., & Linden, K. G. (2003). Standardization of methods for fluence (UV dose) determination in bench-scale UV experiments. Journal of Environmental Engineering, 129(3), 209-215.

Chatzisymeon, E., Droumpali, A., Mantzavinos, D., & Venieri, D. (2011). Disinfection of water and wastewater by UV-A and UV-C irradiation: application of real-time PCR method. *Photochemical & Photobiological Sciences, 10*, 389-395. doi:10.1039/c0pp00161a

Chick, H. An investigation of the Laws of Disinfection. J. Hyg., 8, 92, 1908.

Eramo, A., Morales Medina, W., & Fahrenfeld, N. (2017). Peracetic acid disinfection kinetics for combined sewer overflows: indicator organisms, antibiotic resistance genes, and microbial community. *Environmental Science Water Research & Technology*. doi:10.1039/c7ew00184c

Gehr, R., Wagner, M., Veerasubramanian, P., & Payment, P. (2003). Disinfection efficiency of peracetic acid, UV and ozone after enhanced primary treatment of municipal wastewater. *Water Research, 37*, 4573-4586. doi:10.1016/S0043-1354(03)00394-4

Hijnen, W., Beerendonk, E., & Medema, G. (2006). Inactivation credit of UV radiation for viruses, bacteria and protozoan (oo)cysts in water: a review. Water Research, 40, 3-22. doi:10.1016/j.watres.2005.10.030

Hoyer, O., 1998. Testing performance and monitoring of UV systems for drinking water disinfection. Water Supply 16 (1/2), 424–429.

Kibbee, R., & Ormeci, B. (2017). Development of a sensitive and false-positive free PMA-qPCR viability assay to quantify VBNC Escherichia coli and evaluate disinfection performance in wastewater effluent. Journal of Microbiological

Methods, 132, 139-147. doi:10.1016/j.mimet.2016.12.004Noor, E., Eden, E., Milo, R., & Alon, U. (2010). Central carbon metabolism as a minimal biochemical walk between precursor for biomass and energy. Molecular Cell, 39, 809-820. doi:10.1016/j.molcel.2010.08.031

Lazarova, V., Savoye, P., Janex, M., Blatchley III, E., & Pommepuy, M. (1999). Advanced wastewater disinfection technologies: state of the art and perspectives. *Water Science & Technology, 40*, 203-213.

Li, D., Tong, T., Zeng, S., Lin, Y., Wu, S., & He, M. (2014). Quantification of viable bacteria in wastewater treatment plants by using propidium monoazide combined with quantitative PCR (PMA-qPCR). Journal of Environmental Sciences, 26, 299-306. doi:10.1016/S1001-0742(13)60425-8

Madge, B., & Jensen, J. (2006). Ultraviolet disinfection of fecal coliform in municipal wastewater: effects of particle size. *Water Environment Research, 78*(3), 294-304.

Malley, J.P., Ballester, N.A., Margolin, A.B., Linden, K.G., Mofidi, A., Bolton, J.R., Crozes, G., Laine, J.M., Janex, M.L., 2004. Inactivation of Pathogens with Innovative UV Technologies. American Research Foundation and American Water Works Association, 2004.

Mamane-Gravetz, H., Linden, K.G., 2005. Relationship between physiochemical properties, aggregation and UV inactivation of isolated environmental spores in water. J. Appl. Microbiol. 98, 351–363.

Marsalek, J., & Rochfort, Q. (2004). Urban wet-weather flows: sources of fecal contamination impacting on recreational waters and threatening drinking-water sources. *Journal of Toxicology and Environmental Health, 67*, 1765-1777. doi:10.1018/15287390490492430

McLellan, S., Hollis, E., Depas, M., Van Dyke, M., Harris, J., & Scopel, C. (2007). Distribution and fate of Escherichia coli in Lake Michigan following contamination with urban stormwater and combined sewer overflows. Journal of Great Lakes Research, 33, 566-580.

MOECC. (2016, March 8). *F-5-5 Determination of treatment requirements for municipal and private combined and partially separated sewage systems*. Retrieved from https://www.ontario.ca/page/f-5-5-determination-treatment-requirements-municipal-and-private-combined

Nocker, A., Sossa, K., & Camper, A. (2007). Molecular monitoring of disinfection efficacy using propidium monoazide in combination with quantitative PCR.

Journal of Microbiological Methods, 70, 252-260. doi:10.1016/j.mimet.2007.04.014

Ormeci, B., Linden, K.G., 2002. Comparison of UV and chlorine inactivation of particle and non-particle associated coliforms. Water Sci. Technol.: Water Supply 2 (5-6), 403–410.

Shahraki, A., Chaganti, S., & Heath, D. (2018). Assessing high-throughput environmental DNA extraction methods for meta-barcode characterization of aquatic microbial communities. Journal of Water and Health, 17(1), 37-49. doi:10.2166/wh.2018.108

Sommer, R., Haider, T., Cabaj, A., Pribil,W., Lhotsky, M., 1998. Time fluence reciprocity in UV disinfection of water. Water Sci. Technol. 38 (12), 145–150.

Sommer, R., Lhotsky, M., Hairder, T., Cabaj, A., 2000. UV inactivation, liquid-holding recovery, and photoreaction of E. coli OH157 and other pathogenic E. coli strains in water. J. Food Prot. 63 (8), 1015–1020.

Süß, J., Volz, S., Obst, U., & Schwartz, T. (2009). Application of a molecular biology concept for the detection of DNA damage and repair during UV disinfection. Water Research, 43, 3705-3716. doi:10.1016.watres.2009.05.048

Templar, H., Dila, D., Bootsma, M., Corsi, S., & McLellan, S. (2016). Quantification of human-associated fecal indicators reveal sewage from urban watersheds as a source of pollution to Lake Michigan. Water Research, 100, 556-567. doi:10.1016/j.watres.2016.05.056

Tondera, K., Klaer, K., Gebhardt, J., Wingender, J., Koch, C., Horstkott, M., . . . Pinnekamp, J. (2015). Reducing pathogens in combined sewer overflows using ozonation or UV irradiation. International Journal of Hygiene and Environmental Health, 218, 731-741. doi:10.1016/j.ijheh.2015.09.002

Tondera, K., Klaer, K., Koch, C., Hamza, I. A., & Pinnekamp, J. (2016). Reducing pathogens in combined sewer overflows using performic acid. International Journal of Hygiene and Environmental Health, 219, 700-708. doi:10.1016/j.ijheh.2016.04.009

Watson, H.E. A note on the variation of the rate of disinfection with change in the concentration of the disinfectant. J. Hyg. 8, 536, 1908.

Weatherbe, D., & Sherbin, G. (1994). Urban drainage control demonstration program of Canada's Great Lakes Cleanup Fund. Water Science & Technology, 29, 455-462. doi:10.2166/wst.1994.0694

Whitby, E., & Scheible, K. (2004). The history of UV and wastewater. IUVA News, 6(3), 15-26.

CHAPTER 4:

CONCLUSIONS

Freshwater contamination attributed to high bacterial counts has been the most reported cause of water impairment in recent years (Marsalek & Rochfort, 2004; USEPA, 2012; Pandey et al., 2014). There have also been an increasing number of hospitalizations due to waterborne illnesses. The health of swimmers is of particular importance, because these individuals may come in direct contact with contaminated water. To limit the risk to bathers, regulatory agencies post advisories or close beaches when bacterial concentrations exceed certain thresholds. However, citizens continue to fall ill from poor recreational water quality, and this raises public concern. There is additional economic concern since beach closures and health care expenses reduce recreation and tourism revenue (DeFlorio-Barker et al., 2018).

A significant portion of the contamination has been due to urbanization, or more specifically, urban wet weather flow. Many municipalities still employ combined sewer systems, which tend to overflow during large rainfall events. These combined sewer overflows (CSO) transport not only stormwater runoff, but also untreated sewage to receiving waters. Similarly, sanitary sewer overflows (SSO) may also occur as a result of heavy precipitation, also transporting untreated sewage. Understanding the hazard that these sewer overflows pose to human health, regulatory agencies such as the Ministry of Environment and Climate Change (MOECC) have put together procedures and regulations to establish controls for overflow events (MOECC, 2016). In Ontario, Procedure F-5-5 describes the minimum level of treatment required for CSO that occur in

areas upstream of recreational waters, including primary level treatment of solids and disinfection. For disinfection, three types of methods are commonly used: chlorination, ozonation, and UV radiation. Compared to the other two chemical disinfectants, UV light has gained popularity over time, as it does not produce any known disinfection by-products and has a greater germicidal ability. Therefore, UV was chosen as the disinfectant for this thesis.

The efficacy of treatment is generally measured by standard microbiological methods, which involve culturing techniques. The main drawback of these methods is the long incubation times, thereby delaying beach advisories for the public. Thus, rapid molecular techniques have been explored as alternatives. Currently, the USEPA has issued Draft Method C for *Escherichia coli* detection using qPCR (Aslan et al., 2015). Others have also developed qPCR-based techniques for detection of various waterborne microorganisms. Yet these methods have been suggested for detection and monitoring purposes only, and application with disinfection technologies has not been tested.

Therefore, the ultimate goal for Chapter 2 was to develop a robust method that would be able to quantify UV inactivation of *E. coli*. In order to achieve this, long amplicon qPCR (LA-qPCR) was used with various gene targets. The study conducted a genomic scan of *E. coli* to determine the effect of UV light on different areas of the genome. The results from this study show evidence of widespread damage across the genome, affecting many essential genes and impairing many crucial cellular functions. Furthermore, certain targets were found to be more susceptible to UV damage than others. In particular, the cell division genes *ftsZ* and *ftsQ* were more damaged after UV exposure, whereas the metabolic genes were the least damaged. Damage done to the

conventionally used rRNA gene targets was similar to that of both UV repair and metabolic genes.

Another objective of Chapter 2 was to determine a 'good target' that can be used for quantifying UV damage to *E. coli* with qPCR. It was determined that a suitable target should be present in high concentration in *E. coli*, and be sensitive enough to detect UV damage. Since the sample only contained *E. coli* 8739 cells, specificity to *E. coli* was not tested. All targets were found in high concentration and sensitive. Overall, the cell division genes *ftsZ* and *ftsQ* were the most sensitive to damage. These targets were suggested to be used for quantifying UV damage. If damage done to other gene targets is of interest, a ratio can be calculated based on this study to determine the damage done to the selected target as compared to the cell division gene.

Lastly, results from Chapter 2 showed the correlation between culture-based and qPCR-based methods. The correlation plots show a linear relationship up to a 5-log reduction, or a UV dose of 20 mJ/cm^2. Applying these correlations allows qPCR to serve as a surrogate to the conventional culturing method, and significantly reduces the time between sampling and reporting.

In Chapter 3, the application of the developed qPCR method was tested with artificially generated CSO samples. These samples were made with one-part wastewater and one-part tap water. The main risk lies in the untreated wastewater. As per Procedure F-5-5, primary-treated CSO samples were also used to determine the effect of treatment on UV disinfection.

UV disinfection kinetics revealed several difference between the pure *E. coli* culture used in Chapter 2 and the simulated CSO (sCSO) samples used in Chapter 3. The effectiveness of UV was lower for sCSO, which was assumed to be attributed to the diversity of bacterial strains in wastewater, the different physiological states of the cells, the association with or shielding by particles. All of these factors have been mentioned in previous studies as limiting the disinfection capabilities of UV light (Gehr et al., 2003; Hijnen et al., 2006). Primary treatment improved the efficacy of UV disinfection. The inactivation rates were found to be twice as fast as the untreated sCSO samples. For a 2-log reduction, primary-treated effluent required 10 mJ/cm^2 of UV, whereas the untreated needed twice as much. Additionally, for the primary effluent, UV inactivation continued to occur past 3-log, whereas the dose-response curve of the untreated sCSO started tailing.

The developed qPCR method was used to quantify the damage done to various gene targets. All gene targets showed damage, again emphasizing that UV light causes widespread damage to the genome. When applying this method to the real-world samples, it was found that the primers designed may not be specific to only *E. coli*. The primers over-estimated the initial *E. coli* count, as compared to Colilert. Nonetheless, damage was still calculated as the difference between pre-UV and post-UV exposure. The amount of DNA damage caused by UV was also found to be greater than the pure *E. coli* 8739 culture.

The correlations developed for the sCSO samples were linear in the range of 0 – 20 mJ/cm^2, similar to the pure culture. Although the primer may not be specific enough, the correlations still indicate that the qPCR method can be used as a surrogate for

traditional methods. It is recommended that correlations be made using primers that are more specific to *E. coli*.

Recommendations for Future Work

Molecular techniques for quantifying bacteria, such as qPCR, are much faster than the conventional culturing techniques. It must be noted that when determining disinfection efficiencies, the two methods have different aims: culturing methods quantify the reduction in culturability (often as log reductions), and qPCR techniques quantify the damage of a specific target area in the genome. qPCR methods may be DNA- or RNA-based. Although DNA-based methods are easier and more commonly used, RNA methods have several advantages. RNA provides more information on the viability of a cell, and especially with the controversy of viable but non-culturable (VBNC) post-UV exposure, RNA would give a better representation of the viable bacterial population. Weigel et al., (2017) use a technique called molecular viability testing (MVT) which correlates the viability of a cell with its ability to rapidly produce rRNA precursors (pre-rRNA) in response to nutritional stimuli. After UV exposure, samples were briefly exposed to nutrients in order to increase the amount of pre-rRNA. It was assumed that only those cells that are viable would be able to produce pre-rRNA. This is an improvement from DNA, since even when cell death occurs, the structure of DNA is stable enough to allow it to persist in the environment. Detecting DNA from dead cells would skew the results. On that note, future work should aim to develop and test a robust RNA-based qPCR method for quantifying UV disinfection.

Another improvement that can be made on the method development side is the use of more specific primers and employing TaqMan probes. In this study, SYBR Green qPCR was used. SYBR Green is a fluorescent dye used in molecular biology as a nucleic acid stain. It binds to double-stranded DNA (dsDNA), and once attached, it absorbs blue light and emits an intense green signal which is quantified by the qPCR machine. This technique is not target-specific because the dye will bind to any dsDNA fragment. Often primer-dimers give false signal from SYBR Green. TaqMan is an alternative to SYBR Green to monitor the process of amplification. This technique uses a dual-labeled probe, which are DNA oligonucleotides that have a fluorescent reporter on the 5' end and a quencher on the 3' end. When the report and quencher are in close proximity, no signal is given off. During the elongation step of PCR, Taq polymerase degrades the probe, separating the reporter and quencher and thereby emitting a fluorescent signal which the qPCR machine detects. Compared to SYBR Green, TaqMan is more specific because the unique design of the probe allows for specific PCR products (Tajadini et al., 2014). In this study, SYBR Green was chosen as the method since it is easier to use and cheaper, especially with all the gene targets. However, results from this thesis show that it is crucial to have specific PCR products if qPCR methods are to be applied in real-world situations.

Lastly, to expand on the application of qPCR for detecting UV inactivation, other sources of recreational water pollution should be explored. Although CSO and SSO are the major sources of pollution, there are other non-point sources such as stormwater runoff, bird droppings and animal wastes. The pollution from CSO and SSO was studied in this thesis because there is infrastructure already in place that allows for

implementation of disinfection technologies. For example, UV disinfection may be implemented with overflow retention basins. Aiming to reduce beach closures, a research group from the University of Wisconsin implemented an on-site treatment system (Reimer et al., 2018). This type of system is able to address non-point source pollution. In an inland lake, a five-sided polypropylene barrier enclosed the swimming area of the beach. Within this area, an inlet pipe took in water which passed through an on-site portable treatment system and was then discharged back into the beach through the effluent pipe. The on-site treatment system used three steps: straining of heavy debris, filtration of fine particles, and finally disinfection using UV light. This system was the first of its kind to be successfully employed in the US. The application of such on-site UV treatment trailers should be explored further.

The study conducted by Reimer et al. (2018) used Colilert-18 to quantify the efficacy of UV disinfection. The application of qPCR methods for these types of systems should also be explored, in order to report results faster. One possible drawback of using qPCR with beach water is the low cell count. With the primers and techniques used in this thesis, the qPCR was not sensitive enough to detect the low cell concentrations that are expected to be found in beach water. Large volumes of beach water would need to be filtered in order to detect some qPCR signal.

Overall, UV radiation is an effective disinfection technique that can be used to decrease the microbial pollution from CSO and SSO to receiving waters. Additionally, qPCR is a very promising technique that serves as a faster alternative to traditional culture-based methods. In addition to being used for detection and monitoring, it can be used for quantifying UV disinfection efficiencies.

References

Aslan, A., Kinzelman, J., Dreelin, E., Anan'eva, T., & Lavendar, J. (2015). A guidance document for testing recreational waters using USEPA qPCR method C.

DeFlorio-Barker, S., Wing, C., Jones, R., & Dorevitch, S. (2018). Estimate of incidence and cost of recreational waterborne illness on United States surface waters. Environmental Health, 17(3). doi:10.1186/s12940-017-0347-9

Gehr, R., Wagner, M., Veerasubramanian, P., & Payment, P. (2003). Disinfection efficiency of peracetic acid, UV and ozone after enhanced primary treatment of municipal wastewater. *Water Research, 37*, 4573-4586. doi:10.1016/S0043-1354(03)00394-4

Hijnen, W., Beerendonk, E., & Medema, G. (2006). Inactivation credit of UV radiation for viruses, bacteria and protozoan (oo)cysts in water: a review. Water Research, 40, 3-22. doi:10.1016/j.watres.2005.10.030

Marsalek, J., & Rochfort, Q. (2004). Urban wet-weather flows: sources of fecal contamination impacting on recreational waters and threatening drinking-water sources. *Journal of Toxicology and Environmental Health, 67*, 1765-1777. doi:10.1018/15287390490492430

MOECC. (2016, March 8). *F-5-5 Determination of treatment requirements for municipal and private combined and partially separated sewage systems*. Retrieved from https://www.ontario.ca/page/f-5-5-determination-treatment-requirements-municipal-and-private-combined

Pandey, P., Kass, P., Soupir, M., Biswas, S., & Singh, V. (2014). Contamination of water resources by pathogenic bacteria. AMB Express, 4(51). Retrieved from http://www.amb-express.com/content/4/1/51

Reimer, J., Wu, C., & Sorsa, K. (2018). Water exclosure treatment system (WETS): an innovative device for minimizing beach closures. *Science of the Total Environment, 625*, 809-818. doi:10.1016/j.scitotenv.2017.12.330

Tajadini, M., Panjehpour, M., & Javanmard, S. (2014). Comparison of SYBR Green and TaqMan methods in quantitative real-time polymerase chain reaction analysis of four adenosine receptor subtypes. *Advanced Biomedical Research, 3*(85). doi:10.4103/3377-9175.127998

USEPA. (2012). Summaries of water pollution reporting categories. Retrieved from https://watersgeo.epa.gov/ATTAINS/34PARENTATTAINSDESCRIPTIONS.pdf

Weigel, K., Nguyen, F., Kearney, M., Meschke, J., & Cangelosi, G. (2017). Molecular viability testing of UV-inactivated bacteria. *Applied and Environmental Microbiology, 83*(10). doi:10.1128/AEM.00331-17

Appendix A: Supplementary Information for Chapter 2

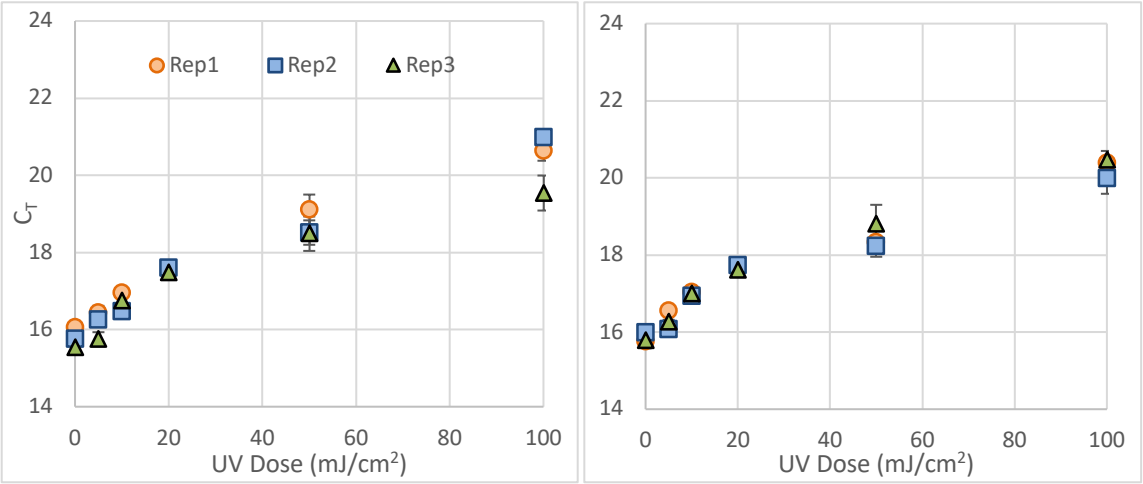

Figure 20: qPCR-based dose-response curves of rRNA genes, *rrsA* (left) and *rrlA* (right). Error bars represent the standard deviation between replicates. Some error bars are smaller than the markers.

Table 5: qPCR results for *rrsA*, used for dose-response curve.

Target	Replicate	Dose	$C_{T\ AVG}$	St. Dev.
rrsA	1	0	16.053	0.149
		5	16.432	0.182
		10	16.954	0.113
		20		
		50	19.110	0.390
		100	20.626	0.248
	2	0	15.755	0.147
		5	16.259	0.058
		10	16.465	0.119
		20	17.593	0.104
		50	18.515	0.317
		100	20.975	0.067
	3	0	15.543	0.069
		5	15.750	0.182
		10	16.757	0.120
		20	17.475	0.113
		50	18.485	0.446
		100	19.540	0.454

Table 6: qPCR results for *rrlA*, used for dose-response curve.

Target	Replicate	Dose	$C_{T\ AVG}$	St. Dev.
rrlA	1	0	15.754	0.176
		5	16.550	0.055
		10	17.023	0.090
		20		
		50	18.324	0.301
		100	20.381	0.317
	2	0	15.986	0.091
		5	16.068	0.129
		10	16.930	0.124
		20	17.734	0.137
		50	18.223	0.270
		100	19.987	0.400
	3	0	15.792	0.060
		5	16.269	0.048
		10	17.004	0.136
		20	17.616	0.028
		50	18.804	0.497
		100	20.464	0.081

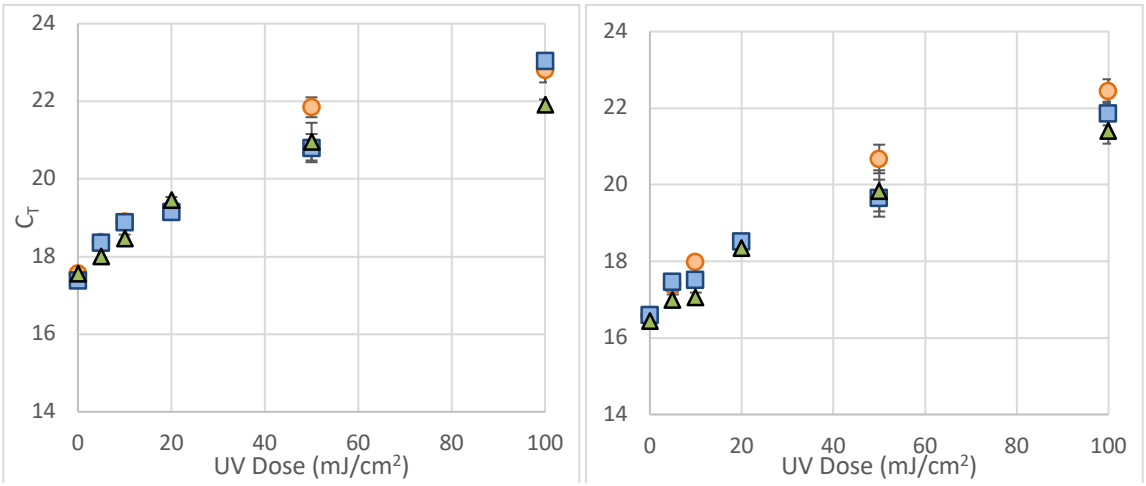

Figure 21: qPCR-based dose-response curves of UV repair genes, *uvrB* (left) and *umuC* (right). Error bars represent the standard deviation between replicates. Some error bars are smaller than the markers.

Table 7: qPCR results for *uvrB*, used for dose-response curve.

Target	Replicate	Dose	$C_{T\ AVG}$	St. Dev.
uvrB	1	0	17.558	0.070
		5	18.378	0.144
		10	18.896	0.163
		20		
		50	21.846	0.256
		100	22.802	0.315
	2	0	17.385	0.117
		5	18.363	0.116
		10	18.875	0.145
		20	19.145	0.085
		50	20.792	0.363
		100	23.031	0.053
	3	0	17.572	0.079
		5	18.017	0.125
		10	18.478	0.087
		20	19.459	0.076
		50	20.960	0.486
		100	21.917	0.130

Table 8: qPCR results for *umuC*, used for dose-response curve.

Target	Replicate	Dose	Ct Avg	St Dev
umuC	1	0	16.574	0.097
		5	17.378	0.176
		10	17.979	0.107
		20		
		50	20.673	0.374
		100	22.443	0.313
	2	0	16.604	0.092
		5	17.466	0.069
		10	17.514	0.183
		20	18.518	0.072
		50	19.651	0.484
		100	21.859	0.310
	3	0	16.451	0.033
		5	16.990	0.144
		10	17.062	0.122
		20	18.355	0.110
		50	19.840	0.537
		100	21.404	0.332

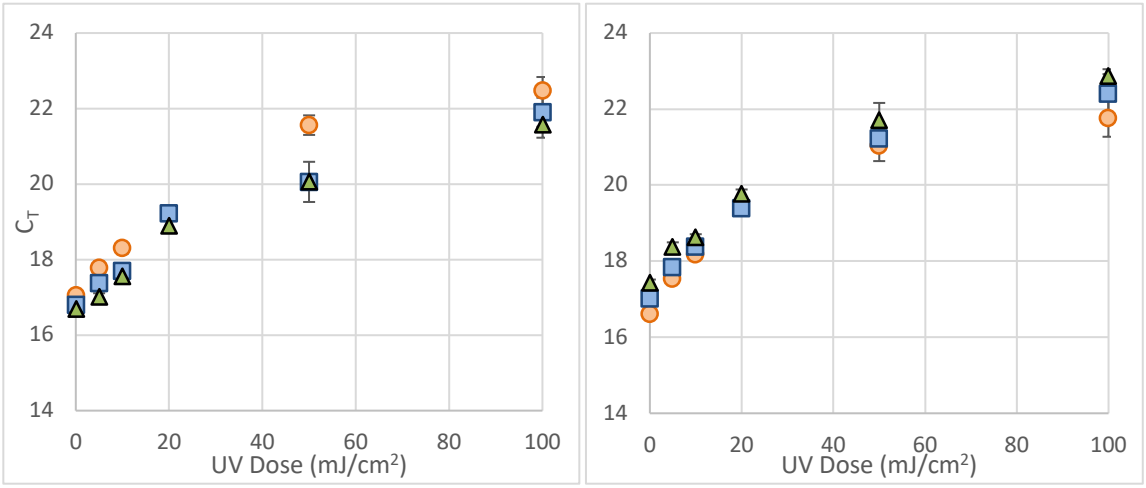

Figure 22: qPCR-based dose-response curves of cell division genes, *ftsZ* (left) and *ftsQ* (right). Error bars represent the standard deviation between replicates. Some error bars are smaller than the markers.

Table 9: qPCR results for *ftsZ*, used for dose-response curve.

Target	Replicate	Dose	Ct Avg	St Dev
ftsZ	1	0	17.050	0.124
		5	17.785	0.160
		10	18.297	0.148
		20		
		50	21.561	0.259
		100	22.477	0.359
	2	0	16.789	0.054
		5	17.363	0.103
		10	17.697	0.116
		20	19.214	0.124
		50	20.044	0.180
		100	21.902	0.384
	3	0	16.692	0.065
		5	17.011	0.098
		10	17.557	0.101
		20	18.894	0.176
		50	20.058	0.532
		100	21.573	0.345

Table 10: qPCR results for *ftsQ*, used for dose-response curve.

Target	Replicate	Dose	Ct Avg	St Dev
ftsQ	1	0	16.611	0.027
		5	17.540	0.045
		10	18.173	0.095
		20		
		50	21.035	0.403
		100	21.761	0.489
	2	0	17.019	0.118
		5	17.837	0.150
		10	18.384	0.159
		20	19.390	0.133
		50	21.212	0.226
		100	22.406	0.514
	3	0	17.432	0.086
		5	18.371	0.125
		10	18.632	0.078
		20	19.768	0.118
		50	21.708	0.454
		100	22.869	0.180

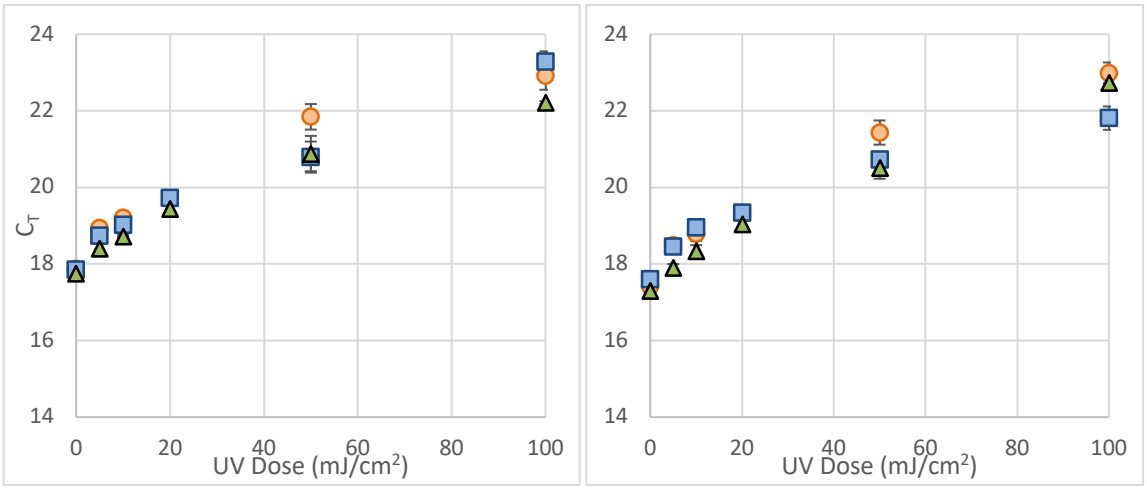

Figure 23: qPCR-based dose-response curves of two metabolic genes, *gltA* (left) and *ptsG* (right). Error bars represent the standard deviation between replicates. Some error bars are smaller than the markers.

Table 11: qPCR results for *gltA*, used for dose-response curve.

Target	Replicate	Dose	Ct Avg	St Dev
gltA	1	0	17.875	0.116
		5	18.948	0.096
		10	19.215	0.109
		20		
		50	21.843	0.333
		100	22.916	0.366
	2	0	17.854	0.077
		5	18.738	0.029
		10	19.025	0.069
		20	19.725	0.104
		50	20.791	0.406
		100	23.290	0.262
	3	0	17.750	0.096
		5	18.403	0.130
		10	18.731	0.028
		20	19.439	0.110
		50	20.883	0.461
		100	22.216	0.036

Table 12: qPCR results for *ptsG*, used for dose-response curve.

Target	Replicate	Dose	Ct Avg	St Dev
ptsG	1	0	17.425	0.084
		5	18.485	0.166
		10	18.788	0.190
		20		
		50	21.432	0.316
		100	22.991	0.270
	2	0	17.597	0.130
		5	18.464	0.105
		10	18.950	0.088
		20	19.340	0.055
		50	20.732	0.100
		100	21.809	0.305
	3	0	17.298	0.106
		5	17.907	0.090
		10	18.334	0.158
		20	19.049	0.087
		50	20.513	0.286
		100	22.735	0.179

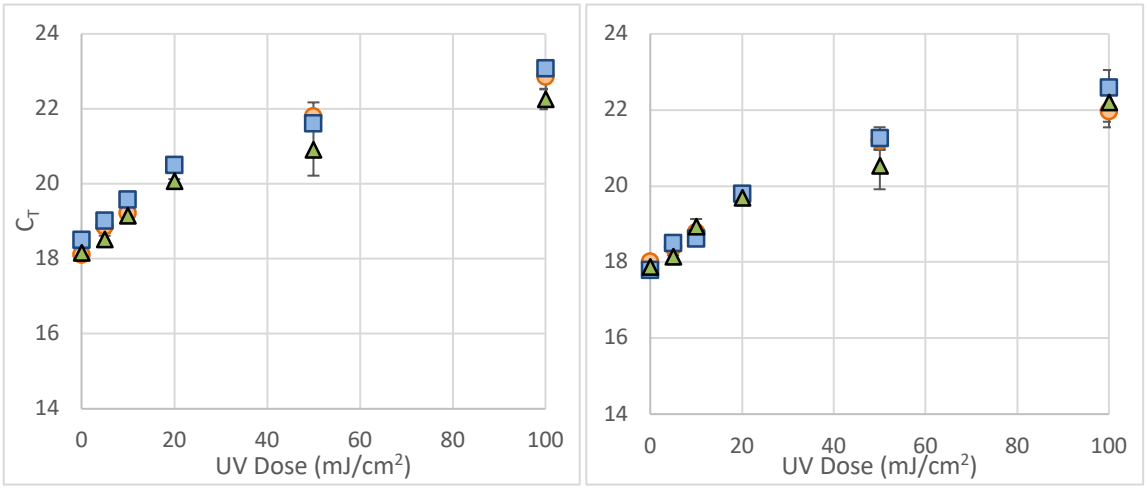

Figure 24: qPCR-based dose-response curves of two metabolic genes, *pgl* (left) and *tktA* (right). Error bars represent the standard deviation between replicates. Some error bars are smaller than the markers.

Table 13: qPCR results for *pgl*, used for dose-response curve.

Target	Replicate	Dose	Ct Avg	St Dev
pgl	1	0	18.109	0.092
		5	18.860	0.169
		10	19.210	0.196
		20		
		50	21.794	0.379
		100	22.857	0.337
	2	0	18.503	0.149
		5	19.021	0.125
		10	19.569	0.030
		20	20.499	0.115
		50	21.607	0.172
		100	23.079	0.090
	3	0	18.151	0.039
		5	18.523	0.095
		10	19.154	0.139
		20	20.076	0.051
		50	20.909	0.691
		100	22.262	0.273

Table 14: qPCR results for *tktA*, used for dose-response curve.

Target	Replicate	Dose	Ct Avg	St Dev
tktA	1	0	17.999	0.165
		5	18.385	0.207
		10	18.784	0.079
		20		
		50	21.181	0.234
		100	21.967	0.424
	2	0	17.793	0.075
		5	18.489	0.134
		10	18.607	0.179
		20	19.794	0.115
		50	21.258	0.287
		100	22.585	0.464
	3	0	17.873	0.164
		5	18.134	0.193
		10	18.927	0.204
		20	19.696	0.053
		50	20.529	0.615
		100	22.204	0.515

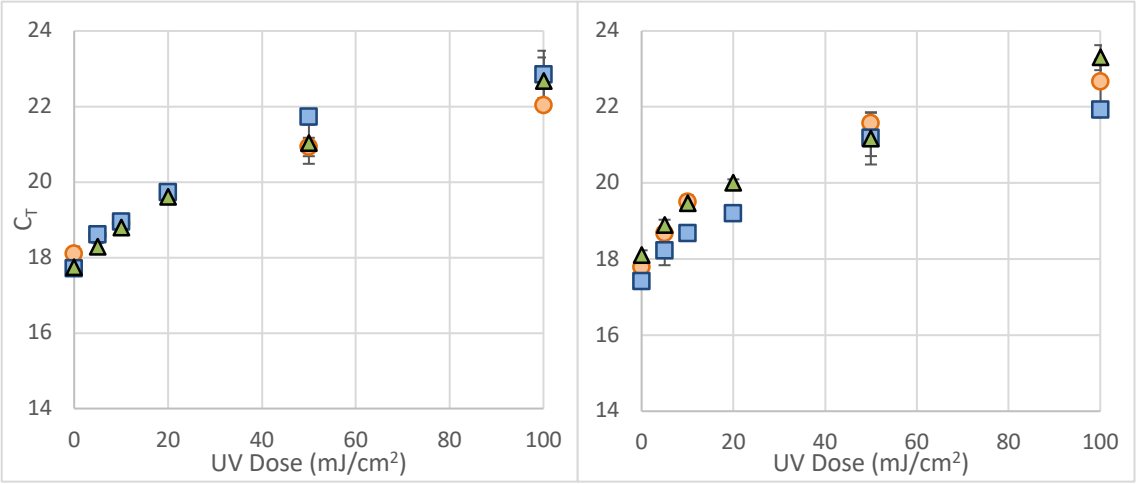

Figure 25: qPCR-based dose-response curves of two metabolic genes, *fbaA* (left) and *tpiA* (right). Error bars represent the standard deviation between replicates. Some error bars are smaller than the markers.

Table 15: qPCR results for *fbaA*, used for dose-response curve.

Target	Replicate	Dose	Ct Avg	St Dev
fbaA	1	0	18.104	0.185
		5	18.587	0.097
		10	18.890	0.195
		20		
		50	20.927	0.244
		100	22.023	0.061
	2	0	17.709	0.083
		5	18.605	0.181
		10	18.936	0.120
		20	19.727	0.068
		50	21.717	0.201
		100	22.850	0.627
	3	0	17.740	0.172
		5	18.276	0.105
		10	18.797	0.093
		20	19.612	0.064
		50	21.034	0.552
		100	22.671	0.628

Table 16: qPCR results for *tpiA*, used for dose-response curve.

Target	Replicate	Dose	Ct Avg	St Dev
tpiA	1	0	17.790	0.109
		5	18.670	0.104
		10	19.506	0.181
		20		
		50	21.565	0.298
		100	22.659	0.590
	2	0	17.408	0.069
		5	18.217	0.377
		10	18.674	0.053
		20	19.198	0.108
		50	21.178	0.469
		100	21.923	0.196
	3	0	18.107	0.125
		5	18.893	0.143
		10	19.461	0.164
		20	20.001	0.097
		50	21.168	0.680
		100	23.298	0.329

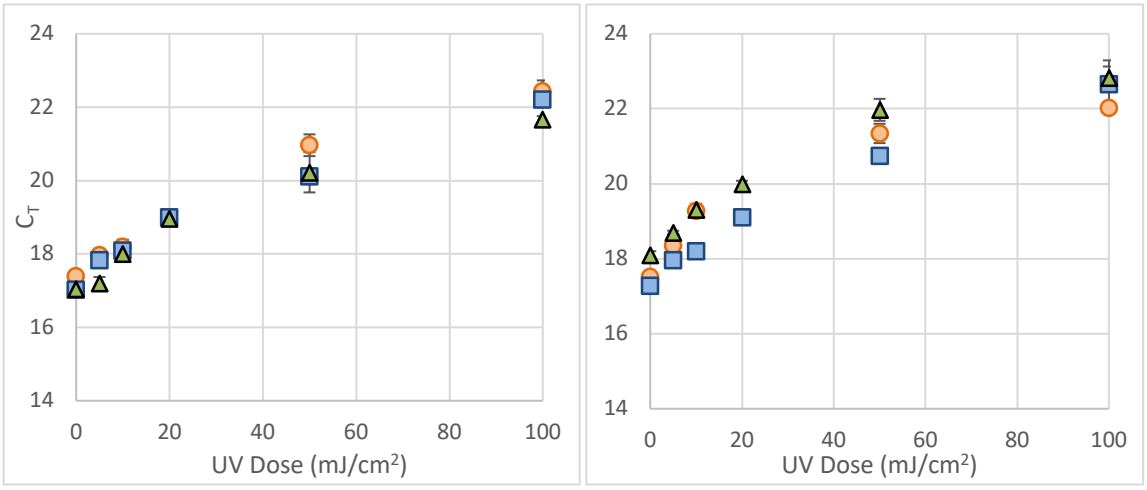

Figure 26: qPCR-based dose-response curves of two metabolic genes, *ppsA* (left) and *pck* (right). Error bars represent the standard deviation between replicates. Some error bars are smaller than the markers.

Table 17: qPCR results for *ppsA*, used for dose-response curve.

Target	Replicate	Dose	Ct Avg	St Dev
ppsA	1	0	17.389	0.083
		5	17.964	0.117
		10	18.192	0.054
		20		
		50	20.964	0.296
		100	22.432	0.300
	2	0	17.037	0.142
		5	17.836	0.050
		10	18.096	0.295
		20	19.008	0.034
		50	20.111	0.208
		100	22.218	0.214
	3	0	17.055	0.076
		5	17.198	0.175
		10	18.013	0.095
		20	18.958	0.110
		50	20.226	0.548
		100	21.664	0.095

Table 18: qPCR results for *pck*, used for dose-response curve.

Target	Replicate	Dose	Ct Avg	St Dev
pck	1	0	17.519	0.055
		5	18.351	0.160
		10	19.283	0.180
		20		
		50	21.343	0.257
		100	22.026	0.036
	2	0	17.283	0.104
		5	17.970	0.205
		10	18.203	0.122
		20	19.111	0.199
		50	20.741	0.208
		100	22.663	0.629
	3	0	18.091	0.112
		5	18.703	0.045
		10	19.309	0.152
		20	20.000	0.081
		50	21.973	0.293
		100	22.821	0.308

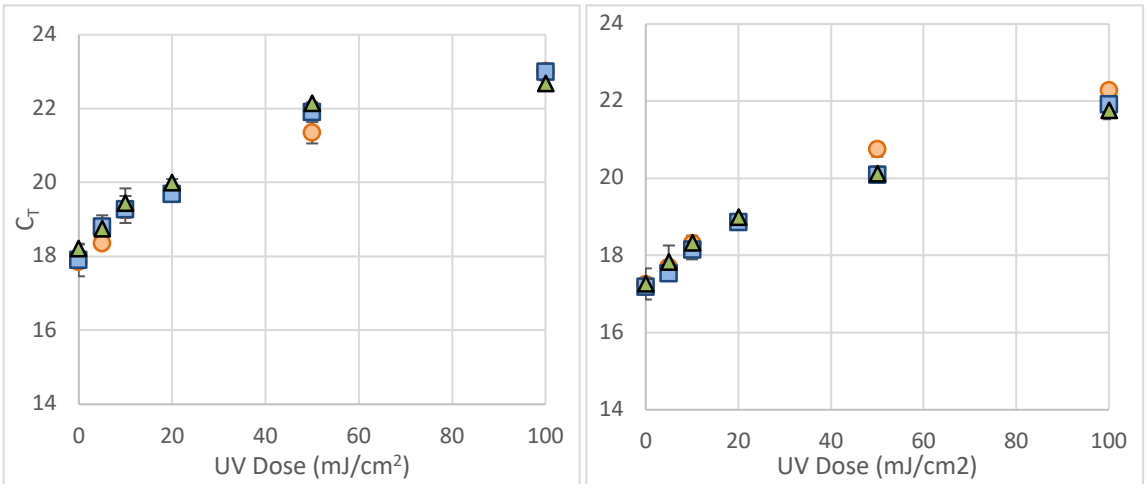

Figure 27: qPCR-based dose-response curves of two metabolic genes, *dfp* (left) and *uidAL* (right). Error bars represent the standard deviation between replicates. Some error bars are smaller than the markers.

Table 19: qPCR results for *dfp*, used for dose-response curve.

Target	Replicate	Dose	Ct Avg	St Dev
dfp	1	0	17.847	0.165
		5	18.352	0.067
		10	19.245	0.178
		20		
		50	21.345	0.288
		100	23.004	0.075
	2	0	17.893	0.430
		5	18.799	0.121
		10	19.270	0.366
		20	19.682	0.068
		50	21.888	0.153
		100	22.995	0.137
	3	0	18.199	0.144
		5	18.750	0.364
		10	19.445	0.397
		20	19.998	0.094
		50	22.141	0.033
		100	22.667	0.095

Table 20: qPCR results for *uidAL*, used for dose-response curve.

Target	Replicate	Dose	Ct Avg	St Dev
uidAL	1	0	17.242	0.105
		5	17.691	0.129
		10	18.314	0.093
		20		
		50	20.743	0.180
		100	22.280	0.158
	2	0	17.172	0.177
		5	17.533	0.114
		10	18.134	0.235
		20	18.859	0.080
		50	20.077	0.074
		100	21.916	0.210
	3	0	17.262	0.404
		5	17.831	0.428
		10	18.329	0.185
		20	18.980	0.085
		50	20.116	0.192
		100	21.760	0.227

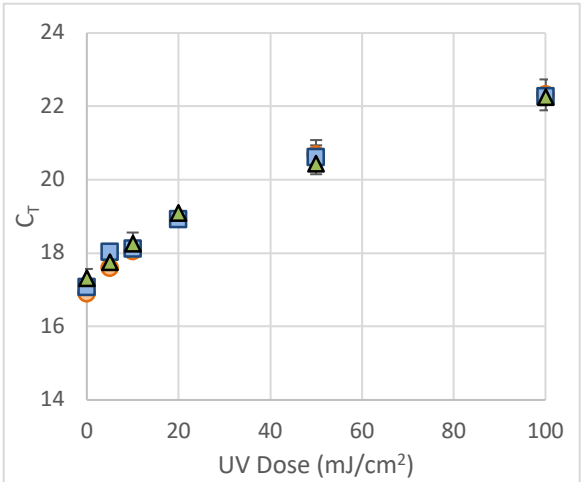

Figure 28: qPCR-based dose-response curves of metabolic gene, *gadA*. Error bars represent the standard deviation between replicates. Some error bars are smaller than the markers.

Table 21: qPCR results for *gadA*, used for dose-response curve.

Target	Replicate	Dose	Ct Avg	St Dev
gadA	1	0	16.903	0.151
		5	17.596	0.042
		10	18.043	0.097
		20		
		50	20.688	0.395
		100	22.315	0.421
	2	0	17.068	0.051
		5	18.037	0.083
		10	18.115	0.178
		20	18.924	0.083
		50	20.614	0.326
		100	22.277	0.226
	3	0	17.315	0.255
		5	17.752	0.218
		10	18.261	0.301
		20	19.097	0.030
		50	20.445	0.293
		100	22.259	0.224

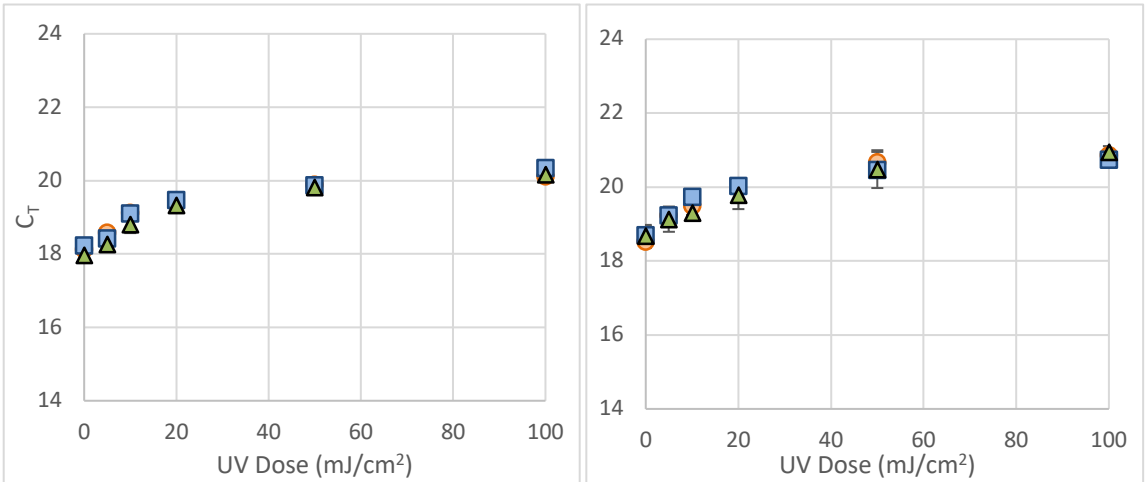

Figure 29: qPCR-based dose-response curves of two short amplicon targets, 23S (left) and *uidAS* (right). Error bars represent the standard deviation between replicates. Some error bars are smaller than the markers.

Table 22: qPCR results for 23S, used for dose-response curve.

Target	Replicate	Dose	Ct Avg	St Dev
23S	1	0	18.135	0.060
		5	18.577	0.135
		10	19.119	0.126
		20		
		50	19.882	0.058
		100	20.108	0.117
	2	0	18.232	0.051
		5	18.428	0.083
		10	19.099	0.061
		20	19.475	0.023
		50	19.879	0.188
		100	20.350	0.049
	3	0	17.973	0.105
		5	18.259	0.043
		10	18.803	0.234
		20	19.327	0.055
		50	19.824	0.054
		100	20.176	0.132

Table 23: qPCR results for *uidAS*, used for dose-response curve.

Target	Replicate	Dose	Ct Avg	St Dev
uidAS	1	0	18.531	0.178
		5	19.234	0.176
		10	19.497	0.077
		20		
		50	20.675	0.276
		100	20.859	0.073
	2	0	18.704	0.243
		5	19.242	0.196
		10	19.735	0.090
		20	20.023	0.141
		50	20.458	0.188
		100	20.747	0.116
	3	0	18.688	0.290
		5	19.133	0.342
		10	19.313	0.065
		20	19.783	0.378
		50	20.486	0.512
		100	20.953	0.156

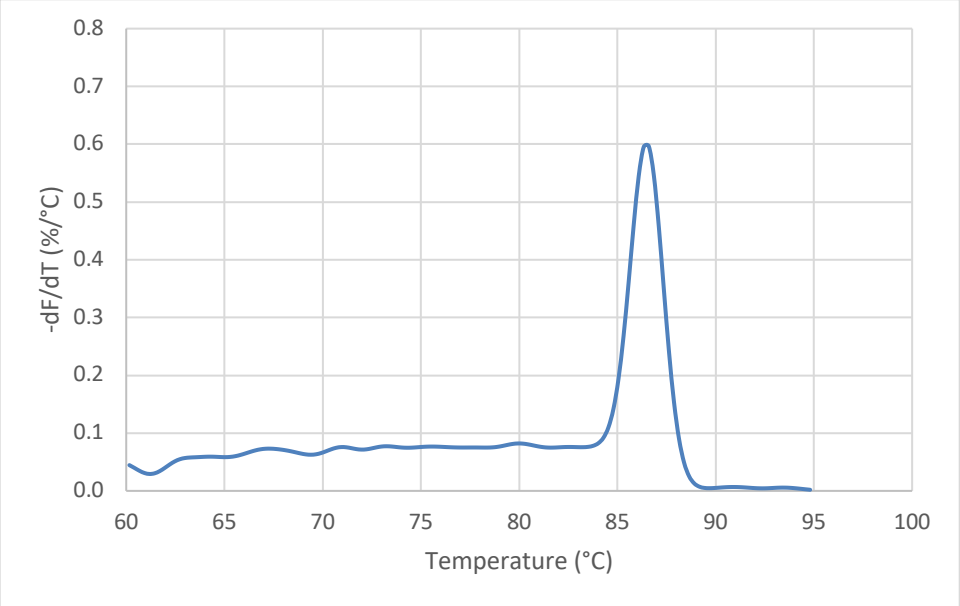

Figure 30: Melt curve for rRNA gene *rrsA*

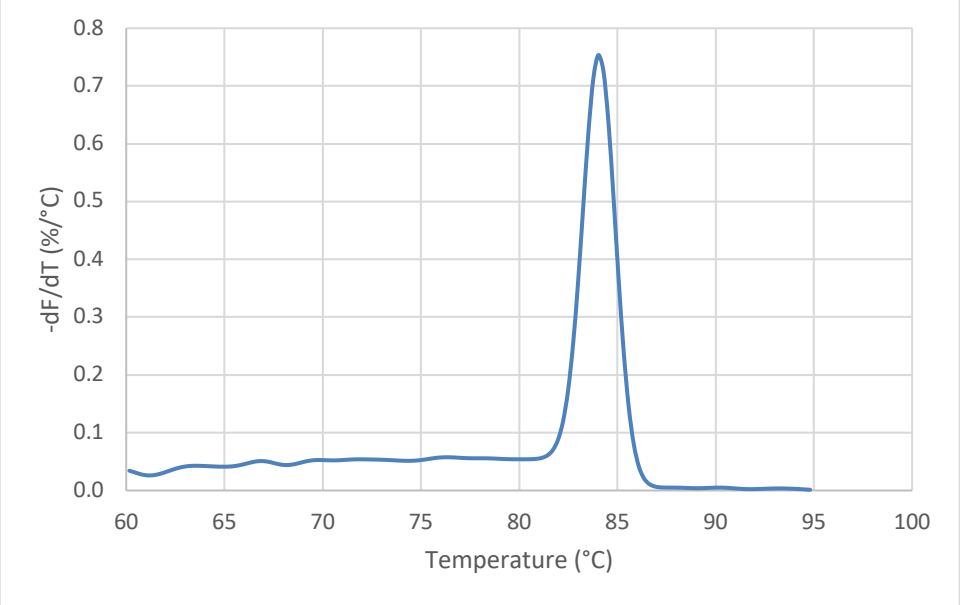

Figure 31: Melt curve for rRNA gene *rrlA*

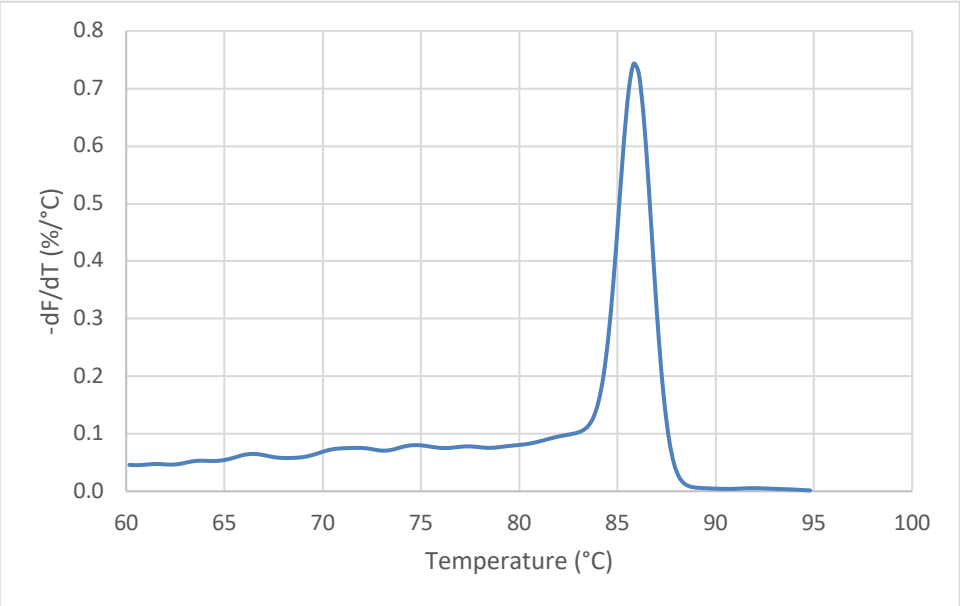

Figure 32: Melt curve for UV repair gene *uvrB*

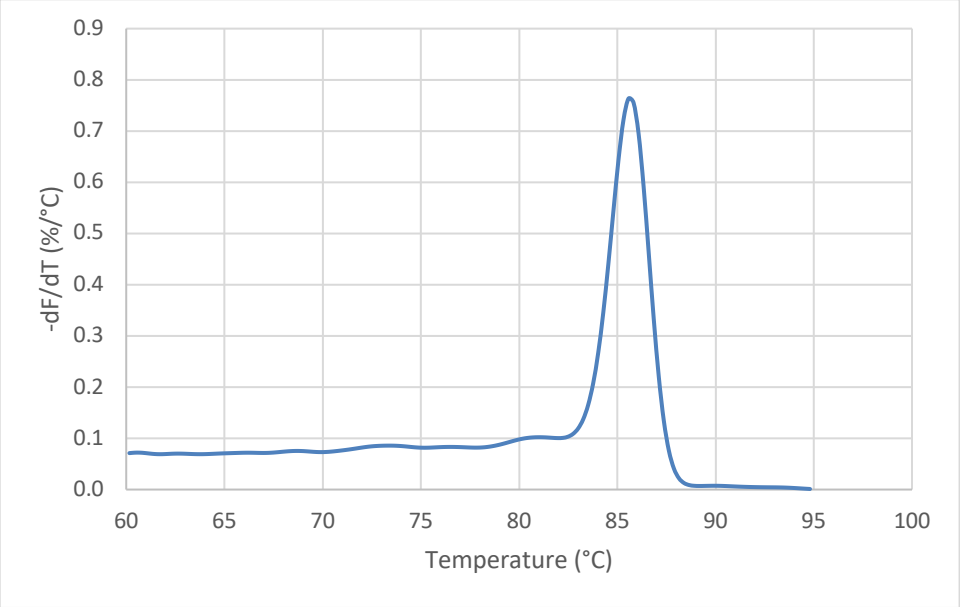

Figure 33: Melt curve for UV repair gene *umuC*

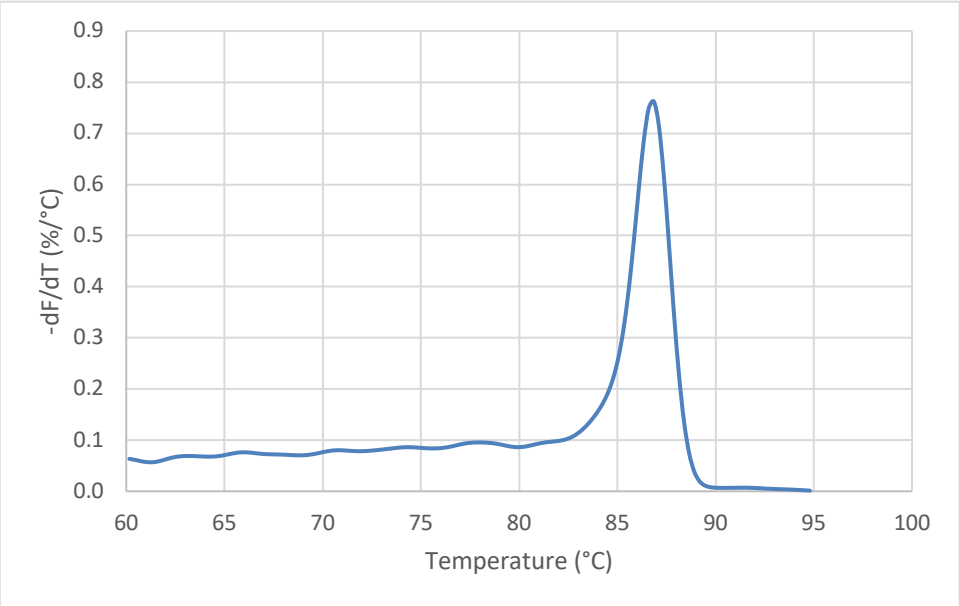

Figure 34: Melt curve for cell division gene *ftsZ*

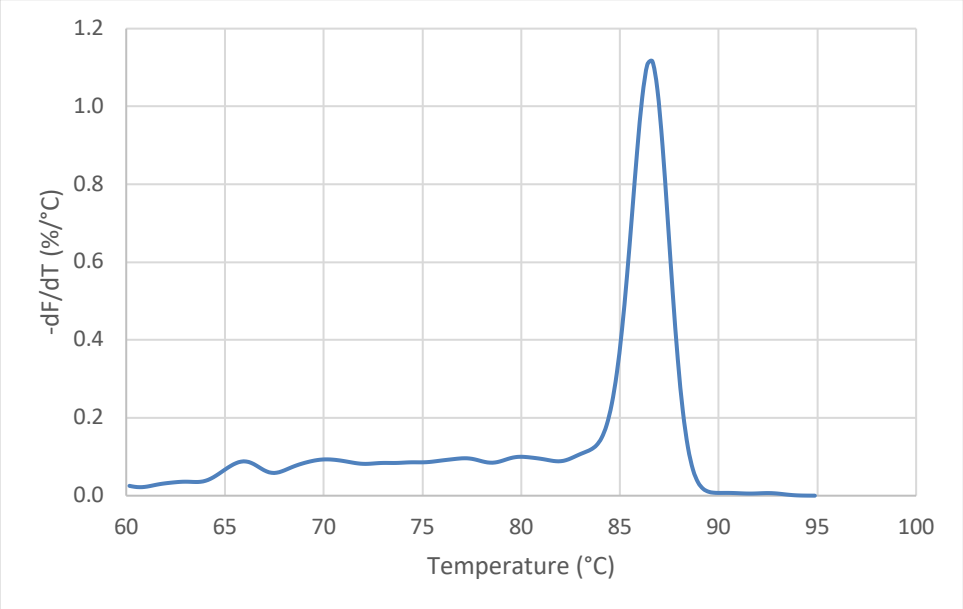

Figure 35: Melt curve for cell division gene *ftsQ*

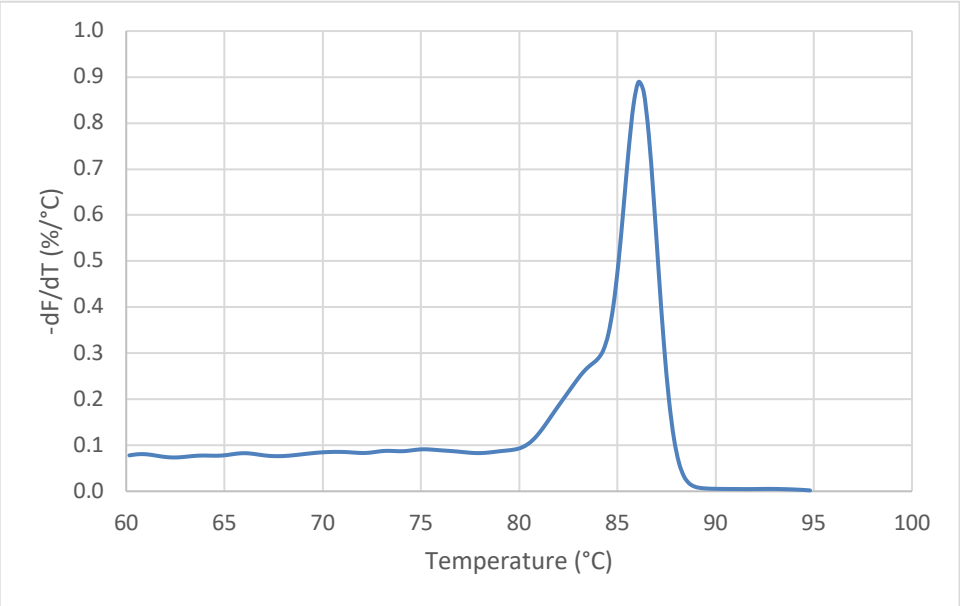

Figure 36: Melt curve for metabolic gene *gltA*

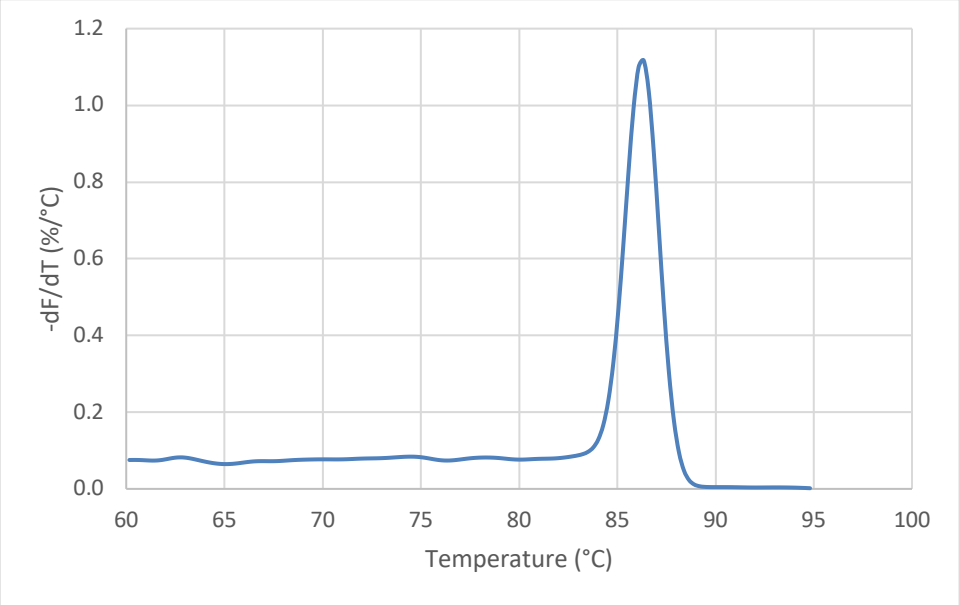

Figure 37: Melt curve for metabolic gene *ptsG*

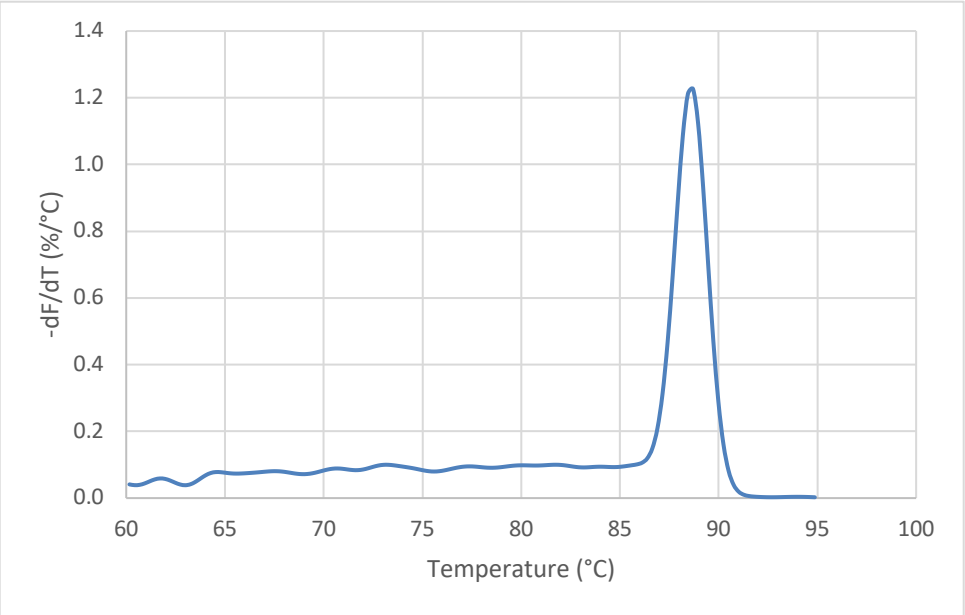

Figure 38: Melt curve for metabolic gene *pgl*

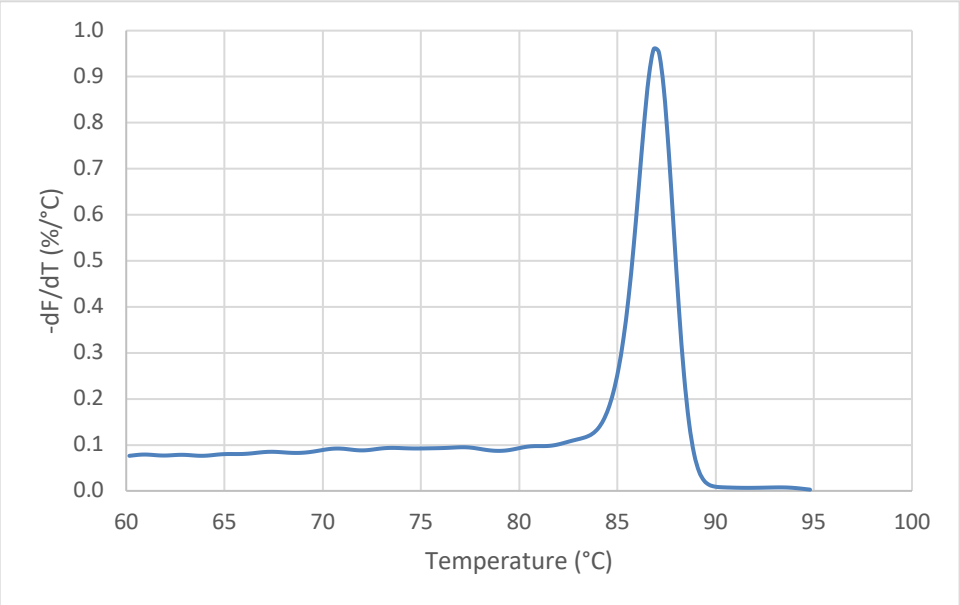

Figure 39: Melt curve for metabolic gene *tktA*

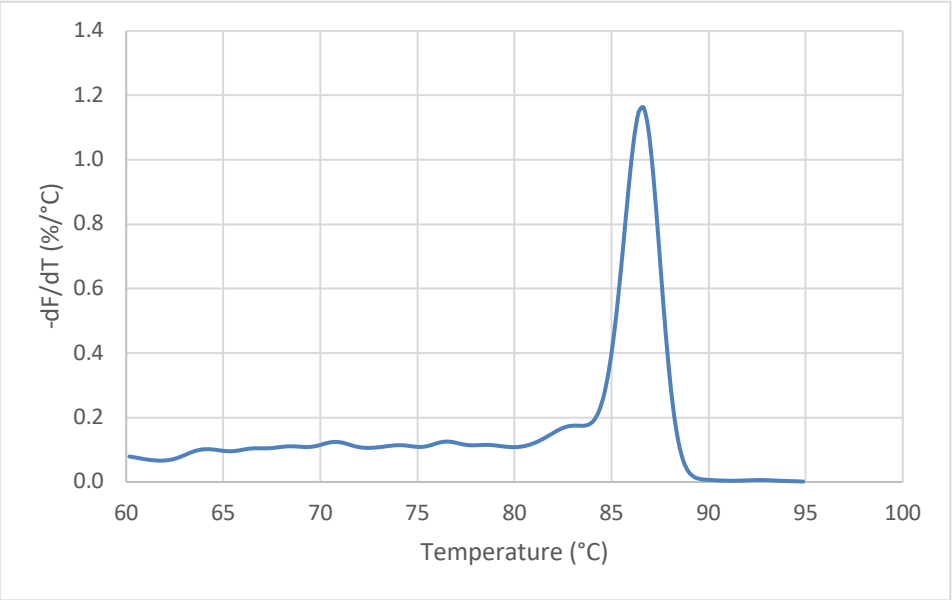

Figure 40: Melt curve for metabolic gene *fbaA*

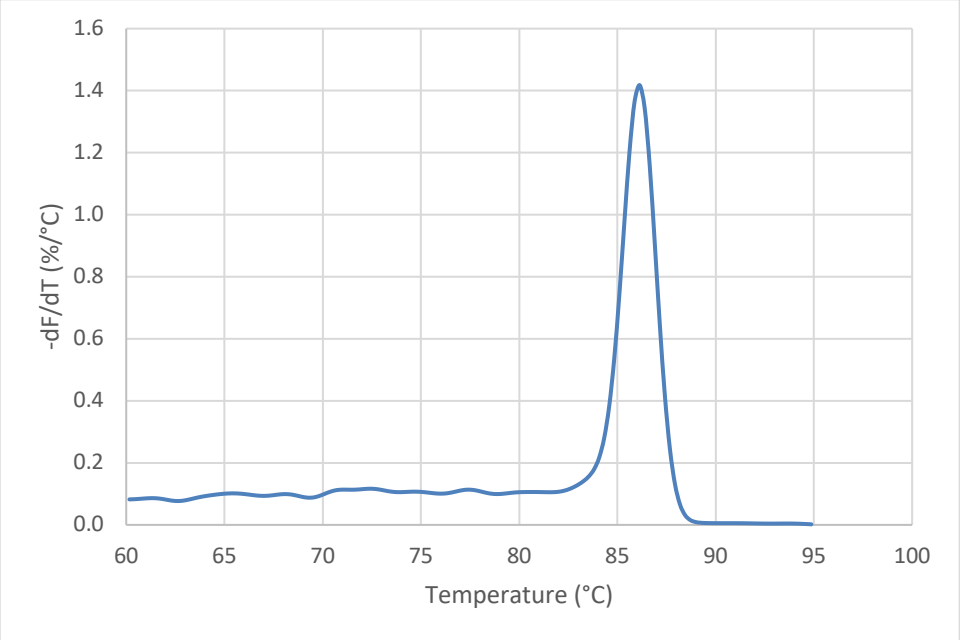

Figure 41: Melt curve for metabolic gene *tpiA*

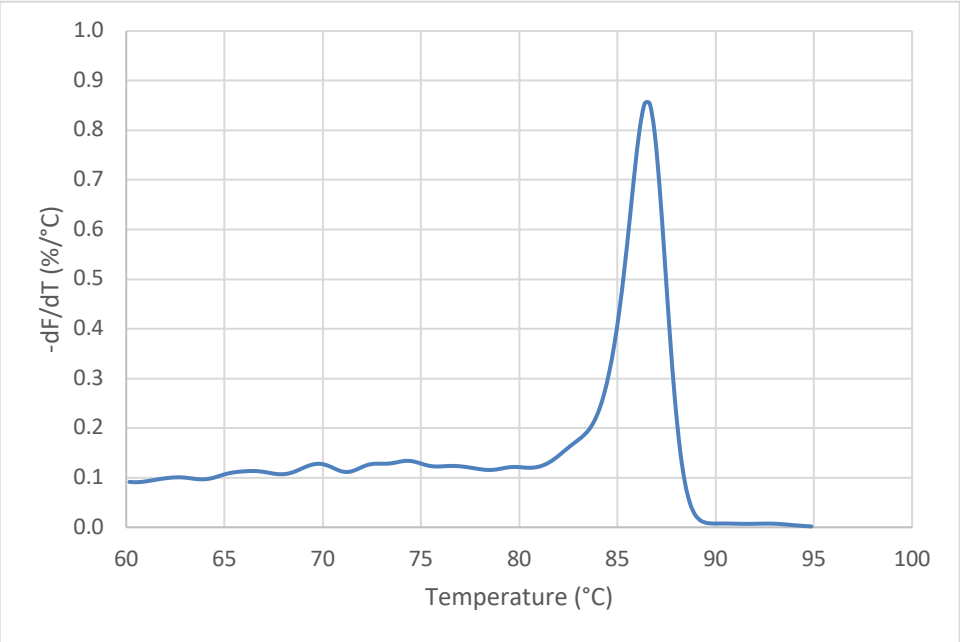

Figure 42: Melt curve for metabolic gene *ppsA*

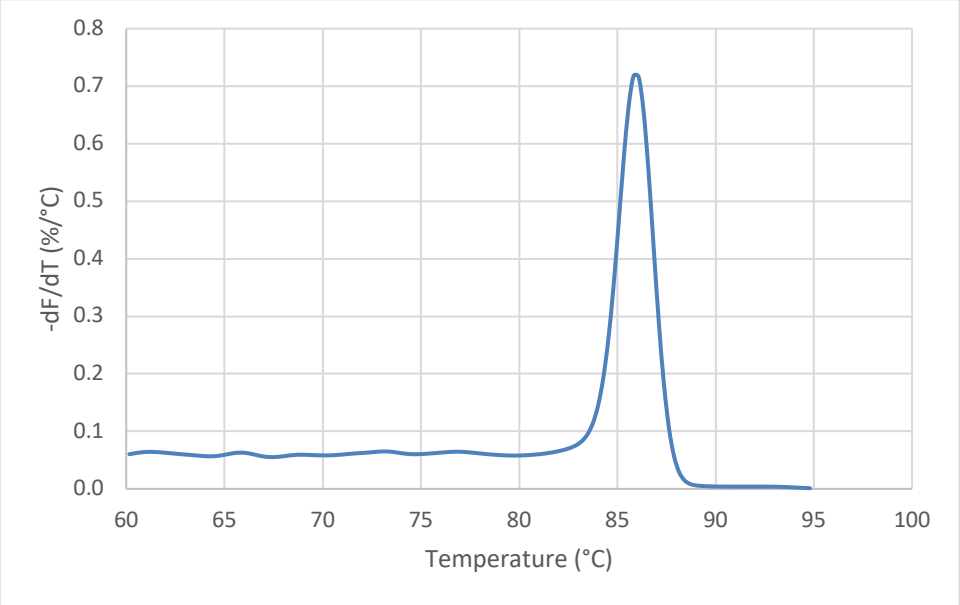

Figure 43: Melt curve for metabolic gene *pck*

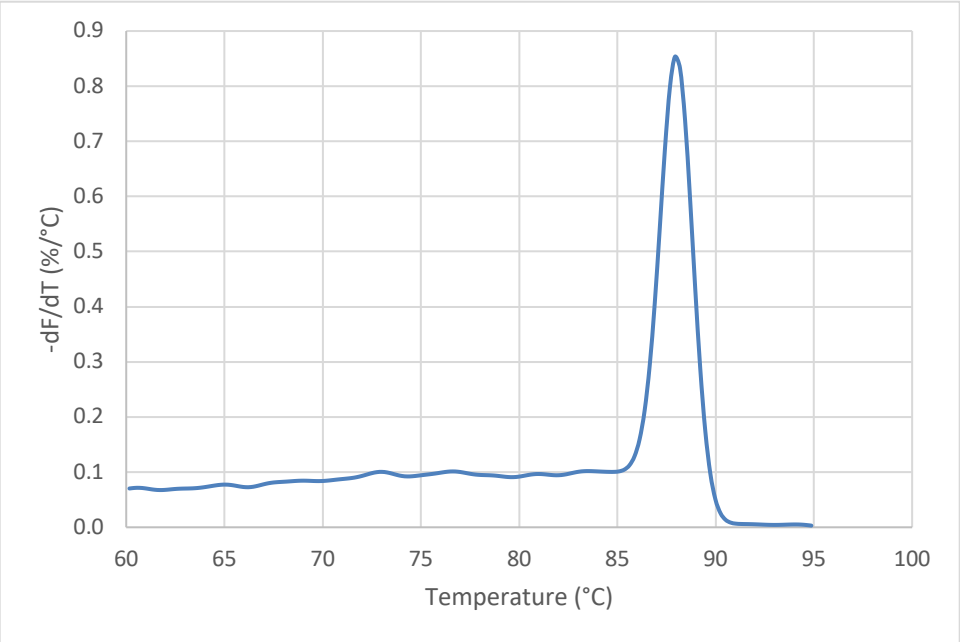

Figure 44: Melt curve for metabolic gene *dfp*

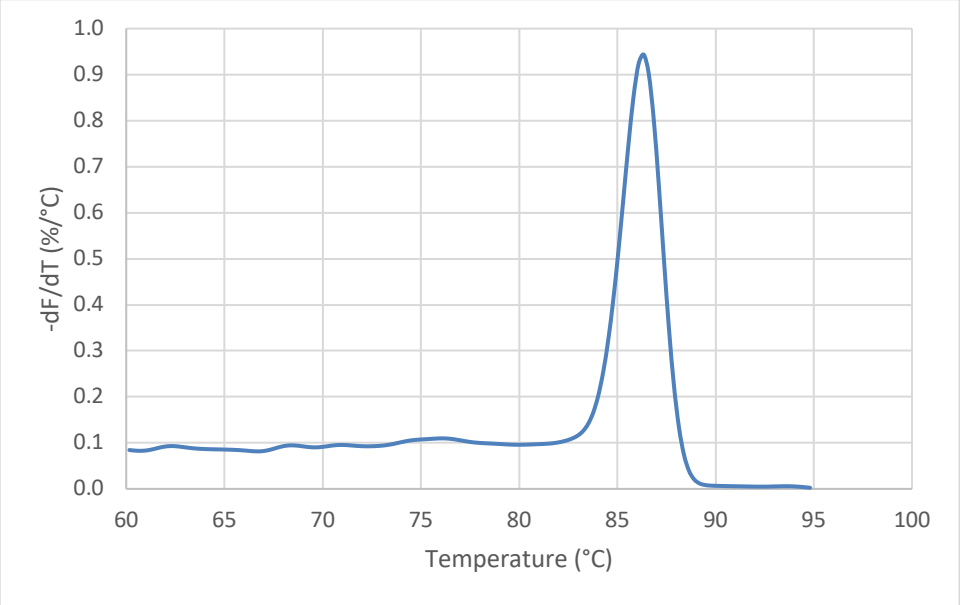

Figure 45: Melt curve for metabolic gene *uidAL*

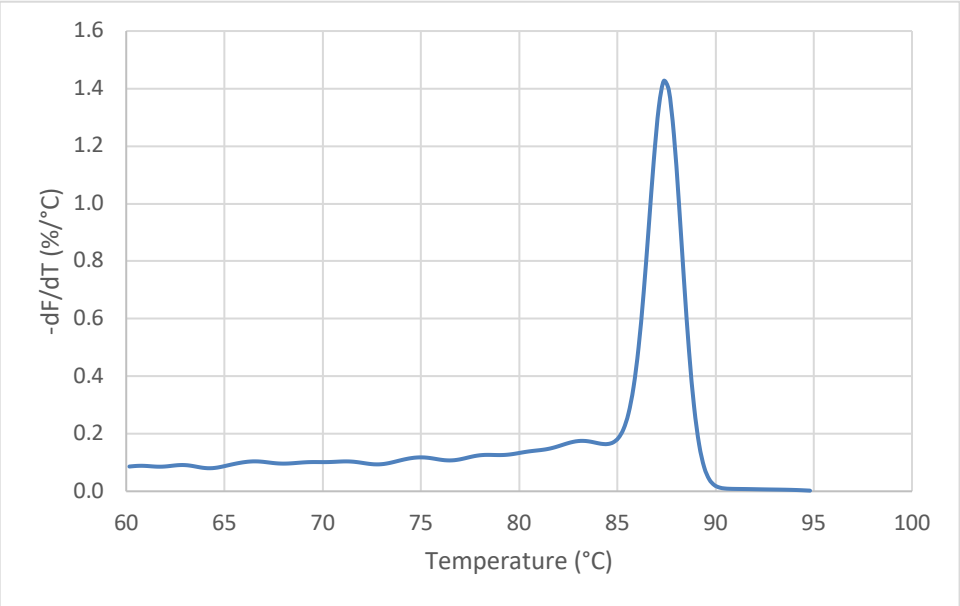

Figure 46: Melt curve for metabolic gene *gadA*

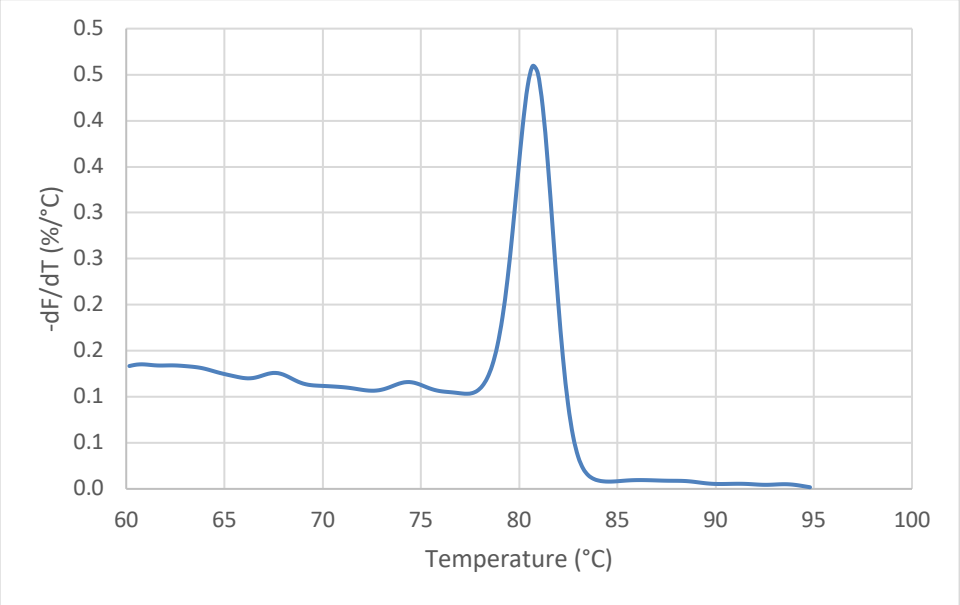

Figure 47: Melt curve for USEPA's 23S gene

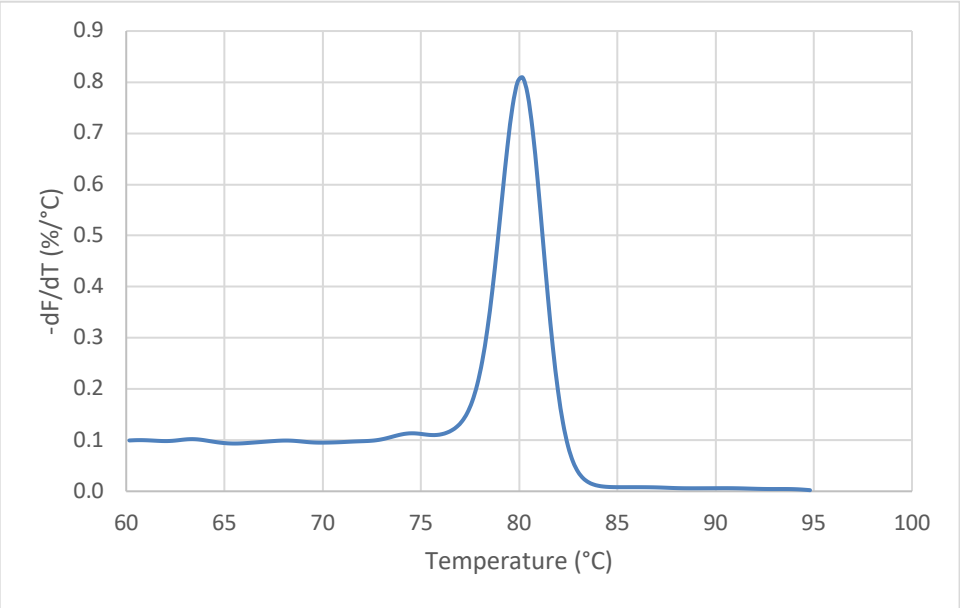

Figure 48: Melt curve for *uidAS*

Appendix B: Supplementary Information for Chapter 3

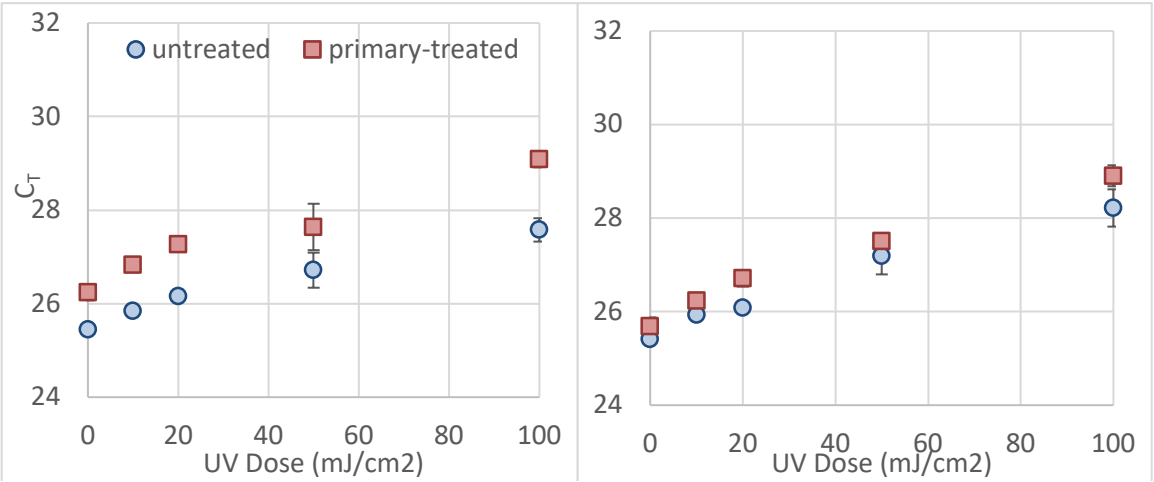

Figure 49: qPCR-based dose-response curves of rRNA genes, *rrsA* (left) and *rrlA* (right). Error bars represent the standard deviation between replicates. Some error bars are smaller than the markers.

Table 24: qPCR results for rRNA genes, used for dose-response curves

Target	Type	Dose	Ct Avg	St Dev
rrsA	raw	0	25.455	0.091
		10	25.841	0.113
		20	26.163	0.092
		50	26.715	0.375
		100	27.577	0.250
	primary	0	26.242	0.171
		10	26.834	0.073
		20	27.273	0.069
		50	27.640	0.496
		100	29.088	0.172
rrlA	raw	0	25.415	0.058
		10	25.932	0.104
		20	26.081	0.089
		50	27.187	0.391
		100	28.216	0.399
	primary	0	25.690	0.186
		10	26.239	0.131
		20	26.710	0.174
		50	27.511	0.028
		100	28.905	0.224

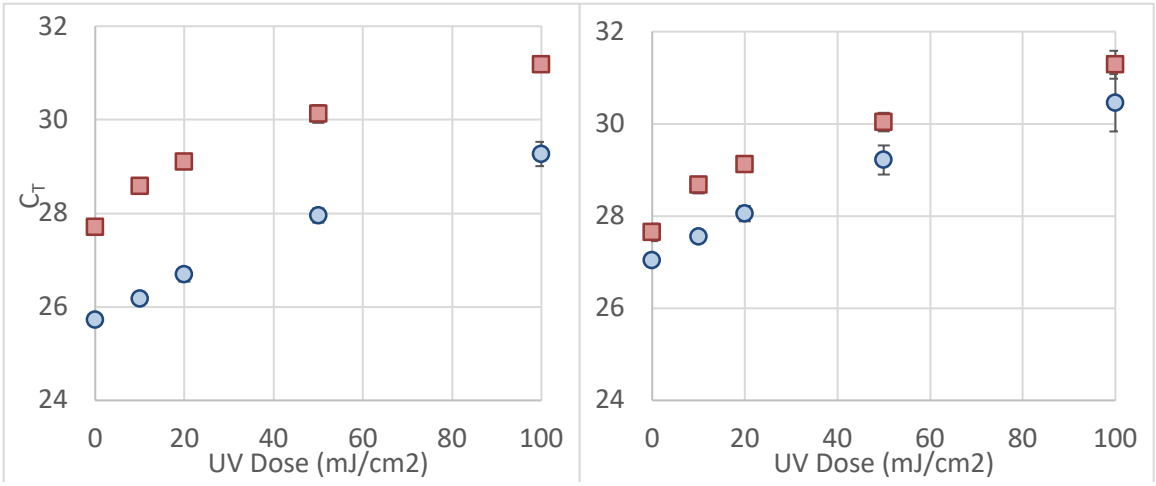

Figure 50: qPCR-based dose-response curves of UV repair genes, *uvrB* (left) and *umuC* (right). Error bars represent the standard deviation between replicates. Some error bars are smaller than the markers.

Table 25: qPCR results for UV repair genes, used for dose-response curves

Target	Type	Dose	Ct Avg	St Dev
uvrB	raw	0	25.722	0.071
		10	26.177	0.069
		20	26.688	0.147
		50	27.953	0.151
		100	29.268	0.260
	primary	0	27.701	0.124
		10	28.586	0.031
		20	29.108	0.145
		50	30.124	0.189
		100	31.179	0.157
umuC	raw	0	27.040	0.081
		10	27.546	0.101
		20	28.052	0.167
		50	29.215	0.316
		100	30.455	0.622
	primary	0	27.644	0.189
		10	28.671	0.181
		20	29.115	0.097
		50	30.037	0.201
		100	31.280	0.303

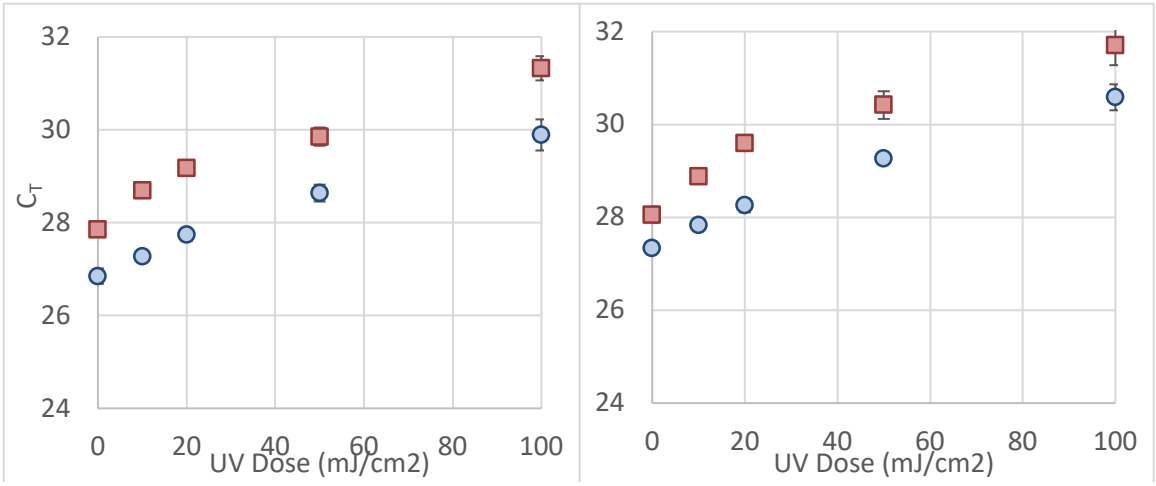

Figure 51: qPCR-based dose-response curves of cell division genes, *ftsZ* (left) and *ftsQ* (right). Error bars represent the standard deviation between replicates. Some error bars are smaller than the markers.

Table 26: qPCR results for cell division genes, used for dose-response curves

Target	Type	Dose	Ct Avg	St Dev
ftsZ	raw	0	26.848	0.166
		10	27.265	0.083
		20	27.736	0.126
		50	28.637	0.181
		100	29.889	0.335
	primary	0	27.856	0.158
		10	28.685	0.132
		20	29.169	0.119
		50	29.853	0.196
		100	31.324	0.261
ftsQ	raw	0	27.337	0.065
		10	27.830	0.116
		20	28.254	0.146
		50	29.264	0.113
		100	30.584	0.280
	primary	0	28.058	0.174
		10	28.886	0.099
		20	29.593	0.153
		50	30.417	0.298
		100	31.700	0.424

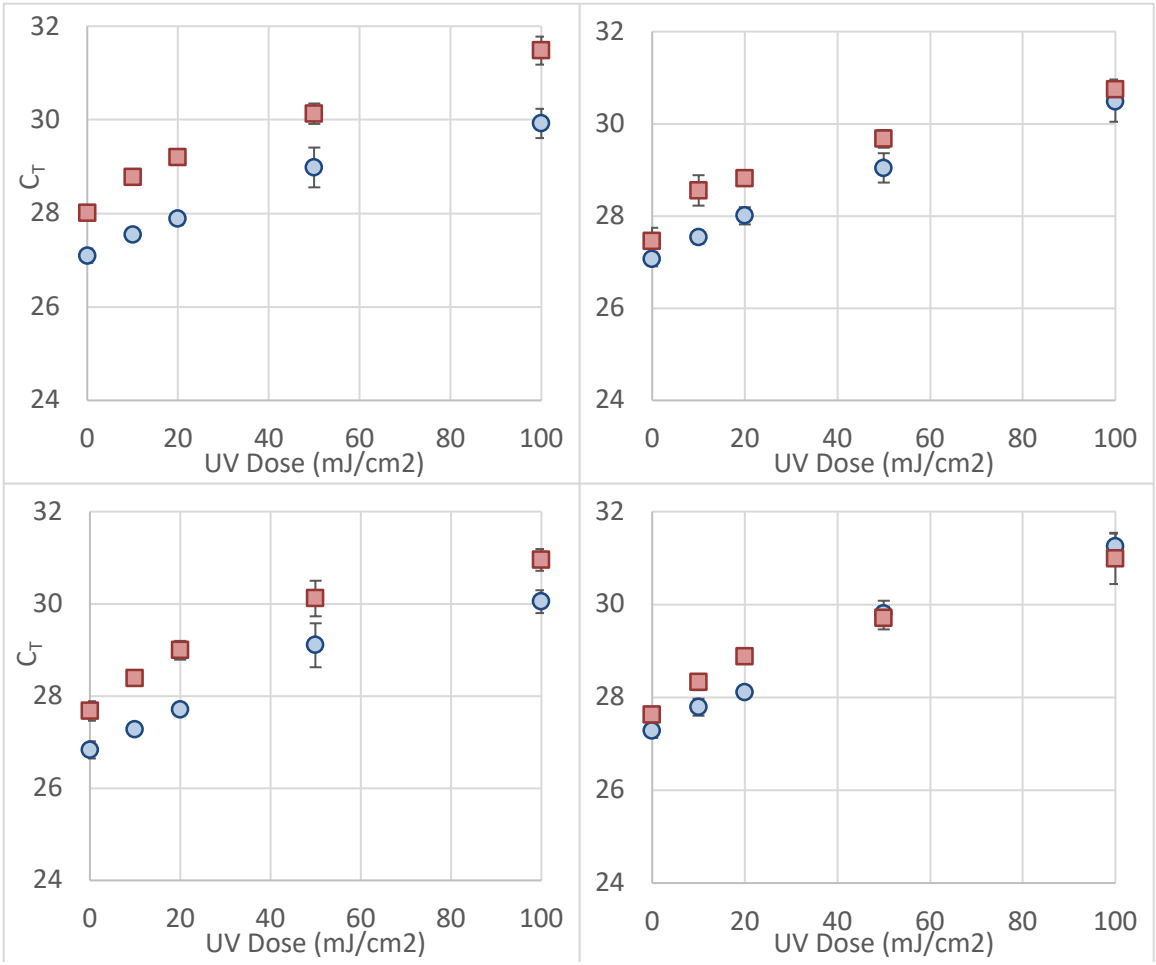

Figure 52: qPCR-based dose-response curves of metabolic genes, *ptsG* (top left), *pgl* (top right), *pck* (bottom left), and *uidA* (bottom right). Error bars represent the standard deviation between replicates. Some error bars are smaller than the markers.

Table 27: qPCR results for three metabolic genes, used for dose-response curves

Target	Type	Dose	Ct Avg	St Dev
ptsG	raw	0	27.093	0.153
		10	27.544	0.113
		20	27.881	0.124
		50	28.981	0.425
		100	29.922	0.313
	primary	0	28.010	0.129
		10	28.769	0.087
		20	29.204	0.093
		50	30.130	0.218
		100	31.479	0.300
pgl	raw	0	27.060	0.152
		10	27.533	0.130
		20	28.004	0.187
		50	29.043	0.318
		100	30.477	0.433
	primary	0	27.456	0.289
		10	28.555	0.330
		20	28.809	0.100
		50	29.673	0.192
		100	30.747	0.214
pck	raw	0	26.831	0.187
		10	27.276	0.115
		20	27.709	0.063
		50	29.100	0.477
		100	30.046	0.248
	primary	0	27.675	0.212
		10	28.388	0.020
		20	28.992	0.204
		50	30.114	0.386
		100	30.951	0.236

Table 28: qPCR results for metabolic gene uidA, used for dose-response curves

Target	Type	Dose	Ct Avg	St Dev
uidAL	raw	0	27.282	0.157
		10	27.787	0.183
		20	28.104	0.096
		50	29.806	0.274
		100	31.256	0.269
	primary	0	27.623	0.078
		10	28.327	0.173
		20	28.882	0.113
		50	29.706	0.244
		100	30.991	0.552

VITA AUCTORIS

NAME:	Natasha Rahman
PLACE OF BIRTH:	Lahore, Pakistan
YEAR OF BIRTH:	1994
EDUCATION:	Vincent Massey Secondary School, Windsor, ON, 2012
	University of Windsor, B.A.Sc., Windsor, ON, 2016
	University of Windsor, M.A.Sc., Windsor, ON, 2019